Design, build and test of a planar biaxial tensile testing machine for skin and other collagenous soft tissues

Jonathan Andrew Caine

Masters of Science Dissertation
in the Department of Mechanical Engineering
Faculty of Engineering and the Built Environment
University of Cape Town

January 2022

Declaration

I, Jonathan Caine, hereby:

(a) grant the University of Cape Town free license to reproduce the above thesis in whole or in part, for the purpose of research;

(b) declare that: I know the meaning of plagiarism and declare that all the work in the document, save for that which is properly acknowledged, is my own. This thesis/dissertation has been submitted to the Turnitin module (or equivalent similarity and originality checking software) and I confirm that my supervisor has seen my report and any concerns revealed by such have been resolved with my supervisor.

I am now presenting the report for examination for the degree of M.Sc (Mechanical).

Signed by candidate

Jonathan Andrew Caine

31 January 2022

Abstract

This investigation forms part of a larger study, investigating the mechanical properties of skin and other soft membrane tissue. The focus of this project was the design and construction of a planar biaxial tensile testing machine, suitable for ultimately testing skin and other soft membrane tissues. The mechanical properties of skin and other collagenous soft tissues are of interest to a wide range of researchers and professionals. Interests include medical device design, research into the change in skin's mechanical properties due to disease, and skin's material characterisation for computational simulation.

None of the laboratories at the University of Cape Town (UCT) were capable of performing planar biaxial tensile tests on soft tissue prior to this project. The machine was designed as a stand-alone, portable and accurate tensile tester with two independent and orthogonal testing axes. The machine was designed to be operated using GRBL software: an open-source motion control system for CNC milling. Two 50 N tensile load cells (K-S2M, Hottinger Baldwin Messtechnik, Darmstadt, Germany) were used for load measurement and a non-contact Digital Image Correlation (DIC) system (Dantec, Denmark) was used for three-dimensional surface displacement measurement.

Commissioning testing was done on a silicone elastomer (Smooth-On, Dragon Skin 10) which was used as a skin surrogate. The commissioning testing did not seek to characterise the surrogate material, but to verify that the machine operated as intended. As testing of biological specimens will involve non-trivial specimen preparation and mounting, this is left to future research. Initially, a single axis of the custom machine was used to perform uniaxial tensile tests on the surrogate material. Specimens of the same surrogate material were tensile tested using a calibrated Instron (Norwood, MA, USA) tensile testing machine at the Centre for Materials Engineering (CME) at UCT for comparison. Twenty specimens were tested on each machine: five specimens per cross-head displacement rate: 10, 50, 120 and 400 mm/min. Sources of error were identified and addressed through minor design and procedure changes. Further uniaxial testing on the revised first axis, and the newly built second axis, was performed at 50 mm/min and 400 mm/min. These results compared favourably to the results from the Instron tensile testing machine.

Planar biaxial tensile tests were performed on cruciform specimens of the surrogate silicone elastomer. Biaxial testing was performed at four different cross-head displacement rates (10, 50, 120 and 400 mm/min) combined with five different loading ratios between the axes (1:1, 1:0.75, 1:0.5, 1:0.25, 1:0). A total of 30 specimens were tested.

The performance of the machine was critically assessed and the areas of difficulty encountered during testing were: handling and gripping the highly pliable specimens, consistency in the boundary conditions of the specimen, inter specimen variability, and alignment issues. The testing demonstrated that the machine functions as intended, and meets the requirements to be used in the testing of skin and other membrane tissue in the future.

Acknowledgements

My sincere gratitude goes to:

My supervisor, Dr Reuben Govender. Whose knowledge, guidance, patience and understanding were essential to the completion of this work.

My wife, Amber. Your love and support mean so much to me.

BISRU staff and my fellow MSc graduate students (Dan, Ruix, Muhsin, Andrew and Dustin) for always being helpful and available to bounce ideas off of.

The Mechanical engineering workshop staff for manufacturing the components of the machine and teaching me so much along the way.

My parents, Grant and Gayle, for always supporting and encouraging me.

Contents

List of Figures

List of Tables

Chapter 1

Introduction

1.1 Background

The mechanical properties of skin and other collagenous soft tissues, such as myocardium, tendons, aorta tissue and many others are of interest to surgeons, medical device experts, biomedical engineers and material engineers. Interests include changes to tissue mechanical properties due to disease or medical intervention, medical device design, and material characterisation for computational simulation of a tissue's response to loading. Understanding the mechanical properties of skin and other collagenous tissues is complicated by the fact that they are heterogeneous, anisotropic, non-linear and some show visco-elastic properties [1][2][3]. There are currently no accepted standards for the tensile testing of biological tissues, whether hard or soft. A variety of testing methods are employed depending on the specific needs of the study and the availability of suitable tissue for specimens. This gives rise to varied results in literature.

The research presented in this dissertation was done at the Blast Impact and Survivability Research Unit (BISRU) at the University of Cape Town (UCT). BISRU is interested in the mechanical properties of skin to better understand the human structural make-up and therefore survivability of people subjected to impact trauma. Previous postgraduate research projects within BISRU have designed, built and commissioned bulge test devices capable of testing skin (or other biological membranes) at different strain rates. These devices all use a pressure differential to inflate a membrane, inducing biaxial tension. However, planar biaxial tensile tests remain an essential part of biological membrane tissue characterisation [4]. Biaxial tensile testing equipment is not commonly available, even for engineering metals or polymers. Testing biological tissues requires sensitive force instruments, suited to the very small forces anticipated. Although planar biaxial tensile testing machines are commercially available, such as the CellScale BioTester [5], these machines are extremely expensive (USD 85 000). As there were no facilities for

planar biaxial tensile tests of any kind at the start of BISRU's broader investigation of tissue properties, it was decided to design and build a custom planar biaxial tensile tester for biological tissues.

1.2 Aim

The aim of this investigation was to design, build and test a custom planar biaxial tensile testing machine, suitable for testing skin and other collagenous soft tissues. This dissertation will detail the design and commissioning testing of the custom built machine. Due to the complexities in harvesting and preparing specimens from human or animal tissue, the commissioning testing of this machine will be performed using silicone elastomers as a surrogate for soft human tissue. The procedures for preparing biological tissue specimens and the actual testing thereof, are left for future research.

The planar biaxial tensile tester will be used by researchers in BISRU and the broader UCT community, so it must be accurate and easy to use consistently. As it may be necessary to perform tissue testing at clinical sites, to limit any degradation after harvesting tissue, the device must be portable. The objectives of the investigation are summarised in the list below:

- Design and build a planar biaxial tensile testing machine, which should be suitable to ultimately test skin and other collagenous soft tissues.
- Verification testing to be performed to prove the concept and build of the custom machine.
- Planar biaxial tensile testing to be performed on a surrogate material.

1.3 Scope and limitations

The planar biaxial tensile testing machine was intended to be a custom built machine, and was not designed with mass manufacture or commercialisation in mind. The device does not need to be novel or patentable.

As this research forms part of an M.Sc in Mechanical Engineering, the focus will be on the mechanical machine design and testing. The electronic instrumentation and associated software makes use of transducers, actuators and software libraries that can be implemented in a modular fashion, rather than designing these from a first principles approach. Additionally, the machine operates in an open loop control mode. Prior BISRU projects using bulge testers had shown that open loop control was stable at low loading rates [6] and that the significant complexity of implementing a closed loop control system

only began to yield benefits at substantially higher loading rates than those intended for this machine [7].

Due to the flexibility and fragility of soft membrane tissues, a non-contact, image based deformation measurement system was used. As there is an existing 3D Digital Image Correlation (DIC) system within the department, it would not be justifiable to develop a new image based measurement system for the machine. Therefore, the existing DIC system was used to measure the deformation of the specimens during testing. The DIC system available at UCT, provided by Dantec Dynamics, does not allow for live feedback as the deformation data is only available after post-processing.

The commissioning testing for this M.Sc project was limited to silicone elastomers as a surrogate for soft biological material. The aim of the testing was not to produce an accurate material model for the elastomer, but to verify that the machine operated as intended. This project made use of simple clamp grips suitable for elastomers, with the detailed design of grips suitable for extremely fragile tissues left for future research.

1.4 Plan of development

This dissertation first establishes the aim and scope of the research. Comprehensive research into the topics relevant to the investigation are then presented in the form of a literature review. Relevant topics include the mechanical properties of skin and soft tissues, testing methods of skin, planar biaxial tensile testing of skin and existing planar biaxial tensile testing machines.

The design process of the custom built machine and its subsystems are then detailed, beginning with the user needs, specifications and concepts. An in-depth break down of the subsystems and their design are presented, discussed and justified.

The experimental plan for the testing of the custom built machine is then presented. The testing was split into first uniaxial testing of individual axes and then planar biaxial testing. The dissertation first presents the uniaxial experimental design, results and discussion. The data from the uniaxial testing was compared against data obtained from a calibrated and commercially available uniaxial tensile testing machine (Instron). Difficulties encountered during the uniaxial tests done on the custom machine were analysed and informed minor revisions to the final design of the planar biaxial tensile tester.

Following the implementation of the revisions, the custom machine was used to perform planar biaxial tensile tests on silicone elastomer specimens as a surrogate for skin. The biaxial testing plan and the test results are presented. The biaxial results are then analysed and discussed. Finally, conclusions are drawn, most notably that the machine

met the design requirements. Recommendations are made to facilitate future testing with biological tissue specimens.

Chapter 2

Literature Review

This chapter reviews the literature needed to understand the background and content of this investigation. First, literature on the mechanical properties of skin and other collagenous soft tissues is reviewed in order to fully understand the complexities and difficulties inherent in testing a soft biological membrane. Then, literature on a variety of methods of testing soft tissue is reviewed, with a focus on planar biaxial tensile testing.

2.1 Skin

Skin is the body's first line of defense against the outside world and is the largest organ in the body [8]. Not only is it a physical barrier, it provides vital structural support to internal organs while simultaneously allowing ease of movement of the body. Skin also regulates the body's heat and fluid losses, it acts as insulation and also protects the body

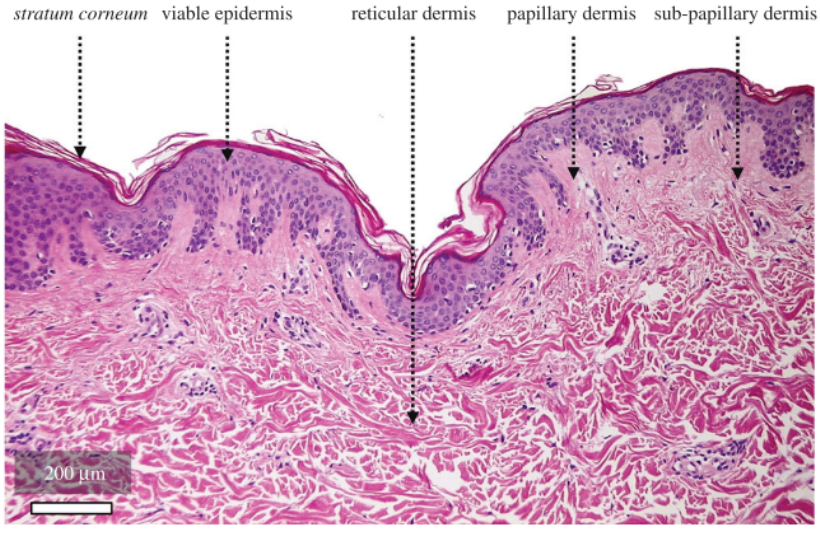

Figure 2.1 Cross-section of stained human back skin [8]

from infection [9]. Skin can be considered as a multi-layered complex fibre reinforced composite structure [1]. Human skin consists of three layers: the epidermis, the dermis and the hypodermis; these layers have different functions and therefore different micro-structural architectures and mechanical properties.

2.1.1 Epidermis

The epidermis is the outer most layer of the skin and is the thinnest, typically measuring between 50 μm and 150 μm [10]. However, this varies substantially with Kolarsick et al stating the epidermis is thinnest on the eyelids with a thickness of 0.1 mm and thickest on the soles of the feet with a thickness of up to 1.5 mm[9]. The epidermis continuously produces a protective outer layer primarily made of keratin through the process of keratinazation. This protective layer of dead keratinocytes is called the stratum corneum and is 15 to 30 μm thick [8], preventing water loss and invasion from foreign substances [9].

2.1.2 Dermis

The tensile mechanical properties of skin are predominantly determined by the dermis [10] as it is the main load-bearing component of skin [8]. The dermal layer prevents mechanical injury, aids with thermal regulation and houses sensory receptors [9]. The dermis is between 0.15 mm and 4 mm thick, and is made up of elastin and collagen fibres which make up approximately 5-10% and up to 70% of the dry weight of skin respectively[1]. These fibres are supported in a ground substance which is mainly made up of proteoglycans [11]. The collagen fibres have the most pronounced influence on the mechanical response of skin to tensile loading [11].

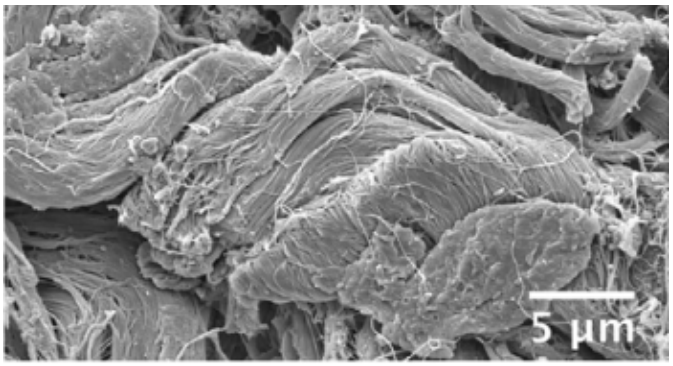

Figure 2.2 An image of the collagen fibres found in the epidermis taken by Pissarenko et al. using SEM microgarphs [10]

The collagen fibres in the dermis (Figure 2.2) are arranged into a complex three-dimensional network [10]. These fibres are initially crimped and have natural preferred orientations (Langer lines) depending on where the skin is on the body. When a load is applied to the skin the collagen fibres uncrimp and reorient themselves in the direction

of the load. Many of skin's mechanical properties, such as being anisotropic, viscoelastic, heterogeneous and nonlinear [1], can be understood by understanding the micro-structural and mechanical response of the dermis.

2.1.3 Hypodermis

The hypodermis, or subcutaneous layer, is primarily made up of fat cells separated by large blood vessels and collagen [9]. The main function of this layer of skin is to store energy, provide shock absorption and to minimize friction with internal organs. Although vitally important, the hypodermis does not contribute significantly to the mechanical response of the skin to loading.

2.1.4 Other collagenous soft tissues

Holzapfel describes soft tissue as "a primary group of tissue which bonds, supports and protects our human body and structures such as organs" he expands on this by stating that "it is a wide-ranging biological material in which the cells are separated by extracellular material"[1]. Skin, ligaments, tendons and blood vessels are all considered as soft tissues and are all fibre reinforced composite structures composed of both collagen and elastin to varying degrees as shown in Table 2.1.

Material	**Ultimate tensile strength (MPa)**	**Ultimate tensile strain (%)**	**Collagen (% dry weight)**	**Elastin (% dry weight)**
Tendon	50-100	10-15	75-85	< 3
Ligament	50-100	10-15	70-80	10-15
Aorta	0.3-0.8	50-100	25-35	40-50
Skin	1-20	30-70	30-70	5-10

Table 2.1 *Mechanical properties of some soft tissues and their biochemical data [1]*

2.2 Mechanical characteristics of skin

Skin and other collagenous soft tissues are non-linear, heterogeneous, anisotropic and exhibit some viscoelastic properties[1][11]. This makes skin a difficult material to accurately characterise. Skin is generally considered to be hyperelastic under loading [12], with several different strain energy functions used to characterise it in literature [13].

2.2.1 Stress-Strain response

The typical stress-strain response of skin under uniaxial tension is shown in Figure 2.3, with the non-linear curve being widely described as J-shaped in literature. The response can be better understood by splitting the curve into three stages and then analysing how the micro-structure of the dermis reacts to the load during each stage. In the first stage, the material's response is linear with a very low elastic modulus [14]. Initially, the collagen fibres are crimped and tangled and do not bear the load, with the elastin fibres being the primary resistance to deformation [2]. During this stage the skin acts isotropically and linearly with a typical elastic modulus between 0.1 and 2 MPa [1]. It is important to note that the slope of the curve in this first stage is also more commonly known as the initial slope, with the gradient in stage 3 of the curve often being referred to as the elastic modulus.

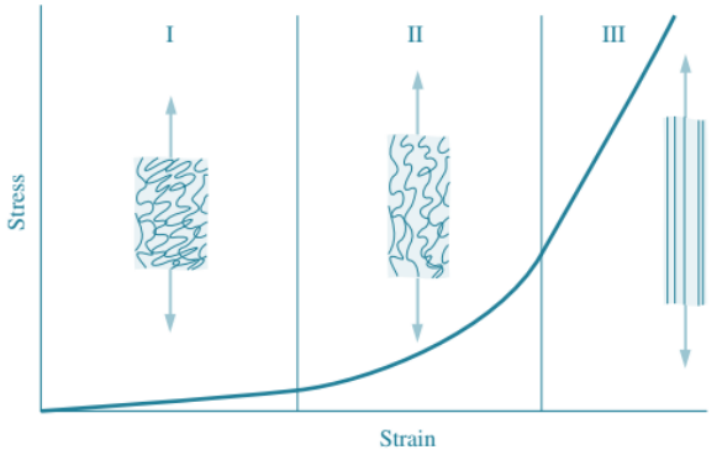

Figure 2.3 A typical stress versus strain response of skin undergoing uniaxial tension [1]

As strain increases into Stage 2, the collagen fibres begin to straighten, untangling and stretching in the direction of the load. Stage 2 is highly non-linear, with the collagen fibres supporting more of the load [1]. Once the collagen fibres have completely untangled and straightened the response enters stage 3, where the tissue behaves almost linearly with a much higher elastic modulus. In Stage 3 the mechanical properties of the skin are dominated by the collagen fibres [3]. The material behaves in a highly anisotropic manner, as the material's response to loading is dependent on the orientation of the collagen fibres.

2.2.2 Anisotropy

The fibres found in soft tissues such as skin have a preferred orientation making skin a highly anisotropic material. This anisotropic behaviour of skin was first mapped by

Langer in 1861. Langer showed that skin had natural lines of tension, a map of these lines which are now known as Langer's lines is shown in Figure 2.4 below [15].

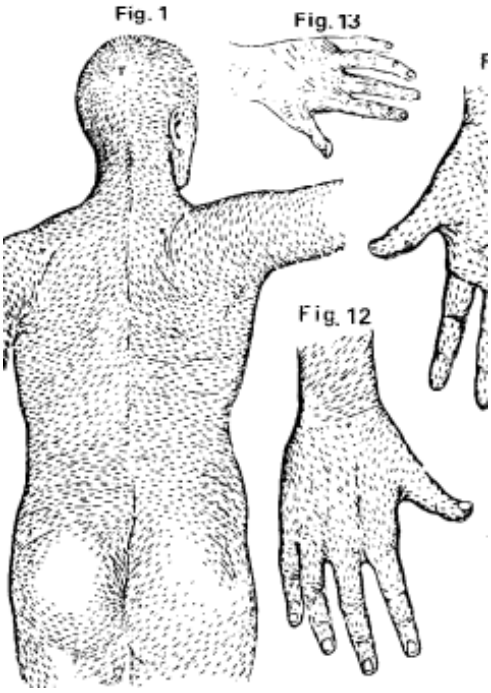

Figure 2.4 Map of Langer's lines [15]

More recently there have been several studies into the affect of skin's natural preferred fibre orientation on its mechanical properties. Ni Annaidh et al [3] studied skin's anisotropic behaviour by performing in vitro uniaxial tensile tests on skin specimens oriented at different angles to the skin's Langer lines. Ni Annaidh et al tested 56 samples from their human subjects' backs, samples were parallel, perpendicular, or at 45° to Langer's lines. It was found that the orientation of the samples with regards to the Langer lines had a significant effect on the ultimate tensile strength, strain energy, elastic modulus and initial slope of the samples [3]. Similar results were found by Ottenio et al [16] who tested the effects of orientation and strain rate on the mechanical properties of skin. Ottenio et al's results [16] are summarised in Table 2.2, highlighting the significant difference in modulus and UTS of skin parallel and perpendicular to the Langer lines.

2.2.3 Heterogeneity

Skin is not homogeneous across the body, varying significantly depending on its location on the body. For example, glabrous (hair free) skin is found on the hands and feet while skin on the top of the head is typically covered in hair. Depending on where the skin is located, its thickness, number of hair follicles and the various types of glands it houses vary significantly. These differences make skin highly heterogeneous when analysing its mechanical response [17].

	Mean UTS (MPa)	**Mean elastic modulus(MPa)**
Parallel	28.0 ±5.7	160.8 ±53.2
Perpendicular	15.6 ±5.2	70.6 ±59.5

Table 2.2 *Effects of orientation on UTS and Elastic Modulus of human skin (Ottenio et al, 2015) [16]*

Ni Annaidh et al [3] found that the specimens' location had a major effect on the ultimate tensile strength, elastic modulus and strain energy, when grouping specimens according to three locations: the upper back, middle back and lower back (Figure 2.5). Ni Annaidh et al also noted that the location of the specimen did not have any statistically significant effect on the initial slope or failure stretch of the specimens [3].

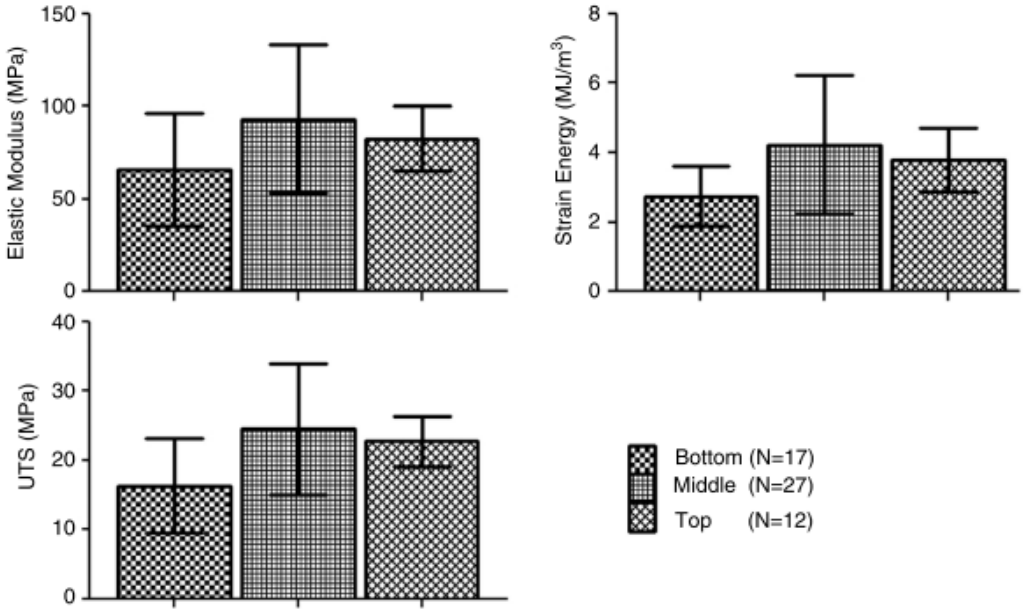

Figure 2.5 The effect of the location of skin specimens on their respective UTS, Elastic modulus and strain energy [3]

.

Agache et al [18] performed torsional tests in vivo on 138 subjects' forearms. It was found that the age of the subject had a significant effect on the results. It was found that up to the approximate age of thirty years old the elastic modulus of the specimens remained more or less constant. For older subjects, the modulus would undergo a rapid increase of approximately 50%, indicating the significant effect of aging on skin [18].

Falland-Cheung et al [19] performed uniaxial tensile tests on human skin taken from the scalp of their subjects with the aim of gaining material data across different ages and regions of the scalp. It was found that there was no statistically significant difference

when comparing the tensile strength between males and females. However, there where differences between male and female subjects when comparing the elastic modulus of samples from the occipital region of the scalp. Falland-Cheung et al also found differences when comparing elastic modulus and tensile strength results between the different regions of the scalp and concluded that their "results highlight the heterogeneous nature of human skin" [19].

2.2.4 Viscoelasticity

The skin's response to loading is comprised of both an elastic and a viscous response. The elastic response is primarily a result of the deformation of elastin and collagen fibres as well as that of the base material of skin's lattice structure. The viscous response is a result of viscous sliding of the fibres as they align in the direction of the applied load [2]. As a result of having both elastic and viscous responses; skin is considered viscoelastic and is therefore strain rate dependent. Soft tissues also display stress relaxation as a result of the shear interaction of the collagen fibres with the base material lattice [1].

There have been several studies into the strain rate dependence of skin. Ottenio et al studied the effect of strain rate on the mechanical properties of skin undergoing uniaxial tensile tests [16]. Specimens were tested at strain rates of 0.06 s^{-1}, 53 s^{-1} and 167 s^{-1}, with reported parameters being UTS, stretch at UTS, stretch at failure, strain energy and modulus. A comparison of the response at 0.06 s^{-1} and 53 s^{-1} showed statistically significant differences in all parameters. However, comparing the responses at 53 s^{-1} and 167 s^{-1} only showed statistically significant variations for strain energy and modulus. An example of the stress-strain curve obtained by Ottenio et al for a single location at varying strain rates is shown in Figure 2.6 [16]. Figure 2.6 does not seem to show the typical J-shape curve shown in Figure 2.3. This is because the initial slope driven by the elastin only happens at very low strains, Ottenio et al preloaded the specimens up to 2 N and all specimens underwent pre-conditioning where a cyclical displacement of 0.5 mm at 1 Hz was applied to the specimens for ten cycles [16].

Shergold et al [20] studied the compressive response of silicone rubber and pig skin over a wide range of strain rates (0.004 s^{-1}, 0.4 s^{-1}, 40 s^{-1} and 4000 s^{-1}). Tests were performed on cylindrical specimens of pig skin and silicone rubber, with a Split Hopkinson Pressure Bar being used for high strain rate tests (4000 s^{-1}), a hydraulic testing machine for medium strain rate tests (40 s^{-1}) and an Instron 5500R screw driven testing machine for low strain rates (0.004 s^{-1} and 0.4 s^{-1}). Shergold et al found that the pig skin strengthened and stiffened with an increase in strain rate, with the shear modulus increasing by a factor of five as strain rate increased from 0.004 s^{-1} to 40 s^{-1} and increased by a factor of four when strain rate increased from 40 s^{-1} to 4000 s^{-1} [20].

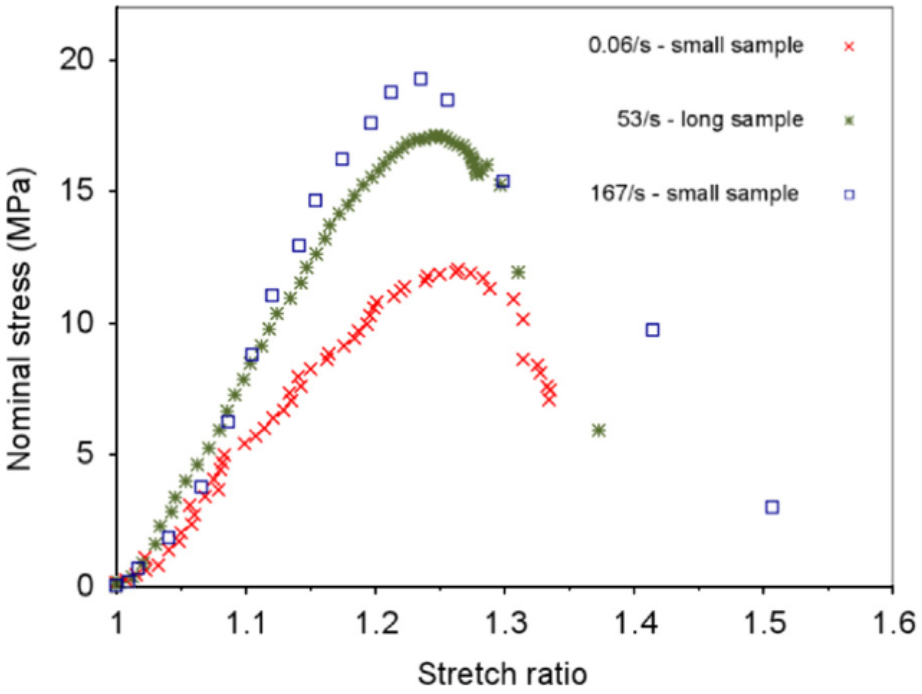

Figure 2.6 The stress-strain response of specimens from the same location at varying strain rates [16]

Pissarenko et al [10] performed uniaxial tensile tests on pig dermis specimens at strain rates of $10^{-4}s^{-1}, 10^{-3}s^{-1}, 10^{-2}s^{-1}, 10^{-1}s^{-1}$ and $0.5s^{-1}$. Pissarenko et al found that inter-specimen differences were significant, and more importantly, greater than the differences attributed to strain rate across all specimens [10]. This highlights the heterogeneity of skin, as discussed in Section 2.2.3. Pissarenko et al then performed tests at variable strain rates on the same specimen to mitigate the effects of the heterogeneity of skin and it was found that strain rate did have a significant effect on the failure stress and the linear region modulus [10].

2.3 Mechanical testing of skin

There are several different methods for testing the mechanical properties of skin, they can be split into two broad categories, in vivo and in vitro testing. In vivo meaning the specimen is in its natural environment (on the body) and in vitro meaning it has been removed from its natural environment before testing.

2.3.1 In vivo

Some widely used in vivo techniques for testing skin are: indentation, suction, torsion and tensile testing. These techniques are non-invasive and therefore quite commonly

used. Results vary widely depending on the type of testing used, the age of the subject, the location of the testing area and the applied strain rate.

Indentation tests are done by applying a small load to the skin in a direction normal to the surface. The displacement of the indentation is typically very small. The deformation is then recorded and the stress-strain response can be analysed. There are difficulties in separating the response of the skin and that of the connected subcutaneous tissue. Pailler-Mattei et al [21] performed indentation tests on the forearms of their subjects as shown in Figure 2.7. Pailler-Mattei et al concluded that it is necessary to take into account the subcutaneous layers' effects in order to accurately estimate the modulus of skin. It must also be noted that the thickness of the skin could not be accurately measured and therefore literature was used to make an assumption on the thickness of the combined dermis and hypodermis layers [21].

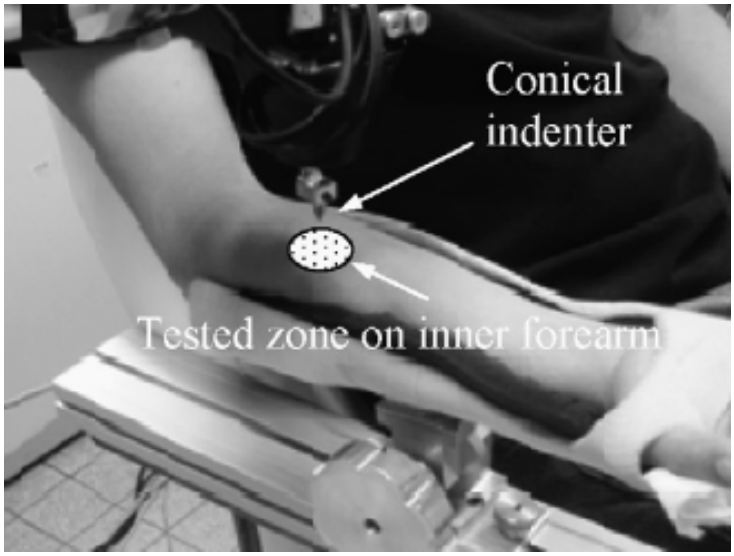

Figure 2.7 Pailler-Mattei et al in vivo indentation test setup [21]

Torsional tests typically provide a constant torque to the skin of a patient and then measure the resultant rotation, where the axis of rotation is perpendicular to the skin. A reported benefit of this method of testing is the ability to mitigate the anisotropic behaviour of skin [14]. The test is repeatable and easily done and therefore relatively popular. Agache et al [18] performed torsional tests on patients' forearms to investigate the effects of ageing on the response of skin as discussed in Section 2.2.3. Agache et al claimed that torsional testing minimised the effects of the underlying tissue connected to the dermis [18].

A suction test is performed by applying a known underpressure, relative to the skin, through an aperture to the skin's surface [22]. The applied suction results in deformation which can then be recorded. The benefits of performing a suction test are that the boundary conditions are more clearly defined than other in vivo techniques and the method can

easily be combined with an imaging technique to measure the deformation. Additionally, the skin is loaded both parallel and perpendicular to the skin surface [22]. Hendricks et al [22] performed suction tests on ten subjects' forearms and successfully characterised the response. Hendricks et al also found that the effect of the fatty subcutaneous layer was negligible for an aperture size of 6 mm [22].

In vivo testing has the benefit of being able to test live healthy tissue in its natural state. Both the microstructural make up of skin and the boundary conditions of any in vivo testing are by definition closer to those of skin undergoing regular deformations. On the other hand it is difficult to determine what response is due to the skin and what is due to connective tissue linking the skin to adjacent muscle or fat. Evans and Holt [12] noted that the pre-stress of skin in its natural loading state cannot be measured in vivo, making it difficult to characterise. Additionally, the boundary conditions of the skin cannot be completely controlled as they can when performing in-vitro testing [12].

2.3.2 In vitro

When performing in vitro testing there is no interference from other connective tissue, therefore the boundary conditions of the specimens are easier to control and the effects of unmeasured pre-stress are mitigated. This means a simple stress-strain relationship is more easily obtained but it must be noted that pre-stress while clamping specimens can be difficult to avoid [14]. A much wider variety of soft tissues can be tested using in vitro testing such as tendons, arteries and heart valves which are very difficult to test in vivo. There are also unwanted confounding factors when performing in vitro testing which have to be taken into consideration; such as the effects of specimen dehydration, specimen degradation and specimen sensitivity to the environment all of which affect the response of skin during in vitro testing [12]. The structural integrity of the specimen may be compromised, either during excision from the host, or during clamping for in vitro testing [14].

Common in vitro techniques include uniaxial, biaxial, multi-axial, bulge, shear and torsional testing. Unlike in vivo tests, the specimens are not in their natural loading state: specimens need to be extracted from the host, possibly stored, then clamped or mounted for testing. How a specimen is extracted, stored, clamped and tested can have a significant effect on the results [23].

In vitro uniaxial tensile tests are used extensively for testing soft tissue: Shergold et al tested pig skin and silicon rubber at differing strain rates [20], Ottenio et al tested human skin at varying strain rates and orientations [16], Ni Annaidh et al tested human skin with regards to its orientation [3] and Kumaraswamy et al studied the response of human female breast skin [24]. Although a significant amount of useful data has been obtained using uniaxial tensile testing, one cannot fully characterize skin with only uniaxial testing

data due to the anisotropic properties of skin. Therefore additional testing is required to fully characterize skin [13]. Furthermore, skin is very rarely loaded in a uniaxial manner in its natural state [12].

Bulge testing allows for the skin to be tested in a state that is closer to in vivo loading than most other in vitro methods, as it constrained along the outer boundary of the specimen. Bulge testing involves applying pressure to a specimen and essentially inflating or deforming the specimen into a hemisphere. Measuring the deformation requires a non-contact measurement technique, such as DIC, due to the flexibility of the specimen. The directionality of the collagen fibres can be found experimentally while doing bulge testing by identifying the direction in which the response is stiffest. Bulge testing with circular clamps does not require prior knowledge of the direction of the fibres in the skin, unlike uniaxial or biaxial tensile testing, which are sensitive to specimen orientation. Tonge et al [25] conducted bulge tests on human skin, finding that preconditioning of the skin or environmental humidity had little effect on the results. However, Tonge et al did note that isolating the effects of bending stress from the assumed membrane stress state of a bulge test was not trivial [25]. Tonge et al's testing setup is shown in 2.8.

Figure 2.8 Tonge et al's bulge testing machine [25]

Previous research into testing the mechanical properties of skin at BISRU was heavily focused on bulge testing machines. Grahame [26], A. Curry [6] and D. Fischer [7] designed, built and tested three separate bulge testing machines for testing skin and other

collagenous soft tissues. Three machines were designed to enable testing at different strain rates; ranging from the quasi-static bulge testing machine designed by A. Curry[6] to the high strain-rate bulge testing machine designed by A. Grahame[26].

2.4 Planar biaxial tensile testing

2.4.1 History

In the 1940s Treloar developed a technique in which two independent strains could be applied in perpendicular directions on a specimen while the resulting stresses in these same directions were recorded [27]. In 1951 Rivlin developed a planar biaxial technique for testing rubbers. Rivlin and Saunders also developed a method in which the constitutive form of the material could be derived directly from the experimental data [28]. These initial works focused on rubber, an incompressible and isotropic elastic material; later research would incorporate these techniques in the testing of biological materials.

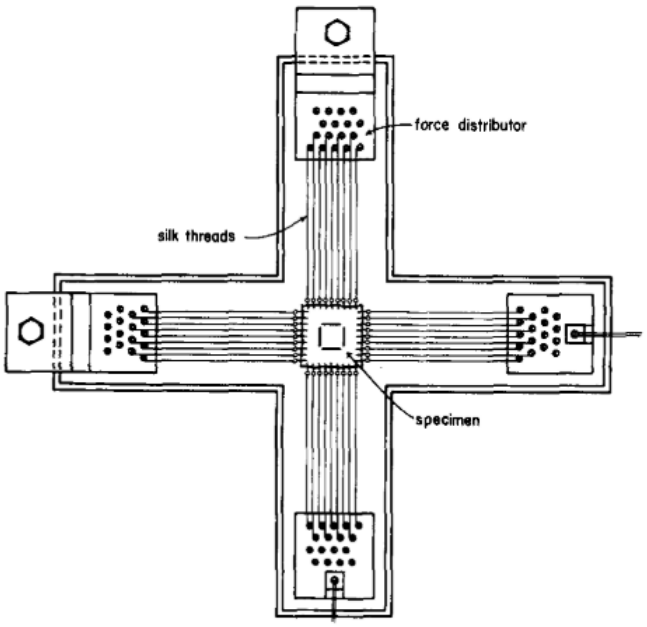

Figure 2.9 Lanir and Fung's setup for testing rabbit skin in 1974 [29]

Lanir and Fung [29] performed planar biaxial tensile testing on soft tissue in 1974. Figure 2.9 shows Lanir and Fung's custom built rig which used up to 17 silk strings attached to staples along each edge of a square specimen of rabbit skin to test its mechanical response under loading. A Video Dimension Analyser (VDA) system was used to continuously record the displacement between two parallel lines on the specimen in order to record the deformation. Lanir and Fung compared their biaxial tensile testing results to uniaxial results and found that stresses were higher for the same stretch value

under biaxial testing than those recorded during uniaxial testing. This helped to justify the need for biaxial testing to properly analyse the response of soft tissues such as skin [29].

2.4.2 Biaxial method

As the name suggests; the planar biaxial tensile testing method is used to apply tensile loads on two perpendicular axes in the same plane to a membrane specimen. Figure 2.10 shows a basic setup of a planar biaxial tensile testing machine. Such tests are necessary because the response of skin under multi-axial loading cannot be predicted or properly understood using uniaxial tests even if multi-axial strain data is recorded [4]. Biaxial testing data and the machines needed to carry out the tests are more complicated than uniaxial ones.

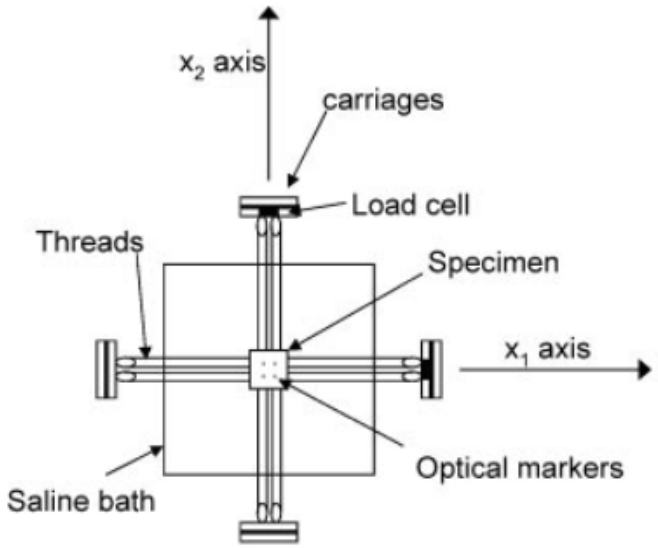

Figure 2.10 Basic setup of a planar biaxial tensile test as depicted by Sacks and Sun [30]

Biaxial testing devices need to control additional boundary conditions and analyse more complex deformations than is typically done during uniaxial testing. Devices need to allow specimens to expand in the lateral direction of each of the two testing axes. Additionally, the unwanted effects due to the various types of grips on the usually small specimens need to be mitigated [30]. The target region is typically far from the specimen edges for this reason, as well as to ensure that uniform stress and strain states are created at the target region for simplified data analysis [30]. Due to the often complex and sensitive response of specimens under biaxial loading (especially for anisotropic specimens) optical means of strain measurement are used, which ensures there is no interference with the specimen when measuring the strain. Unlike uniaxial testing, biaxial tensile testing

typically stops short of rupture. Considering the previously discussed sensitivity of excised skin to environmental conditions, tests are often performed in a saline solution heated to temperatures similar to that which skin would experience in vivo.

2.4.3 Existing planar biaxial testing machines

Several planar biaxial tensile testing machines for testing skin and other soft tissues already exist, some being custom built in research laboratories and others being commercially manufactured. These machines can be grouped as either stand-alone machines or mechanisms which are added to existing uniaxial tensile testing machines.

Examples of commercially manufactured, stand-alone planar biaxial tensile testers for soft tissues are the Zwick-Roell biaxial testing machine, the Test Resources 574 Series planar biaxial testing machine (Figure 2.11) and the CellScale Biotester (Figure 2.12).

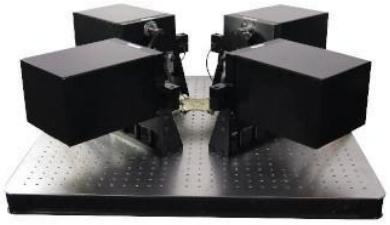

Figure 2.11 Test Resources 574 Series [31]

Figure 2.12 CellScale Biotester [5]

All the above mentioned machines use four separate linear actuators to form an X shape device with the specimen loaded at the centre of the X with the two axes of the device perpendicular to each other. Force measurements are recorded using load cells and the strain is measured using optical measurement techniques. It is also common practice in literature to perform tests in a saline solution to keep the skin or other soft tissues hydrated and at a constant temperature during testing. As a result, many of the commercially available machines include heated baths so that the specimen can be submerged in a heated saline solution during testing.

Uniaxial tensile testing machines may be modified with linkage mechanisms, to allow the application of biaxial tension to a specimen. Such mechanisms have been used extensively in planar biaxial testing of sheet metals [32][33] but are not as popular when testing soft tissues.

Link mechanisms allow for tests to be carried out using equipment which is already readily available in most materials science laboratories. Due to the use of physical links, the range of strain rates which are tested is reduced. Both axes are powered by the same compression or extension motion of the tensile tester; therefore differences in rates between axes are determined by the physical links themselves. This is limiting as physical adjustment is required to adjust rates, which is further complicated by the fact that the relationship between the rates of the testing axes and the rate of the uniaxial machine's compression/extension is not necessarily linear as in Figure 2.13. Additionally, the links can obscure the view of non-contact displacement measurement systems such as DIC. Alternatively, an additional actuator which is orthogonal to the existing actuator can be added to a uniaxial tensile testing machine.

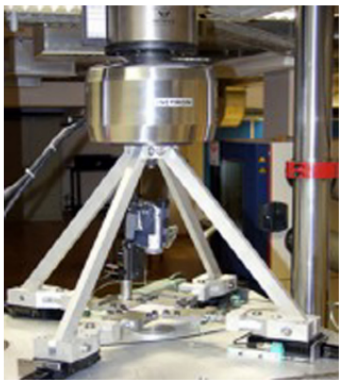

Figure 2.13 Horizontal bed link attachment mechanism [32]

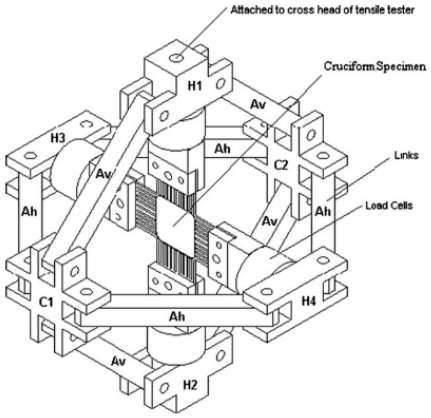

Figure 2.14 Vertical link attachment mechanism [33]

2.4.4 Planar biaxial testing studies

There have been several studies on biological soft tissues using planar biaxial tensile testing in literature. Table 2.3 summarises a sample of published studies using planar biaxial tensile testing of soft tissue, without being an exhaustive list. As can be seen in Table 2.3 a wide variety of materials were tested, including human ventricular myocardium [34], bat wing skin [35] and porcine gastric tissue [36].

Author, year	**Title**	**Material tested**	**Device used**
Lanir and Fung, 1974 [15] [37]	Two-dimensional mechanical properties of rabbit skin I and II	Rabbit skin	Custom built stand-alone device
MS Sacks and CJ Chuang, 1998 [38]	Orthotropic mechanical properties of chemically treated bovine pericardium	Glutaraldehyde-treated bovine pericardium	Custom built stand-alone device
MS Sacks and W Sun, 2003 [30]	Multiaxial mechanical behavior of biological materials	Non-treated and glutaraldehyde-treated bovine pericardium	Custom built stand-alone device
Bellini et al, 2011 [39]	Biaxial mechanical modeling of the small intestine	Porcine intestine (duodenum, jejunum and ileum)	Custom built stand-alone device
O'Connell et al, 2012 [40]	Human annulus fibrosus material properties from biaxial testing and constitutive modeling are altered with degeneration	Human annulus fibrosus	Custom built stand-alone device
Szczesny et al, 2012 [41]	Biaxial tensile testing and constitutive modeling of human supraspinatus tendon	Human supraspinatus tendon	Custom built stand-alone device
Perez et al, 2014 [42]	Biaxial mechanical testing of posterior sclera using high-resolution ultrasound speckle tracking for strain measurements	Posterior porcine sclera	ElectroForce planar biaxial TestBench

Sommer et al, 2015 [34]	Biomechanical properties and microstructure of human ventricular myocardium	Human ventricular myocardium	Stand-alone device
Skulborstad et al, 2015 [35]	Biaxial mechanical characterization of bat wing skin	Bat wing skin	Custom built stand-alone device
Deplano et al, 2016 [43]	Biaxial tensile tests of the porcine ascending aorta	Porcine ascending aorta	Custom built stand-alone device
Aydin et al, 2017 [36]	Experimental characterization of the biaxial mechanical properties of porcine gastric tissue	Porcine gastric tissue	MediX0.1, Messphysik Materials Testing
Huang and Lu, 2018 [44]	Biaxial mechanical behavior of bovine saphenous venous valve leaflets	Bovine saphenous venous valve	Biotester 5000, CellScale
Jett et al, 2018 [45]	An investigation of the anisotropic mechanical properties and anatomical structure of porcine atrioventricular heart valves	Porcine atrioventricular heart valves	Biotester, CellScale

Table 2.3 *Summary of planar biaxial tensile tests from literature*

Some of the articles from Table 2.3 were used to determine the loads encountered during planar biaxial tensile testing of various soft tissues. This data is summarised in Figure 2.15. As can be seen the loads vary with a maximum of 16 N shown in Szczesny et al's investigation into the mechanical properties of human supraspinatos tendon [41].

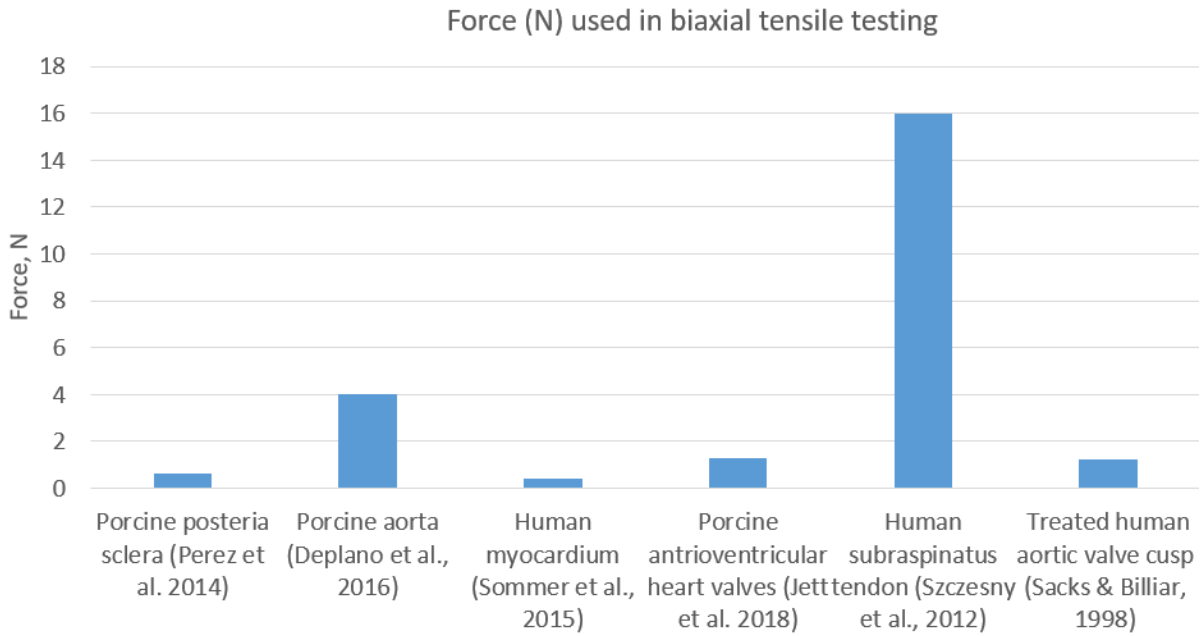

Figure 2.15 Forces recorded in literature [42] [43] [34] [45] [41] [38]

Multi-axial tensile testing can be done as an extension of the biaxial testing method. Jor et al [11] tried to mitigate the unwanted effects found in bulge testing and uniaxial testing by performing multi-axial tensile tests. Circular porcine skin specimens were used and loaded by 12 automated motor axes with the deformation recorded using optical measurement techniques. With 12 axes, Jor et al found that the response of the specimens showed a high sensitivity to fibre orientation and that knowledge of fibre orientation before testing was a priority [11].

2.4.5 Difficulties in planar biaxial testing

Sacks and Sun [30] list some common difficulties encountered when performing planar biaxial testing: "Just a few of the experimental problems include small specimen sizes, structural and compositional heterogeneity, difficulty in gripping (without doing damage), dramatic effects of different gripping techniques (St. Venant–like effects), difficulty in precisely identifying material axes, difficulty in assuring constant forces along specimen edges, large specimen-to-specimen variability, and time-dependent changes due to biological degradation. In addition, a question of homogeneity of deformation within the specimen is paramount"[30]. As pointed out by Sacks and Sun there are several obstacles to overcome when biaxially testing skin and other collagenous soft tissues.

Boundary conditions, specimen preparation, testing environment, and the extreme variability between samples due to the age, location, orientation and condition of specimens can all have a significant effect on the results. As stated in Section 2.2.3, the heterogeneity of skin even between specimens from the same subject can produce large variations in results. Therefore researchers need to be mindful of inter-specimen variability and take due care when sourcing specimens. Ottenia et al [16] list accidentally applying a preload to the specimen, varying thickness across a specimen and specimens being difficult and cumbersome to grip, as some of the difficulties encountered when dealing with biological membrane specimens.

How to grip the specimens in a repeatable manner without applying a large unknown pre-load is not a trivial matter. The proper alignment of the preferred orientation of the specimen with that of the testing axes is also essential in order to properly understand the response of the specimen [46].

2.4.6 Specimen boundary conditions

As mentioned in Subsection 2.4.5 one major source of difficulty reported when performing planar biaxial tensile tests is that of gripping the specimens. Additionally, a key requirement is that the region of interest reaches a state of uniform stress and strain [30], which can be difficult to achieve due to St. Venant effects, unknown in-plane shear stresses and unknown contra-lateral forces. Contra lateral forces are a result of the specimen boundary being fixed in the direction perpendicular to the testing axis. This results in resistance to the deformation in the lateral direction which can negatively effect the results especially if the grips are close to the target region [4]. Saint Venant's principal states that local stresses due to gripping of the specimen becomes negligible at some distance from the boundary [23], therefore it is beneficial to have the target region at a set distance from the boundary of a specimen.

It has been found that the shape of the specimen and how it is constrained by the grips greatly affects the experimental results [23]. In Figure 2.16 the most common specimen profiles and gripping methods are shown. When performing planar biaxial tensile testing on elastomers, sheet metal and other non-organic materials, cruciform specimens are typically used. When testing biological tissue the specimen material is often more difficult to acquire or naturally small in size. The cruciform specimen is not an efficient use of material, hence most experiments are done using square specimens to reduce material waste [47].

The three most commonly used gripping mechanisms are: sutures (or tethers), rigid clamps and rakes [47]. When using clamps no lateral deformation is permitted and the magnitude of the axial displacement is equal across the length of each clamped boundary [47]. Sutures can be considered as a series of point loads along each boundary. As

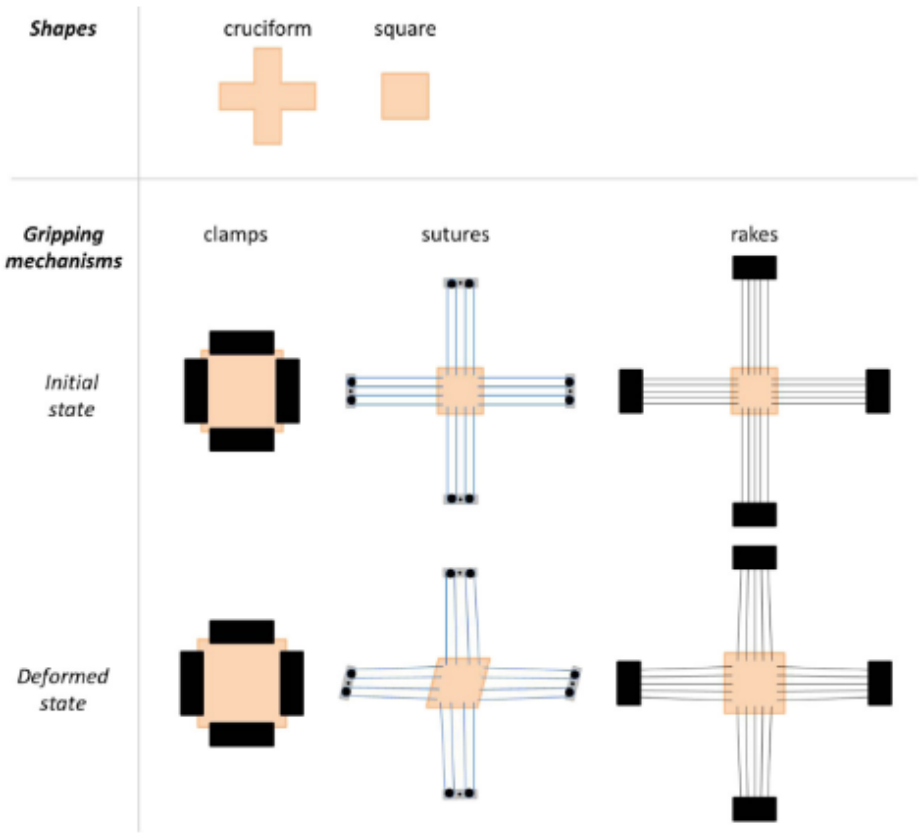

Figure 2.16 Different specimen types and gripping methods commonly used in planar biaxial testing [47]

the points are connected to pulleys via individual tethers, they do not necessarily result in equal displacements in the direction of loading and allow for motion in the lateral direction, therefore they do not create unwanted contra-lateral forces. They also allow for some rotation of the specimen. However, the pulleys and hinges ensure that forces are evenly distributed amongst the tethers. Rakes, like sutures, create point loads. Unlike sutures, rakes have bending rigidity and therefore do not allow completely free lateral motion. They also do not allow for differing axial displacements to the same extent as sutures due to the absence of pulleys nor do they allow for any rotation of the specimen.

All three of the above gripping techniques have some unwanted effects. Clamped grips result in unwanted and unmeasured contra-lateral forces along the gripped edges. Waldman and Lee compared the results of biaxially tensile tested bovine pericardia using sutured and clamped specimens and found that clamps result in a significantly higher recorded stiffness of the specimen [23]. This can be mitigated by using cruciform specimens if enough material is available [48].

Sutures have more localised loading than clamps. Sutures also suffer with repeatability, as they have to be connected individually - requiring very dexterous and skilled

testing personnel. Unlike clamps, sutures do not create unwanted contra-lateral forces as they allow for lateral motion along the boundary as well as in-plane rotation of the specimen. This means that in-plane shear loading can be induced and the effects of in-plane shear studied. In-plane shear is induced by rotating the specimen so that the specimen's preferred fibre directions are at 45° to the testing axes [49]. The specimen edges also need to be able to rotate freely in plane and a non-uniform system of forces can be applied [49]. Sun et al [48] found that the boundary effects were less significant when using sutures compared to when using clamps and concluded that sutures appeared best suited for biaxial tensile testing of soft tissues.

Rakes also result in localised loading but are more uniform than sutures due to better repeatability when connecting the rakes to the specimens [47]. Rakes also create small unmeasured contra-lateral forces as they allow restricted lateral motion. They do not allow rotation of the specimen and therefore in-plane shear cannot be induced. Rakes are therefore only advantageous to use when the material axes are known and there is no specific shear term in the material model [47].

2.4.7 Biaxial testing standards

There is currently no standard for the planar biaxial tensile testing of soft tissues. BSI ISO 16842:2014 [50] details the method and standards for testing cruciform specimen planar sheet metal with a biaxial tensile tester. Although some of the information and requirements listed in the standard are useful, much of the difficulties of testing soft tissue specimens are not addressed.

The specimen dimensions and designs listed in BSI ISO 16842:2014 [50] are not feasible for testing skin and other soft tissues, with the width of the cruciform arm needing to be greater than 30mm and the minimum overall length of the cruciform specimen being 120mm. Such specimens are much larger than typical biological membrane specimens. Additionally the standard specifies strain gauges be mounted onto the specimen for strain measurement, it also states where and how they should be mounted. Once again, this is not feasible for testing skin and other soft tissues as the in-plane stiffness of the strain gauge would be higher than that of many membrane soft tissues and would therefore skew the measured stiffness.

2.4.8 Constitutive modelling of skin

In 1974, Lanir and Fung [29] claimed that as skin can be considered an incompressible material, a full three-dimensional test is not necessary as a two-dimensional test could be be used to derive a three-dimensional model of the skin [29]. Sacks and Sun make the same claim in 2003 about biological tissues [30]. Holzapfel and Ogden countered these claims

in 2009 when they noted that this was only true when the material is an incompressible isotropic material and that a planar biaxial tensile test was not sufficient when creating a three-dimensional model for an anisotropic material [13]. Holzapfel and Ogden then go on to state that to fully characterize a transversely isotropic material both a planar biaxial tensile test which includes in-plane shear and an additional through thickness shear test are necessary [13].

To characterise the mechanical response of skin one has to mathematically define the material and populate model variables which approximate the experimental response of the skin. In literature skin is generally accepted to behave as a hyperelastic material. In continuum mechanics this means that it is a nonlinear elastic material whose stress strain response derives from its strain energy function (ψ) and whose deformation is described by its deformation gradient **F**. In planar biaxial tensile testing this deformation gradient **F** is obtained experimentally through optical measurement of the surface deformation of the specimen.

There are several examples in literature of investigations which characterised soft biological tissues using planar biaxial tensile testing. O'Connell et al [40] characterised human annulus ficrosis using biaxial testing data, Skulborstad et al [35] characterised bat wing skin using a custom built planar biaxial tensile testing machine, and Aydin et al [36] characterised porcine gastric tissue using a commercial planar biaxial tensile testing machine.

2.5 Digital Image Correlation (DIC)

2.5.1 Theory

Digital Image Correlation (DIC) is a contactless optical measurement technique first developed at the University of South Carolina in the 1980s [51]. It has since undergone much improvement and is widely used in experimental mechanics. DIC tracks the deformation of the specimen surface in sets of images. Unlike grid methods, which track displacement of discrete points, DIC can achieve a much finer spatial resolution and therefore more accurate measure of deformation.

Each image is split into several much smaller regions called facets, which are identified and tracked relative to both the image's preceding and succeeding images. The motion and deformation of each facet can then be calculated. In order to identify each facet correctly the specimen surface needs to have a random pattern which deforms along with the specimen (Figure 2.17) [52]. This random pattern is typically called the speckle pattern, which can either be the natural surface of the specimen or added to the surface of the specimen.

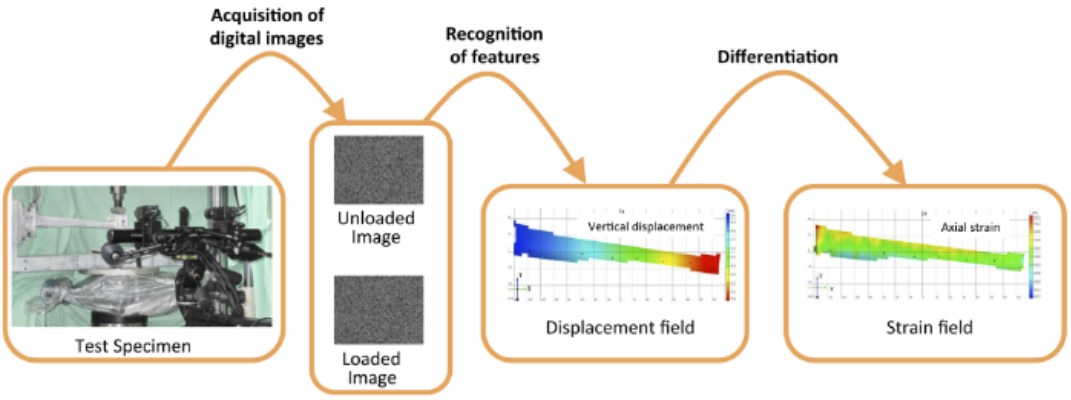

Figure 2.17 DIC workflow needed in order to get strain measurements of a specimen [52]

DIC can be done in 2D or 3D. For 2D DIC a single camera perpendicular to the surface is used, which assumes planar deformation. For 3D deformation, it is necessary to use two or more cameras, whose axes are not parallel. It is essential to calibrate the system using a target of known dimensions to establish the precise relative positions and orientations of the cameras to the region of interest. The calibration target also facilitates correcting for lens distortion effects. The accuracy and precision of DIC is highly dependent on the quality of the images, quality of speckle pattern, accuracy of the calibration and the parameters of the numerical processing [52].

2.5.2 Specimen marking

In most cases when testing biological specimens the natural texture of the specimen's surface does not provide an adequate random pattern for DIC. Specimens are usually marked with a speckle pattern prior to testing. The quality of this speckle pattern influences the accuracy of the displacements and strains measured [52].

Palanca et al [52] list some of the requirements that a good speckle pattern should have. Firstly the pattern must be random, to ensure that the DIC software can easily track the deformation and translation of the individual facets. The contrast between the background and the speckle should be high in order to more easily differentiate the speckle from the background. The speckle should be sized appropriately for the specimen size. Palanca et al note that when using a 5 Megapixel (2448 x 2050 pixel) camera for a region of interest of 2 m x 2 m the optimum speckle size is around 3.25 mm [52].

There are two main techniques used to create speckle patterns on biological specimens. The first is to use an airbrush to create a speckle on the surface of the specimen (Figure 2.18) and the second technique, is to use a toner or graphite powder on the surface of the specimen (Figure 2.18). Barranger et al [53] reported that graphite did not work as well

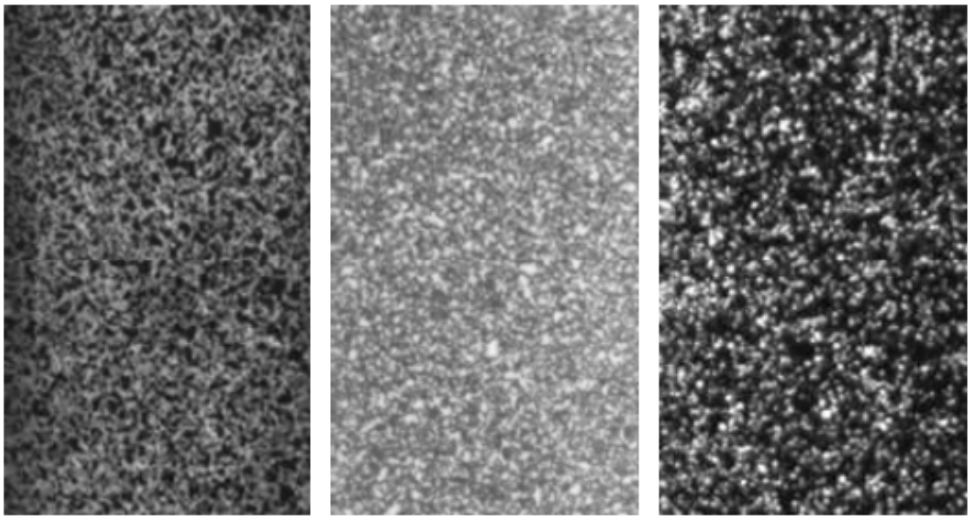

Figure 2.18 Three different types of speckle pattern; black paint (left), white paint (centre) and black powder (right) [53]

for large strains because, unlike airbrushed paint, the graphite did not deform with the specimen but was displaced. In both cases a background paint or dye is used to provide contrast between the speckle and the specimen. The effects of layering paint or dyeing the specimen must be carefully considered as they may adversely affect the results of the experiment [53].

Chapter 3

Design of Biaxial Tensile Testing Machine

The focus of this MSc project is the design, manufacture and verification of a planar biaxial tensile testing machine, suitable for soft biological tissue specimens. It is not necessary for the machine described in this paper to be patentable or novel. Existing methods and experiments were critically analysed in literature (Sections 2.3 and 2.4) to gain an understanding of the difficulties which may be unique to testing biological soft tissue as well as to determine the user needs of the machine.

Once the requirements and specifications were determined, concepts were generated and chosen. The biaxial machine would have the same means of actuation along both axes. It was therefore decided to initially build a single axis and ensure the concept worked as expected before making a fully operational biaxial machine. This would make it possible to test the design against an existing tensile testing machine before adding the second axis, making it easier to implement any design revisions. The comparison to the existing uniaxial tensile testing machine along with other physical testing would serve as a verification of the design.

3.1 Overview of final design

Figure 3.1 shows an image of a 3D CAD model of the final design of the planar biaxial tensile testing machine, with the saline bath and electronics omitted for clarity. The machine was modelled on SolidWorks and drawings of the sub-components which were machined at the UCT Mechanical Engineering Workshop are shown in Appendix A.

Figure 3.2 shows an image of the machine in use during planar biaxial testing as a part of this investigation.

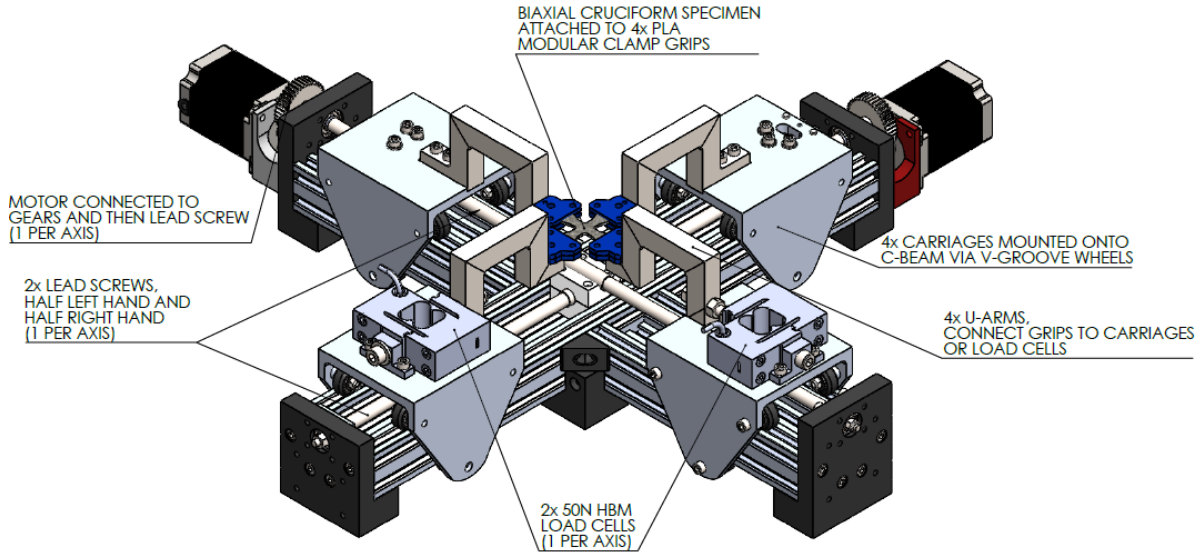

Figure 3.1 Final assembly of biaxial tensile testing machine

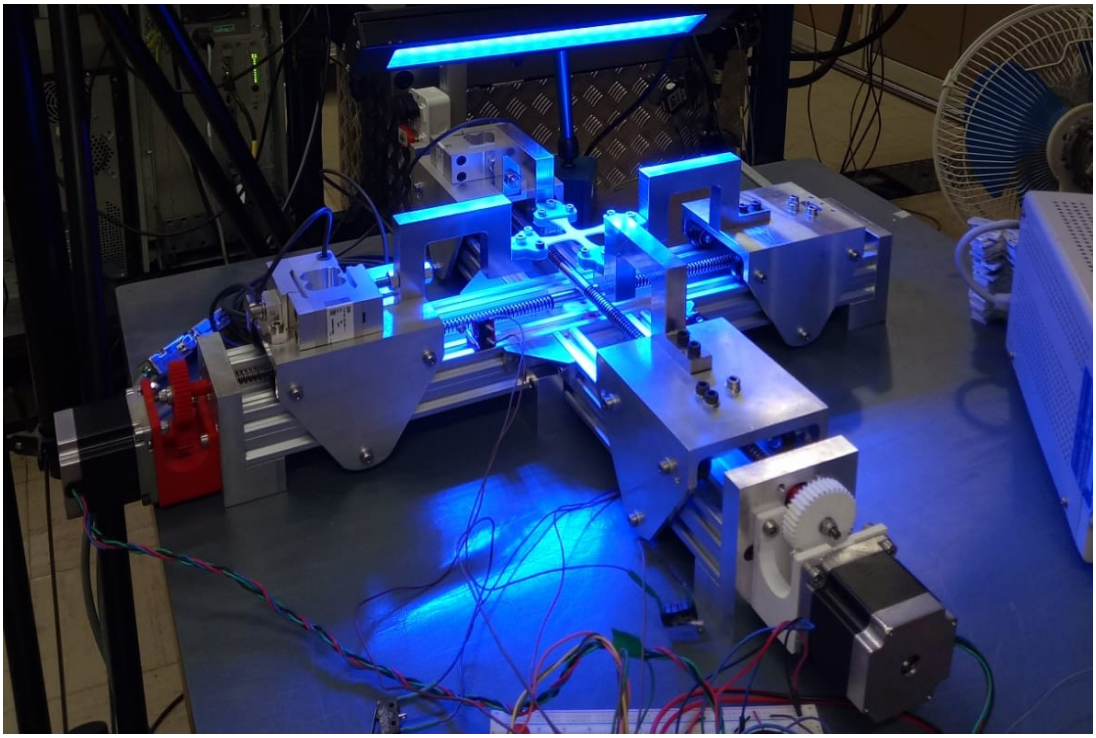

Figure 3.2 Photo of the final planar biaxial tensile testing machine in use

3.2 User needs and design inputs

Before any design work could begin the user needs and design inputs had to be determined. This was done by extensively analysing literature on physical testing of skin and examining existing planar biaxial and uniaxial tensile testing machines.

3.2.1 User Needs

First, broader user needs were determined, then more specific design inputs were determined in order to quantify and meet all the user needs, these inputs are detailed in Section 3.2.2. The design inputs were used to create the design outputs which were recorded to ensure all design inputs were addressed. Furthermore, verification of design inputs was done to ensure that all design outputs were functioning as designed and therefore fulfilling the design inputs. The user needs determined for the machine are listed below;

Number	**User Need**
UN 1	**Planar biological specimens:** Can test skin and other planar collagenous soft tissues
UN 2	**Strain rate:** To be used at variable low strain rates
UN 3	**Biaxial loading:** Capable of biaxial tensile loading, with different tensions on each axis
UN 4	**Force data:** Measure and record force data along the axes of deformation
UN 5	**Deformation data:** Measure and record deformation data of specimen surface
UN 6	**Safe to use:** Machine does not pose safety risk to users or observers
UN 7	**Easy to use:** Machine is easy to use
UN 8	**Portable:** Machine can be moved to various work-spaces by the user

UN 9	**Reliable:** Produces repeatable and consistent data
UN 10	**Manufacturable:** Device sub-components and key sub-systems are manufacturable at the UCT Mechanical Engineering Workshop and/or commercially available

Table 3.1 *User Needs*

3.2.2 Design inputs and design control matrix

Design inputs were then formed to address the user needs. Table 3.2 lists the Design Inputs, with these addressed in subsequent sections. As far as possible all design inputs are to be verified through testing of the manufactured machine.

Number	Design Input	Linked User Needs
DI 1	**Grips:** Can grip soft tissue surrogate material without slipping during testing. Grips providing different boundary conditions can be mounted onto the device.	UN 1
DI 2	**Specimen shape:** Machine to be designed to test specimens across 2 perpendicular, independent axes, with specimens anticipated as being both square and cruciform in geometry	UN 1 and UN 3
DI 3	**Specimen size:** Specimen's size and therefore machine size to be appropriate for human biological specimens; region of interest (ROI) between 6x6 and 20x20 mm.	UN 1
DI 4	**Saline Bath:** Make provisions for a saline bath for testing tissue in temperature controlled environment	UN 1

DI 5	**Sanitary:** Device can be cleaned easily	UN 1 and UN 6
DI 6	**Forces:** Machine capable of loading specimens and recording data at expected loading range of soft tissue specimens up to 50 N.	UN 1, UN 4 and UN 9
DI 7	**Force resolution:** Force data is digitally recorded to a resolution of 0.01N or better	UN 4 and UN 9
DI 8	**Cross-head/carriage speeds:** Cross-head speeds between 10 and 400 mm/min	UN 2
DI 9	**Biaxial:** All loads and rates of actuation can be applied simultaneously and independently to the two separate axes.	UN 3 and UN 9
DI 10	**Maximum deformation length:** Machine to be able to provide a minimum of 30mm of continuous deformation to the specimen per axis	UN 3
DI 11	**Deformation measurements:** Deformation is to be measured using a non-contact, image based system such as DIC.	UN 5 and UN 9
DI 12	**Device is DIC compatible:** Machine allows for DIC cameras to record test; no mechanical components in way of cameras and specimen ROI to be stationary for ease of deformation measurement. Load measurements interface with existing Dantec DIC system for synchronized load and deformation data.	UN 5

DI 13	**Instructions for use:** Instructions for use created with clear and concise instructions for user.	UN 6 and UN 7
DI 14	**Emergency shut down button:** Physical emergency stop button, that is easily accessible, which stops all machine movement.	UN 6
DI 15	**Machine motion limits:** Motion of carriages are limited by physical limit switches. Machine stops if limits are reached.	UN 6
DI 16	**Load limits:** Limits on maximum loads can be set by user. Machine stops if limit is reached	UN 6
DI 17	**Machine mass:** Weighs no more than 20kg	UN 8
DI 18	**Overall Dimensions:** Overall dimensions of machine are smaller than 600x600x300 mm (length x width x height)	UN 8
DI 19	**Machinability:** All sub-components which are intended to be manufactured can be machined at the UCT mechanical engineering workshop	UN 10
DI 20	**Bought parts:** All sub-components which are intended to be bought as standard items are readily available to users in South Africa	UN 10
DI 21	**Single user:** Can be operated by a single user given the appropriate training	UN 7

Table 3.2 *Design inputs*

A review of planar biaxial tensile testing data was conducted from literature (Figure 2.15) to obtain the expected forces needed to adequately deform the specimen, and it was concluded that 50 N would be suitable. This would give the user more flexibility with regards to the materials and sample sizes which could be tested on the machine, while still providing suitable resolution of the expected loads, documented Figure 2.15.

3.3 System design

3.3.1 Stand-alone versus adjustment mechanism

As previously discussed in Section 2.4.3 there are two broad types of existing planar biaxial tensile testing machines: stand-alone machines and link adjustment mechanisms. Although both options were considered it was decided to design a stand-alone machine. The link-adjustment mechanism was inferior to the stand-alone machine when it came to several requirements. The ratio of the displacement rates in the two axes is determined by the linkage lengths. Hence the user would have to physically change linkages, if different rates are desired. Additionally, the portability of a link-adjustment mechanism is limited to the location of an existing tensile testing machine. A stand-alone machine of the appropriate size could be moved to different clinical environments to facilitate testing of fresh specimens. The physical links are likely to obstruct the view of the specimen region of interest, which is an obstacle for optical measurement of specimen deformation. While a link adjustment mechanism would be inexpensive and have good repeatability, these factors did not outweigh the prior negatives, therefore only stand-alone machines were considered further.

3.3.2 System

The machine was broken down into basic subsystems for ease of design. As discussed previously the machine was to be designed and constructed as two uniaxial tensile testing machines, which are assembled together. A breakdown of the sub-systems for the planar biaxial tensile testing machine is shown in Figure 3.3.

3.3.3 Motion constraint

The linear actuator determines the strain rates, displacements and forces for which a specimen can be tested at. It also determines the constraints and therefore the allowable motion of the machine. Typically, a uniaxial tensile testing machine will have one end of the specimen clamped in a stationary grip, with the other end mounted in a grip on a movable cross-head. This means the centre of the specimen moves relative to a stationary observer. If a biaxial tensile testing machine keeps two adjacent grips stationary, while

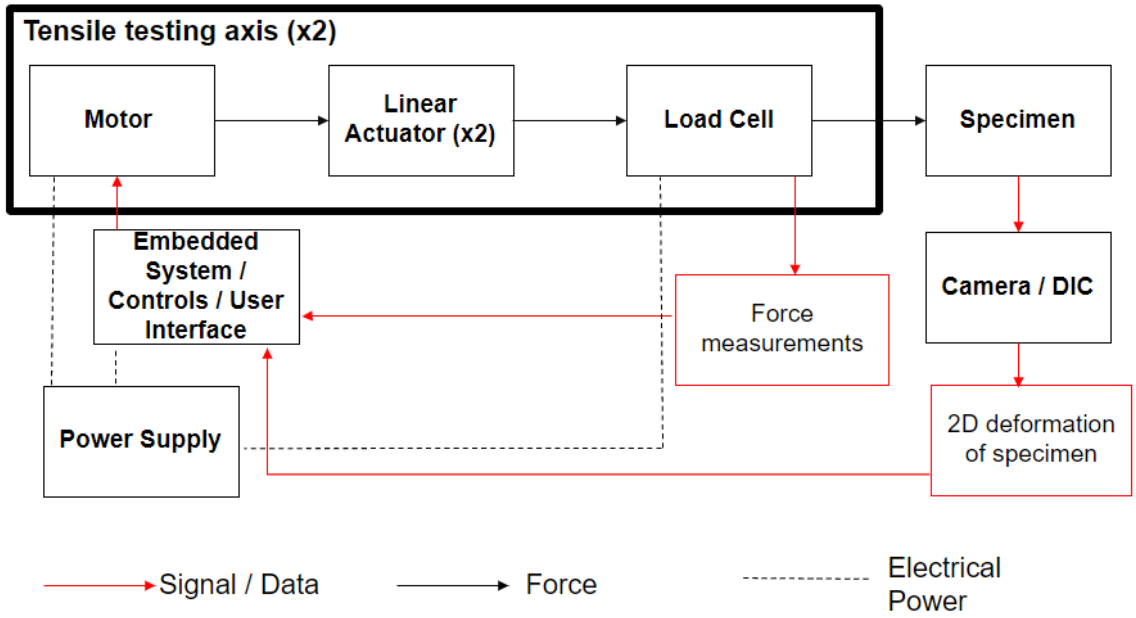

Figure 3.3 System design of custom built biaxial tensile testing machine

the opposite grips move, the specimen deforms in a non-symmetric manner, illustrated in Figure 3.4 (left). However, if both grips on an axis displace symmetrically as seen in Figure 3.4 (right), the specimen deformation is symmetric and more uniform in the region of interest. Furthermore, keeping the region of interest stationary is very desirable for image based deformation measurements as the position will remain stationary relative to a stationary observer or optical deformation measurement device.

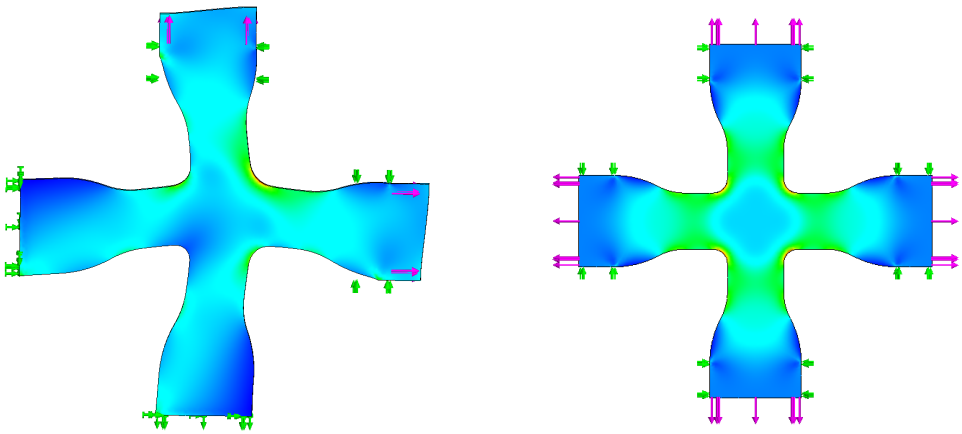

Figure 3.4 Left; deformation of specimen where one carriage of each axis is fixed. Right; deformation when both carriages of each axis move equally.[1]

In order for the specimen to remain centered, both cross-heads (carriages) of the same axis of the biaxial tensile testing machine need to undergo equal but opposite displacements and velocities along the axis as shown in Figure 3.4 (right). This means that the

[1]Image was made as part of this investigation using SolidWorks Simulation

designed machine requires four degrees of freedom as opposed to the single degree of freedom that a typical uniaxial tensile testing machine has. This adds significant complexity to the design when compared to a uniaxial tensile testing machine.

Furthermore, the motion of the carriages is to be constrained to only allow axial motion along each of the two planar deformation axes. All angular and radial degrees of freedom on all axes are to be fully constrained and axial motion on the 3rd axis (out of plane) is to be constrained as well.

3.3.4 Linear actuation

The machine was designed so that both carriages on a single axis are powered by the same source, and are mechanically coupled. Without mechanical coupling of the carriages, separate drives on the same axis would need closed loop control to avoid having different displacements or speeds on the same axis. Therefore, carriages on the same axis were mechanically coupled to mitigate any errors that may arise due to the carriages on a single axis not moving in unison.

Two carriages on the same axis are connected to a single lead screw which is connected to a stepper motor. Half of the lead screw has left-handed thread and the other half has right-handed thread, with the carriages connected to either half of the lead screw with the appropriate lead screw nut. This means that when the screw is rotated by the stepper motor the two carriages move an equal distance in opposite directions along the same axis as shown in Figure 3.5. Therefore the two carriages are physically constrained to move together. This ensures that the specimen remains centered on a given axis and that the displacement and velocities being applied to either end of the specimen are equal in magnitude but opposite in direction.

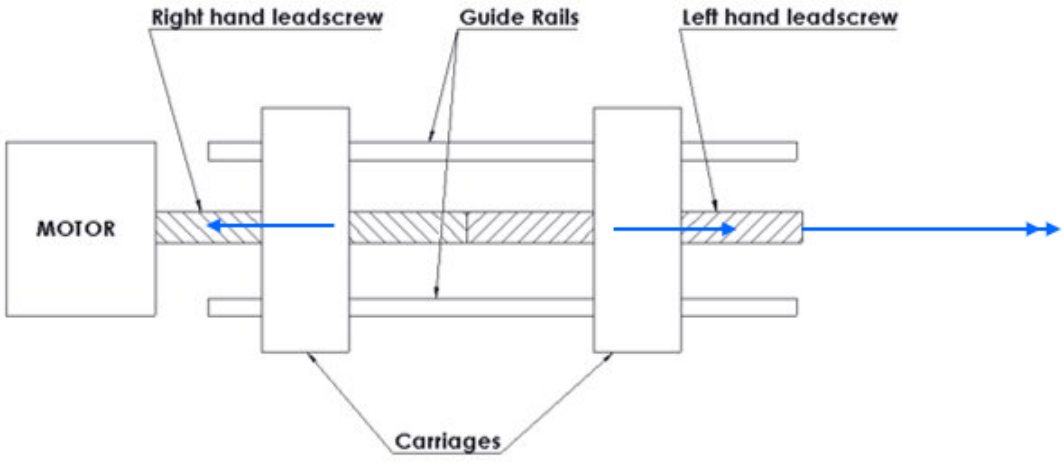

Figure 3.5 Linear actuation concept

A lead screw was selected as opposed to a ball screw as lead screws are more customisable, which is important for a proof of concept. Ball screws are typically commercially available in right hand thread. Sourcing a left hand ball screw was seen as prohibitively expensive. Other concepts such as belts and pulleys were considered. However, these are better suited for higher speed / low force applications. For the range of deformation rates desired, an electrically driven lead screw is the most commonly used system.

3.4 Subsystem design

3.4.1 Carriage and guide rail design

Various carriage and guide rail concepts were considered. Most of the concepts were based on one of two main methods of motion constraint. The first method of constraint was cylindrical guide rails connected to linear bearings which are mounted to the carriage. The second was V-slot aluminium extrusions and V-slot wheels mounted onto the carriage. Both of these forms of constraint can be applied in various configurations with differing amounts of bearings or wheels depending on the type of loading and motion anticipated. The various concepts were assessed using a concept selection matrix and the highest scoring concept was chosen for the design. The matrix is shown in Appendix B and shows the concepts' score tallies and has brief descriptions of the concepts themselves.

The concept which was chosen uses an aluminium V-slot C-beam extrusion as the guide rail, with each partially constrained carriage fitted to the C-Beam by six V-wheels that fit into the V-slots of the C-beam. These were chosen as they provide guide slots with a relatively fine tolerance for straightness as received from the factory, and can be assembled perpendicular using stock brackets - hence reducing machining costs. They are also lightweight and strong. Many 3D printers use similar V-slots to constrain the motion of the 3D printer extruder. Additionally, the guide system needs to be able to interface with the linear actuation system. On either end of the extrusion a fixed end-plate is fitted which houses the lead screw bearings, therefore, fully constraining the system.

Figures 3.6 and 3.7 show two different views of the final concept which uses V-wheels and the aluminium C-beam extrusion. It has six wheels, three on either side of the carriage with the bottom wheel on both sides being adjustable with an eccentric nut for ease of assembly. The carriages are connected to the lead screw via the anti-backlash nuts which will be discussed in Section 3.4.3. The carriages were designed to have a flat top section for mounting load cells and specimen grips. In Figure 3.6 (side view) it can be seen that the the specimen interface (end of the arm) and lead screw are not on the same plane, in order to counteract the moments that this would cause three wheels are needed to properly constrain the carriage. This allows motion along the axis while counteracting the moments caused. In Figure 3.7 it can be seen that to prevent the unwanted moments

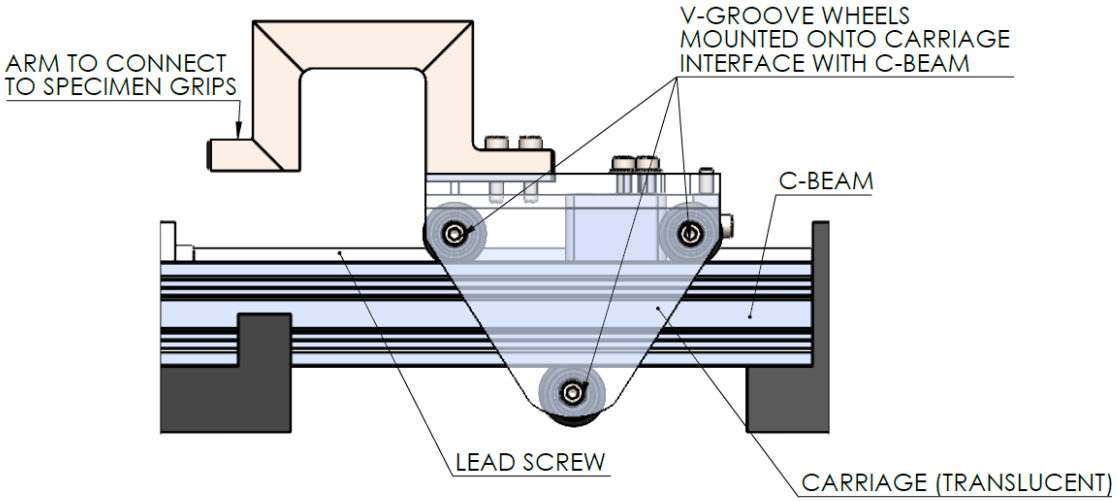

Figure 3.6 Carriage and aluminium extrusion guide system, side view

caused by the guide rail plane being offset from the lead screw and specimen plane an additional set of three wheels was added to the carriage, mirrored across the lead screw plane. The carriages are now constrained so that they can only move axially along the deformation axes and all other axial or angular motion is constrained.

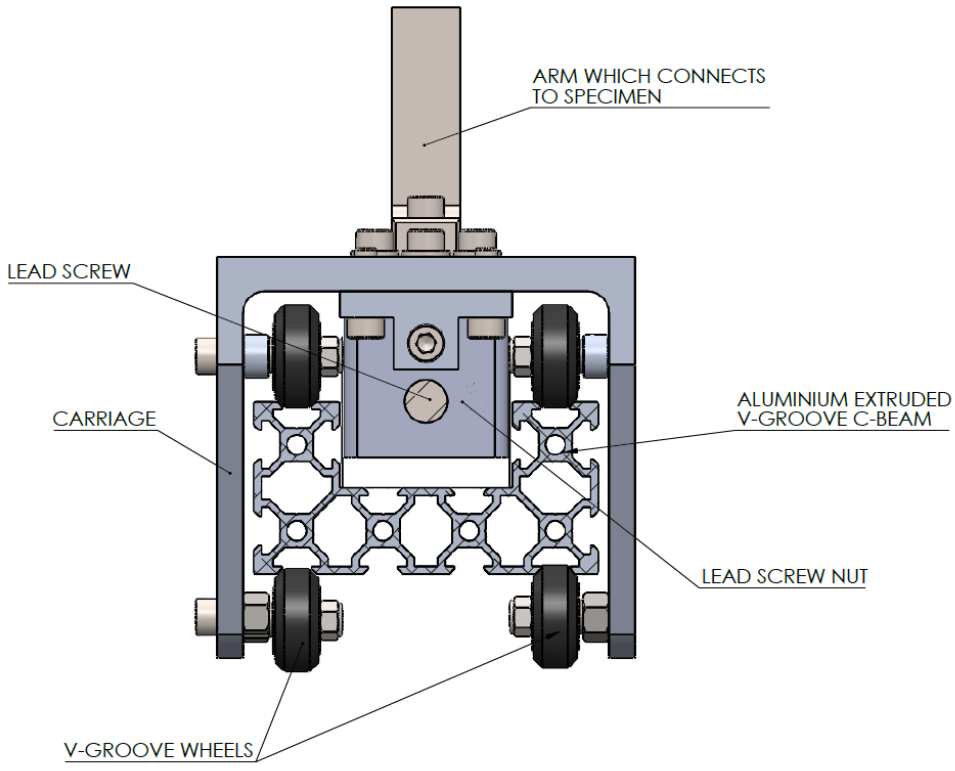

Figure 3.7 Carriage and aluminium extrusion guide, rear view

3.4.2 Lead screw selection and calculations

When designing the lead screw, the strength, length, diameter, pitch and number of thread starts all had to be considered. The following calculations were done in order to determine the required dimensions of the lead screw. The lead screw was designed to move a load (F) of at least 200 N. This was based on the requirement of 50N specified in the design inputs, with a safety factor of 4 to compensate for inertia and friction forces from the carriages and to ensure that the lead screw could withstand load fluctuations in undesired situations such as the carriages jamming or larger specimens being used. The machine also needed to be strong enough to ensure it would be durable during assembly and transportation. There was no benefit to having the machine designed to the minimum required strength in this instance.

It was decided to buy the lead screws, as the UCT Mechanical Engineering workshop staff were uncertain whether they could manufacture a lead screw of the desired length and diameter to the necessary accuracy. The available lead screws were limited to those supplied as both left hand and right thread. The number of thread starts, pitch, material and outer diameter specified by the manufacturer were then used to ensure the potential screws would be strong enough and to determine the required motor torque. The calculations used to check the screw specifications are listed in Equations 3.1 to 3.3.

A 10mm outer diameter lead screw was chosen as a standard size screw which met all the loading requirements. The mass reduction in selecting a smaller screw diameter did not justify the increased risk of buckling. A single start screw with a 3mm pitch was chosen. The smaller pitch was selected as displacement resolution was considered a higher priority than machine speed. As a single start thread met the mechanical and performance requirements therefore there was no need for a double or triple start thread to be used. Stainless steel 304 was chosen due to its high strength and corrosion resistant properties. A high helix dryspin (Igus) thread was selected.

First the torque (T) required to move a load (F) was calculated using Equation 3.1. A Matlab code was written which allowed the different screw variables (which were available for purchase) to be added to the code to calculate the required torque. See Appendix C for the Matlab code used.

$$T = \frac{Fd_m}{2}\left(\frac{\pi\mu_t d_m + L\beta}{\pi d_m \beta - \mu_t L}\right) = 0.4Nm \tag{3.1}$$

Where d_m is the mean diameter of the screw, L is the lead of the screw, μ_t is the coefficient of thread friction (0.25 for static friction of Sustarin C on Stainless Steel, 0.21 for dynamic friction) and $\beta = cos\alpha_n$ where α_n is the normalised flank angle of the thread.

The lead screw needed to be self-locking to ensure that a loaded specimen did not cause motion of the carriages when the motor was not powered. Rather it would remain in place unless the motors were purposefully driven by the user. Equation 3.2 displays the condition that needed to be met to ensure that the screw was self locking.

$$L < \pi \mu_t d_m \tag{3.2}$$

The critical load (F_c in Equation 3.3) is the force at which the lead screw will buckle. This load was calculated to ensure there would be no unwanted buckling of the screw for the expected loading it would undergo during regular use.

$$F_c = \frac{C\pi^2 E}{L_c^2}\left(\frac{\pi d_r^4}{64}\right) \tag{3.3}$$

Where C is the buckling end-condition constant ($C = 1$), L_c is the column length and d_r is the minor diameter of the lead screw. A value of $C = 1$ is a used as the bearing supports on either end of the device are considered as floating bearings and the entire span of the screw was used for L_c. These are both conservative values as the screw is also supported by the lead screw nuts which have a variable displacement always less than the length of the screw.

3.4.3 Anti-backlash nut

A regular nut transmits loads in both directions but has a small backlash displacement when changing direction, where the nut and screw are briefly not in contact before being able to transmit a load in the opposite direction. Backlash within the lead-screws' interfacing nuts are a potential source of inaccurate specimen deformation. If the backlash on any two nuts is not the same then there can be errors even if the nuts are interfaced with the same lead-screw. In order to mitigate these errors anti-backlash nuts were custom built. The manufacturer of the lead-screw could not provide anti-backlash nuts for left-hand thread and therefore the nuts were custom designed and manufactured.

The nut was split into two halves which are preloaded to ensure that the backlash is fully taken up by the two halves of the nut. The one half of the nut is used to transmit the load in a certain direction, then when the screw changes direction the load is transmitted by the other half of the nut.

The nut was made from Sustarin C, a polyoxmethylene (POM) thermoplastic, with a low coefficient of friction (0.21), high abrasion resistance and a yield strength of 67MPa. Stresses within the nut were calculated to ensure that the nut thread does not strip due to the forces it is transmitting. The nut was considered as a point of potential failure as

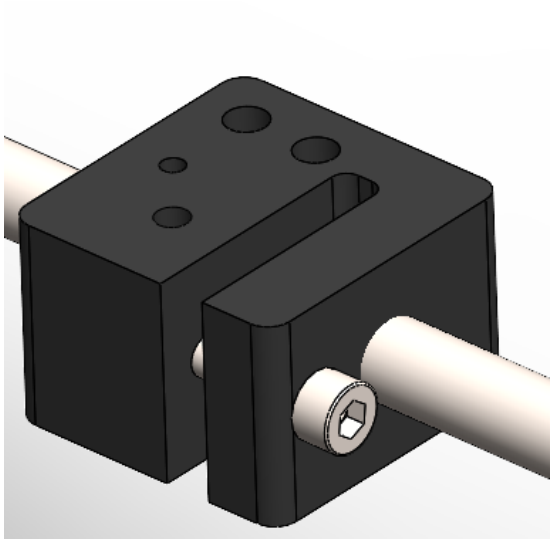

Figure 3.8 CAD model of anti-backlash nut on lead screw

it is interfacing with a stainless steel lead screw and would therefore wear over time; so, the nut would require periodic lubrication and tightening.

The anti-backlash nut displayed in Figure 3.8 shows the nut's two halves are on either end of a C shaped block. The larger half is designed to transmit the forces while the system is in loading and the smaller half while it is unloading. The two halves are preloaded with a bolt across the open end of the C-block ensuring that the two halves are always in contact with the thread. This anti-backlash nut design is commonly used in DIY CNC machines. When appropriately tightened there is no play between the carriage and the screw in either direction. If the anti-backlash nut needs to be tightened due to wear the user simply needs to tighten the bolt on the anti-backlash nut.

3.4.4 Arm design

"Arms" were designed to connect the carriages and load cells to the specimen grips. They were designed to accommodate a saline bath and therefore had a "U" shape to allow the arm to pass over the edge of the bath. The arm was designed to not create unwanted bending moments on the load cell as this would skew the data. Some slight bending within the arm was unavoidable so the arm was designed out of Stainless Steel 316 alloy with a relatively large cross section to mitigate the effects of bending within the arm. Although the arm is not straight the force acting through the specimen is co-linear with the connection to the load cell as seen in Figure 3.9. This mitigates the risk of non-tensile forces acting on the load cell. The length of the arm shown in Figure 3.9 is 101 mm and the height is 59 mm.

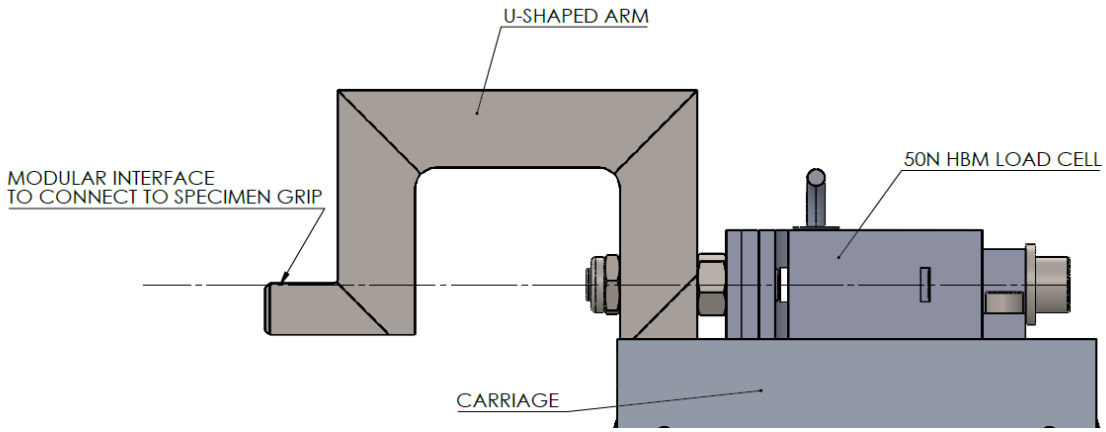

Figure 3.9 Arm designed to connect load-cell to grips

The load cell is slightly raised above the carriage, with the arm sitting in a slot in front of the load cell. The slot is toleranced for a locational clearance fit, to minimise any impact on the forces on the arm, while still keeping accurate alignment. The normal force and therefore frictional force of the arm in the slot is negligible, lubricant is also used to further mitigate any risks of unwanted friction. A simple finite element analysis was done on SolidWorks Simulation to assess the deformation of the arms as seen in Figure 3.10. The deformation is minimal, with a maximum of less than 0.02mm, the deformation of the arm in Figure 3.10 has been scaled for deformation visualisation. These results were backed up with hand calculations using Castigliano's method.

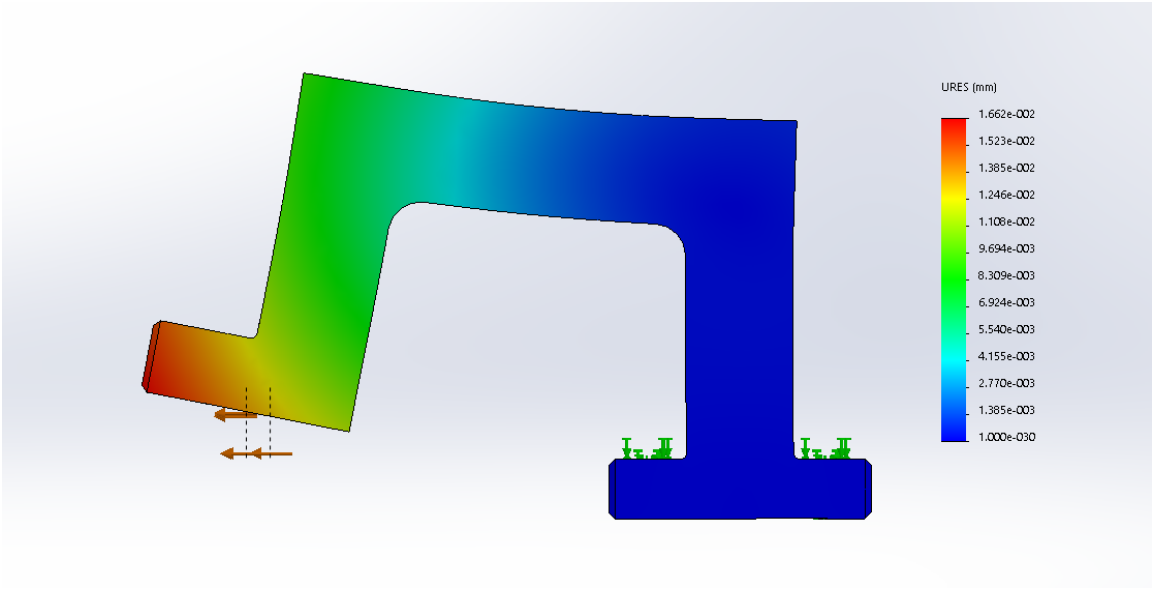

Figure 3.10 Scaled deformation of Arm at 200N

3.4.5 Grip design

The grips were designed as modular attachments to the arms. As the commissioning testing was to be done with silicone elastomer cruciform specimens, simple modular rigid clamp grips were designed and are shown in Figure 3.11. The interface between the arms and the grips was designed so that different grips can be manufactured in the future depending on the needs of the user. Each grip is connected to the arm with an M5 socket head screw and/or a 3mm stainless steel pin. Each grip consists of a top and a bottom half. The bottom half has two M4 nuts embedded into it which connect with two M4 screws which pass through the top half to clamp down on the specimen.

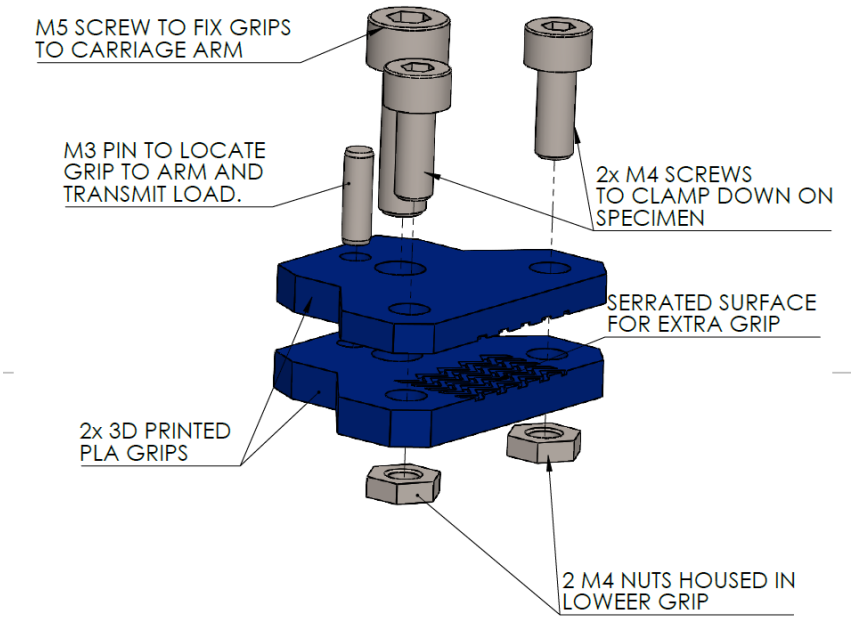

Figure 3.11 Grips designed to connect specimen to arms

The grips are made of 3D printed Ploylactic Acid (PLA) which allows for a certain amount of flexibility which can securely grip the specimen without easily damaging the specimen, like grips made from harder material such as stainless steel could. The surfaces which come into contact with the specimen are serrated to allow for extra grip and therefore mitigate the risk of specimens slipping in the grips during testing. Follow up projects that test biological tissue will need to investigate the use of other gripping techniques such as sutures or rakes. This is because rigid clamps are not very effective in gripping smaller square specimens which are typically used when testing biological specimens, they are effective when used with cruciform specimens.

3.5 Force and deformation measurement

3.5.1 Load cell

A single axial load cell on each axis is used to measure the axial load applied through the specimen. Two 50 N HBM (Hottinger Baldwin Messtechnik, Darmstadt, Germany) K-S2M tensile load cells were purchased along with two HBM ClipX devices. The ClipX is a combined load cell amplifier and signal conditioner which connects to a PC via an ethernet connection. If load cells with different maximum loads are needed they can easily be switched with other HBM load cells which interface with the ClipX devices.

3.5.2 Surface deformation measurements

The custom biaxial machine needed to integrate with the already existing Dantec DIC system at CME at UCT due to the large expense of having a dedicated DIC system for the machine. In order to integrate with the existing system the cameras need to have an unobstructed view of the specimens and the specimens cannot shift out of the region of interest of the cameras. For the most part the DIC system is a standalone system, with the only connection between the DIC system and the custom machine being an analogue connection which sends load cell force data from the ClipX device to the DIC system. This ensures the force and DIC data is synchronised correctly and can be analysed together on the Dantec Istra4D software in post processing. The force data is also recorded separately from the DIC system, by automatically recording the data on the PC used to control the machine. This ensures that if other DIC systems are used in the future the force data can still be recorded reliably, so that the design can be used with a wide selection of non-contact image based surface deformation measurement systems.

3.6 Electrical and embedded system design

As this project forms part of a Mechanical engineering masters, the focus is not on design of the electrical and embedded systems from first principles. Rather, existing solutions and systems were integrated with the mechanical design of the custom built machine. This Section describes the electrical and embedded systems used and justifications for their use.

3.6.1 Electrical and embedded system overview

The electrical and embedded control system consists of the following; a single Arduino Uno microcontroller board, a GRBL shield board, 2 motor drivers, two stepper motors, 4 limit switches, one emergency stop button, two load cells and two ClipX devices. Figure

3.12 shows a schematic of how the system is connected, with the blue arrows depicting the transfer of electrical signal or data and the red arrows depicting the transfer of power to the system.

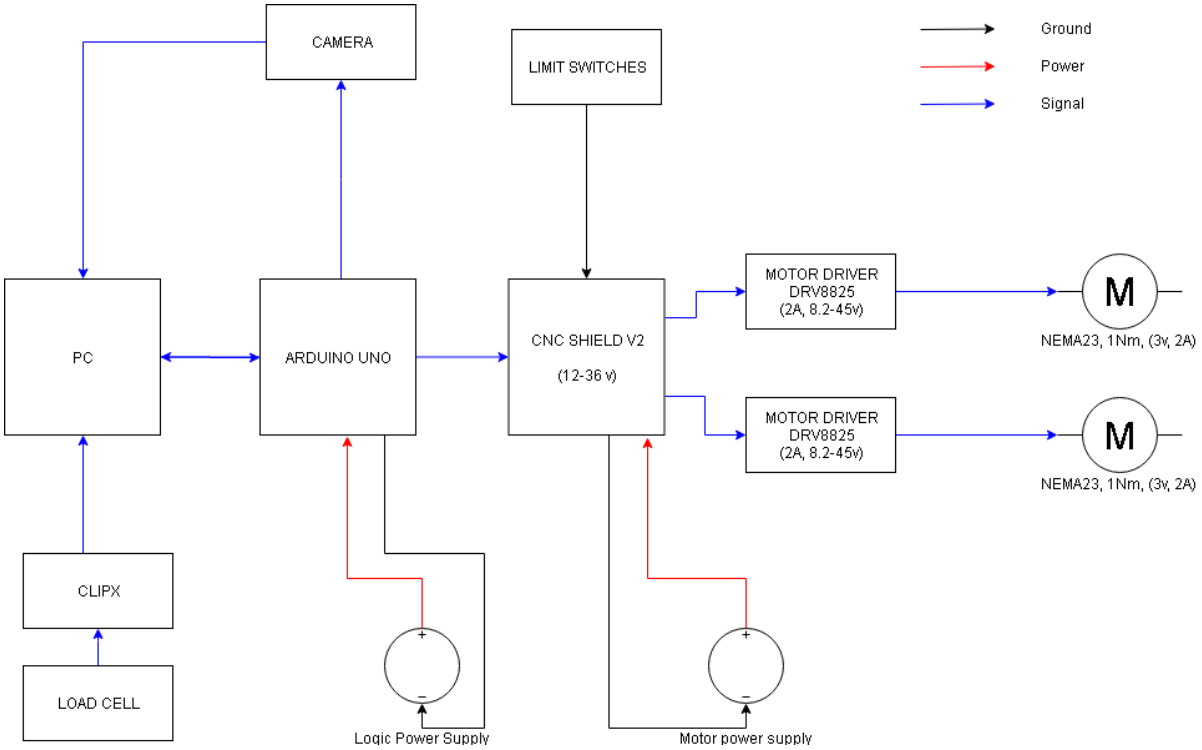

Figure 3.12 Electrical system

GRBL is an open source CNC motion control system which can be run off an Arduino Uno. The GRBL system is designed to use open loop control and stepper motors to run a CNC mill. The GRBL shield board can be purchased and plugged directly into an Arduino, the software is then downloaded onto the Arduino. The shield board has marked ports for the motor drivers, motor connections and power connections. Instructions are then sent to the Arduino as GCode commands using Universal GCode Sender - an open source software used for interfacing with CNC controllers.

In order to move the axes of the planar biaxial tensile testing machine the X and Y axes on the GCode sender are used to send instructions to the two machine axes, known as the red and white axes respectively. The axes are named the red and white axes as the motor mounts and gears for the two axes are red and white respectively, giving the user an easy visual marker to differentiate the two axes. The Z-Axis of the GRBL system is used to send signal to the data acquisition system in order to record data via the ClipX. The ClipX requires a constant signal to record data, not just a trigger. The GCode instruction to move the Z-Axis is used to record data via the ClipX and does not send motion instructions. Alternatively, other GCode commands - such as spindle speed - could be used as long as the signal could be held while the X and Y axes were in motion.

3.6.2 Motor selection

Stepper motors with open loop displacement control were selected as the simplest solution for controlling the motion of the machine. This was done with the use of the open source GRBL system. With the low loads needed to be tested, it was calculated that stepper motors connected to spur gears and then to the lead screws would provide enough torque to power the machine without any unwanted losses. Other options such as servo motors with closed loop load control were considered but deemed unnecessarily complicated for this project. Closed loop load control with such small forces, and specimens of a biological nature, would add an unrealistic amount of complexity to the project.

For the desired 50 N of force, it was calculated that the motor needed to provide at least 0.4 Nm of torque while the carriages were running (Equation 3.1 in Section 3.4.2). The additional torque needed to accelerate the loaded carriages up to speed was calculated and found to be negligible. Spur gears with a ratio of 3:1 were mounted between the motors and the lead screws to increase the displacement resolution and torque at which the machine could operate. The gears were 3D printed out of PLA. The motor selected was a 1 Nm Wantai stepper motor, which could easily operate at the required 0.4 Nm. The backlash potentially introduced by the gears was not a substantial concern. Firstly, specimen deformation is measured directly via DIC, so this does not negatively affect deformation measurement. Secondly, as both carriages are mechanically constrained to the same screw any backlash between the gears would result in the same losses (if any) across the two carriages. Therefore, equal and opposite motion of the carriages is ensured. If greater precision of cyclic loading is required, a means of minimising gear backlash should be investigated.

3.6.3 Safety features

Several safety features were built into the machine to ensure that it would not harm the user, or damage itself. The machine was designed to have the ability to detect predetermined dangerous scenarios and stop all functions which are a danger. The machine was also designed to be able to be safely stopped by the user in an emergency situation not detected by the machine. The list below details the safety features of the machine:

- A physical emergency stop button, which stops all motors and GRBL commands. The system alarm needs to be turned off on the Universal GCode sender by the user before the machine can be put into motion again.

- Limit switches to prevent carriages from moving beyond limits of the machine. When limit switches are hit an alarm is triggered and all motors are stopped.

- Soft limits set in Universal GCode Sender do not allow GRBL commands beyond the user specified limits. If a command is sent which would result in motion beyond the specified limits an error message will be sent and the machine will not perform the motion command.
- Load limits can be set by the user on the ClipX which stops machine if a load above the limit is detected.
- Clear and concise step by step user instructions provided to the user for starting the machine (See Appendix D).

Chapter 4

Uniaxial Experimental Planning and Procedure

In order to verify that the custom built machine met the design requirements and worked reliably and safely, physical testing was performed. First, subsystem commissioning testing was done and then testing of the individual axes with specimens was performed and results compared to a calibrated Instron uniaxial tensile testing machine. Only once the uniaxial systems and subsystems were verified could the machine be reliably used to perform planar biaxial tensile testing. This section details the experimental planning and procedure to verify the uniaxial systems and subsystems.

4.1 Commissioning testing

4.1.1 Planned subsystem commissioning

The subsystem commissioning testing was done to ensure the machine worked as expected, that the design requirements were met and that the machine could be used reliably before the testing of skin surrogate specimens could begin. The following machine functions and requirements were verified during machine commissioning: carriage speed, carriage displacement, carriage reliability, safety features, data acquisition and stepper motor settings.

4.1.2 Displacement commissioning testing

The accuracy of the location of the carriage was tested to ensure that both carriages were moving the predetermined amount as specified by the GCode command sent to the machine. This was done by running the machine over a given displacement and

measuring both carriages before the carriage movement and then again afterwards using a vernier caliper. Tests were carried out by giving the carriages a series of displacement commands and then measuring their locations after each instruction. This was done while the carriages were both loaded and unloaded; carriages were loaded by using elastic bands as specimens to provide resistance to the motion of the carriages. Safety features, homing accuracy and settings were also tested and adjusted as needed during the displacement testing. The motion of both carriages on a given axis was measured individually, relative to fixed reference points, to ensure displacement was symmetrical.

4.1.3 Speed commissioning testing

Speed tests were done by first tracking a point on a specimen to ensure the speed was constant. A point very close to the grips on a speckled specimen was tracked using the Dantec DIC system and the speed plotted. Although this is not a very accurate way to measure the speed it would allow for valuable insight into whether the speed was constant and into the acceleration and deceleration of the machine.

Speed testing was then done by measuring the amount of time taken by the carriage to travel a predetermined displacement; the displacement was then confirmed through physical measurements of the distance travelled by the carriage. This was done over a distance of 5mm and 20 mm (per carriage: 10 mm and 40 mm total displacement per axis) over four different carriage speeds; 8 mm/min, 20 mm/min, 50 mm/min and 180 mm/min (which equates to a total speed of 16, 40, 100 and 360 mm/min per axis). This was done for both an unloaded (no resistance) and loaded system. Forces were also recorded during the speed testing; firstly, to ensure that the data acquisition from the load cell was working correctly but also as a safety feature to ensure excessive force was not transmitted through the load cell. Furthermore, load cell data was used to confirm the time of the tests as the starting and stopping point of the test is clearly visible when load data is analysed, even in an unloaded test, due to the slight - but visible - vibrations detected by the load cell.

4.2 Specimens

4.2.1 Specimen material

As per the scope of the investigation, both uniaxial and biaxial tensile tests were done using a skin surrogate rather than skin. This would allow the machine and proposed testing method to be critically assessed before testing on an actual soft tissue which has the additional complexities of preparing and gripping the specimens.

Dragon Skin 10 [54] (Smooth-On) was chosen as the skin surrogate. Dragon Skin 10 is a Shore 10A platinum cure liquid silicone compound predominately used for special effects in the film and entertainment industries [54]. It was chosen as it has a similar Young's modulus to that of skin in the toe region, it is also highly pliant (1000 % elongation at break [54]), it is readily available and easy to use. This material was also previously used as a surrogate by A. Curry [6] and A. Graham [26] at BISRU, which allowed specimen design and manufacture to be built on past knowledge of using the material.

4.2.2 Specimen manufacturing and speckling

Dragon Skin 10 [54] is translucent - in order to get the contrast needed between the base material and the speckle pattern needed for DIC, pigment was added to the base material to colour it white. Black speckle pattern was used to provide the adequate contrast. Various substances and means of speckling the white Dragon Skin 10 were attempted with varying degrees of success; spray paint, paint, and silicone were all used along with paint brushes, air brushes and even milk frothers.

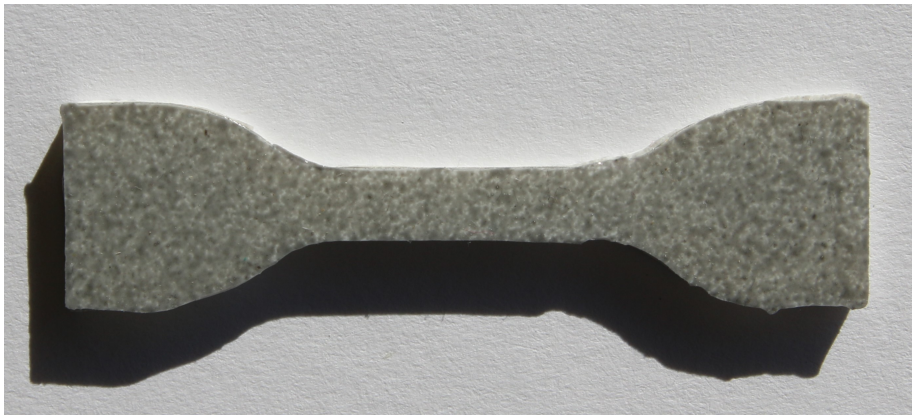

Figure 4.1 Photograph of a failed uniaxial Dragon Skin 10 specimen which was speckled using an airbrush

Initially Dragon Skin 10 with black pigment was used to speckle the specimens using a milk frother [26]. This was done by using the milk frother to spray the black Dragon Skin 10 onto the specimens. This method, although time consuming and highly prone to error, did produce reasonable specimens but only when making larger specimens.

It was found that a platinum cure liquid silicone based paint called Psycho Paint [55] (made by Smooth On, manufacturers of Dragon Skin) when used with an airbrush was able to provide the consistently fine speckle pattern needed when working with such small specimens, an example of which is shown in Figure 4.2.

The Dragon Skin 10 comes as two parts (Parts A and B) which are mixed and cured at room temperature to form the surrogate material. For the base of the specimens it

Figure 4.2 Photograph of a successful biaxial Dragon Skin 10 specimen after being speckled with an air brush, before having the excess silicone trimmed

was found that the following quantities provided the best results: 1 part Part A, 1 part Part B, 0.1 parts solvent (Dimethylsiloxane) and 0.05 parts white pigment. The solvent was added as Dragon Skin 10 is highly viscous and difficult to work with while curing. The mixture was then left to cure in a custom made Plexiglas mould for 2 hours before adding the speckle. For the Psycho Paint it was found that in order to achieve the desired contrast less solvent was to be used than the recommended amount: with 1 part Part A, 1 part Part B, 3.5 parts thinner and 0.125 parts black pigment. The black speckle was added with an air gun after the specimens had partially cured, which meant they bonded but did not mix. This ensured a clear contrast between the base material and the speckle. Care had to be taken to ensure the speckle material was the correct consistency and opaqueness otherwise it was prone to run and be a light grey rather than black as shown in Figure 4.1, which did not provide the needed contrast between the base and speckle.

Figure 4.3 shows the specimens curing in their Plexiglas mould after speckling; this method of curing the specimens resulted in some inter-specimen differences in thickness. This was due to the very high viscosity of the Dragon Skin 10 while curing, a 2.5 mm thick plexiglass sheet was used to aid in making 2.5 mm thick specimens the mould could not

be sealed to ensure an even thickness however as the speckle needed to be added during the curing process.

Figure 4.3 Photograph of uniaxial Dragon Skin 10 specimens in their mould after being speckled with an air brush

4.2.3 Uniaxial specimen design

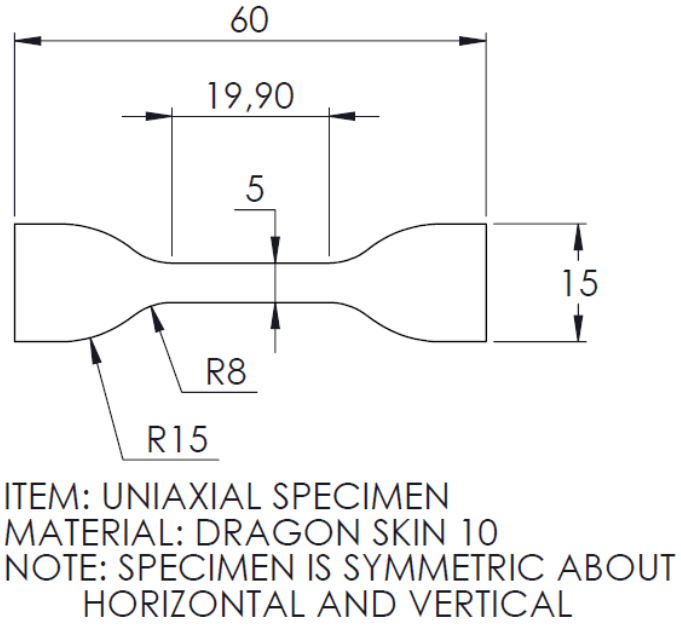

Figure 4.4 Drawing of the uniaxial specimen

The specimen dimensions were constrained by the size and range of motion of the planar biaxial testing machine. The machine was designed to test specimens which are

considerably smaller than those typically used when performing uniaxial tensile tests on non-biological materials. ASTM D412−16 (Standard test methods for vulcanised rubber) was used to design the shape of the specimen but the size was scaled down in order to fit into the testing machine (Figure 4.4).

In order to mitigate any unwanted complications from the deviation from standard ASTM D412-16 it was decided that the same size specimens would be used for uniaxial testing on the custom built biaxial testing machine and for testing done using the Instron uniaxial tensile testing machine. Additionally, the specimens for both rounds of testing would come from the same batch to avoid small variations in manufacturing between batches affecting the results.

4.3 Uniaxial testing

4.3.1 Method

In order to critically assess the machine design and build, it was decided to do a comparative study of the results obtained when using the designed biaxial tensile testing machine versus that of a calibrated and commercially available machine. The commercial machine chosen to compare results with was the Instron uniaxial tensile testing machine with a calibrated 100 N load cell, with a resolution of 0.001 N, at the Centre for Materials Engineering (CME) at the University of Cape Town. The same batch of specimens was used for the testing done on the custom machine and the Instron to ensure an accurate comparison could be made. Additionally, the same DIC system (Dantec) would be used for testing on the Instron and custom machine.

As the custom biaxial tensile testing machine could essentially run as two separate uniaxial tensile testing machines, it was not an issue to run only a single axis during this phase of testing. It also meant the controls and recording of data would be simplified which would allow for the ironing out of any issues which could then be rectified before moving to full biaxial testing. These factors, along with lack of access to a commercially built biaxial tensile tester, meant that uniaxial testing of each axis individually was the best method to verify the machine design and build.

The acceptance criteria was set as either the stress-strain data for the designed machine lying within the limits of the stress-strain data obtained via the Instron machine, or the means varying by less than 2%, with a Coefficient of Variation of less than 5%.

4.3.2 Uniaxial tensile testing plan

The specimens for both the Instron machine and the custom built biaxial machine were all made together from a single batch of Dragon Skin 10. This was done to ensure the same material was used and that no differences in mixture or curing environment could have an effect on the specimens; and therefore the results. The testing protocols for the uniaxial testing on the self built machine (Table 4.1) and Instron testing machine in CME (Table 4.2) are given below.

Test Speed (mm/min)	**Number of specimens tested**	**DIC sample frequency (Hz)**	**Maximum displacement (mm)**
10	5	1	30
50	5	5	30
120	5	12	30
400	5	20	30

Table 4.1 *First round of uniaxial testing done using designed planar biaxial tensile testing machine (Axis 1)*

Test Speed (mm/min)	**Number of specimens tested**	**DIC sample frequency (Hz)**	**Maximum displacement (mm)**
10	5	2	50
50	5	5	50
120	5	15	50
400	5	30	50

Table 4.2 *Uniaxial testing done using the Instron uniaxial tensile tester at CME*

As shown in Tables 4.1 to 4.3 the DIC sample rate was not the same across tests of different speeds. This is because DIC can be become computationally expensive if the sample rate is too high, or inaccurate if it is too low. A 400 mm/min test over 30 mm lasts approximately 4.5 seconds and requires the sample frequency of the DIC to be higher to adequately capture the deformation of the specimen, hence a sample rate of 20 Hz. Conversely, a 10 mm/min test over 30 mm lasts 180 seconds and is computationally expensive to run with a DIC sample frequency of 20 Hz, as this would result in 3600 DIC

images being taken as opposed to the 90 of the 400 mm/min test Therefore, to not have large inconsistencies in the resolution of the deformation data, the DIC sample rate was adjusted depending of the speed of the test. It must also be noted that the Instron test was run over 50 mm and not 30 mm, this does not have any effect on the results.

After the first set of uniaxial tests, some revisions to the machine were necessary and are detailed in Section 5.2.2. After completing these revisions, an additional round of testing was performed on the custom built biaxial tensile testing machine. The testing protocol for this second round of testing is given below in Table 4.3. In the second round of testing both axes of the custom machine were tested individually. The axes are named the red axis and the white axis to easily identify them by the colour of the motor mounts on each axis.

Test Speed (mm/min)	**Number of specimens tested**	**DIC sample frequency (Hz)**	**Axis Tested**
50	5	10	Red
50	5	10	White
400	5	25	Red
400	5	25	White

Table 4.3 *Second round of uniaxial testing done using the custom built machine*

4.3.3 Uniaxial tensile testing procedure

The DIC system and software; Istra4D (Dantec Dynamics, Skovlunde, Denmark) were used to track and record the deformation of the specimens. Calibration of the cameras for DIC was done at the beginning of each testing session. If testing lasted more than a day then the cameras were calibrated at the beginning of each day. The first round of testing on the custom built machine and the Instron tensile testing machine were done using 2D DIC which meant that only a single camera was needed. 3D DIC was used for the second round of testing on the custom built machine, which meant that two cameras were used. This was done in anticipation of the need to use 3D DIC when doing full biaxial tensile tests on the machine.

In order to calibrate the DIC system a series of 10 images of a Dantec calibration plate were taken. The Istra4D software would then determine camera positions, focal lengths and image distortion using known features on the calibration target, which are later used in processing the images from the experiment into displacement data. In order

to accurately calibrate the system, the region of interest needs to be in focus and the lighting should be bright but without causing any glares. During calibration, the Istra4D software would provide the residuum value, which is the uncertainty (in pixels) of the location of any facet. A residuum of less than 0.4 pixels was deemed sufficient. The initial placement of the calibration plate is important as the axes that the software uses align with the first calibration image during the calibration setup.

Once the cameras are calibrated and the machine has been powered up and homed the following testing procedure is followed:

- Measure and record the thickness of the specimen at multiple locations in the region of interest, using a vernier caliper.
- Ensure the correct G-Code is selected for the current test on GRBL software.
- Ensure the carriages are at the predetermined start point (this could be the home position or a distance from the home position depending on the specimens).
- Ensure the force data acquisition system has the correct file name for saving the test data. The name should include the test number with an underscore used to differentiate different specimens of the same test regimen.
- Ensure the camera sample frequency and settings are correct.
- Mount the specimen into the grips and then mount the grips onto the arms of the machine. Ensure the specimen is not slack or accidentally pre-loaded.
- Start the capture of the images on the DIC Instra4d software.
- Run the test. Data collection from the load cells is started by a trigger which forms part of the every G-Code written for testing.
- When the test is finished, stop DIC data collection. The force data is automatically saved at the end of the test.

Chapter 5

Uniaxial Commissioning, Results and Machine Revision

As the custom built biaxial tensile testing machine can be run as a uniaxial tensile testing machine along either of the machine's two axes, it was decided to do a comparative study against the Instron uniaxial tensile testing machine at CME at the University of Cape Town. Before the comparative study could be done displacement, speed and safety commissioning tests were done to verify the machine was working as intended.

5.1 Commissioning testing

5.1.1 Displacement tests

As described in Section 4.1.2, testing was done to ensure that the carriages moved the amount specified by the GCode command given to the machine. The results of the displacement tests are detailed in Table 5.1 below. Testing was done while the machine was loaded to ensure the displacement is correct under test conditions.

As can be seen in Table 5.1, the measured displacements were slightly less than the commanded displacement, but by less than 0.13 mm at most. The average error was 0.2% and 0.4% for the white and red axes respectively. However, the variation between the results of the two speeds tested is very small - the difference in measured displacement for all tests on the white axis spans 0.02 mm, while the red axis measurements span 0.08 mm. It should be noted that a vernier caliper (with a resolution of 0.02 mm) was used to measure the displacement, this combined with human error in aligning the vernier caliper would account for some of the error. A total of 5 samples per axis were tested at each speed.

Axis	**Test speed (mm/min)**	**Average measured displacement (mm)**	**Variance**
White	50	29.89	0.00012
Red	50	29.97	0.00043
White	400	29.89	0.00032
Red	400	29.96	0.00092
White	500	29.87	0.0003
Red	500	29.89	0.00067
White	**All speeds**	**29.88**	0.00029
Red	**All speeds**	**29.94**	0.0029

Table 5.1 *30mm Displacement tests while loaded*

5.1.2 Speed tests

Once the displacement testing was completed testing was done to verify that the speed of the carriages was correct and constant. Displacement was measured using a vernier caliper and time was measured using measurements from the load cell. Additionally, DIC was used to further verify that the speed measured was constant during testing. This was done by tracking the displacement of a point on the specimen which was close to the grips. This displacement wouldn't equal the grip displacement precisely, due to the small deformation between the grip and the point tracked. However, the testing would still show whether the speed varied appreciably. Table 5.2 shows the speed verification results and Figure 5.1 shows the speed of a point on the specimen close to the grips.

Table 5.2 shows that the speeds recorded closely match those commanded in the GCode. The speeds commanded seem to be quite arbitrary; this is because a 1 mm motion step in the Z-Axis (which does not physically exist in the machine) was used in the GCode to trigger the data capture. This 'motion' in the Z-Axis then unknowingly altered the speeds tested as the speed specified in the GCode is the absolute speed. For example: if a displacement of 10 mm along the X-axis and 1 mm along the Z-Axis was specified at 16 mm/min the actual speed along the the X-axis would be 15.69 mm/min and the absolute speed would be 16 mm/min if a Z-axis existed. For all future testing, the Z-Axis displacement was taken into account when making the GCode commands to ensure trigonometry played no part in determining the speeds set in the machine post testing.

Machine Settings			**Experimental Results**
Speed (mm/min)	**Distance (mm)**	**Acceleration (mm/s^2)**	**Measured speed (mm/min)**
15.69	10	20	15.65
15.98	40	20	16.01
39.22	10	20	39.10
39.95	40	20	39.88
98.06	10	20	98.19
99.88	40	20	100.18
353.01	10	20	351.99
359.55	40	20	359.96

Table 5.2 *Speed tests done while unloaded*

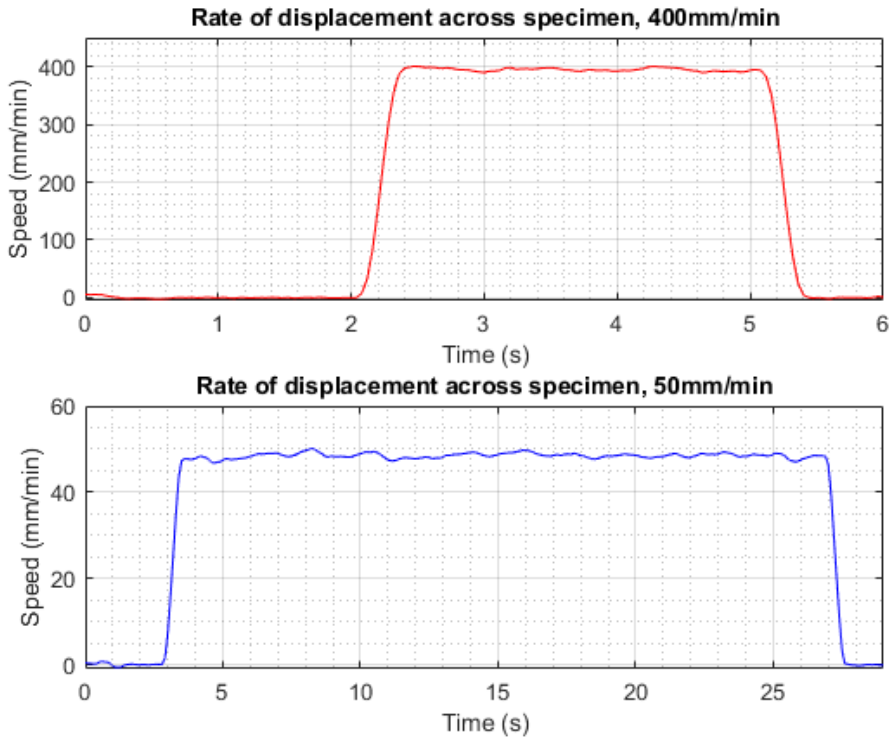

Figure 5.1 Average relative cross-head speed v Time; Red Axis 400mm/min (top) and White Axis 50mm/min (bottom). Measured using DIC

Figure 5.1 shows the instantaneous speed as recorded by DIC for tests at 400 mm/min and 50 mm/min. While there is variation between the instantaneous speed and the nominal set speed, over a test the average is typically within 0.15 mm/min. It wasn't clear whether the apparent variation was due to noise in the DIC measurements, or if this was actual speed variation in the machine. However, further refinement of this would need an independent speed measurement and possibly closed loop control, which was deemed to be beyond the scope of this project. The speed recorded by the point on DIC is not perfectly linear as can be expected when tracking an arbitrary point on the specimen but it does maintain the intended speed across the test. The ramp-up acceleration for all testing was set at 20 mm/s^2, for the the 400 mm/min and 50 mm/min tests shown in Figure 5.1 the ramp up time took approximately 0.4 s and 0.07 s respectively. A test which tracked the rigid grips themselves, rather than a point on the specimen, would have been useful in eliminating potential unknowns.

5.1.3 Vibration analysis

During commissioning testing it was observed that the load cell raw data had significant noise. As the magnitude of the noise was greater than anticipated, a vibration analysis was used to investigate the possible source of the noise and what mitigation options could be undertaken. This was investigated and it was determined that the noise came from the vibrations of the machine while in operation. In order to mitigate the adverse effects of the noise on the data collected, testing was done to analyse said vibrations. Micro-stepping of 1, 1/8th and 1/16th were tested to see what effect the stepper motor stepping had on the noise, as well as testing the machine when loaded as opposed to unloaded. The frequencies of the undesirable noise was then found using Fast Fourier Transforms.

Figure 5.2 shows the dominant frequencies in the force noise (from a zero load test) were considerably higher than the frequencies anticipated when loading a typical specimen at the anticipated rates. It can also be seen that 1/16th stepping provided the best results in terms of noise reduction. The noise at higher frequencies can be removed using a low pass filter on the ClipX amplifier system which the load cell interfaces with. Bessel low pass filters were used to filter out frequencies above 20, 50 and 100 Hz with the results of the 20 Hz low pass filter shown in Figure 5.3.

As can be seen in Figure 5.3 the noise in the force data was successfully filtered out using the software supplied with the load cells. It was therefore determined that 20 Hz Bessel low pass filters would be used for all future testing using the custom built planar biaxial tensile testing rig. It should be noted that the noise was much less evident when the machine was loaded with a specimen (even if highly compliant), than when the machine was running unloaded. It is hypothesised that the soft elastic specimens have a damping effect, thus the decrease in noise of the machine when loaded during this investigation.

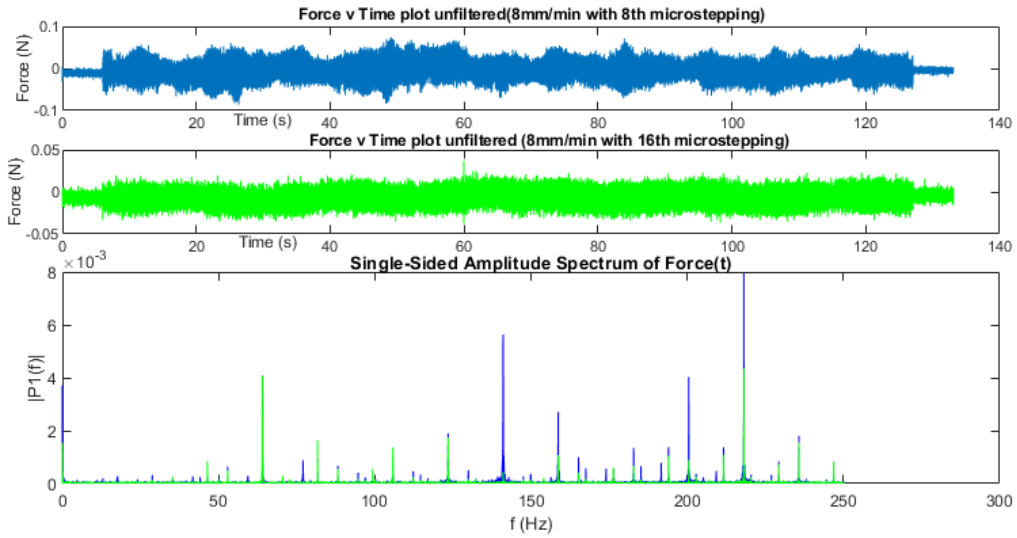

Figure 5.2 1/8th and 1/16th micro-stepping noise comparison

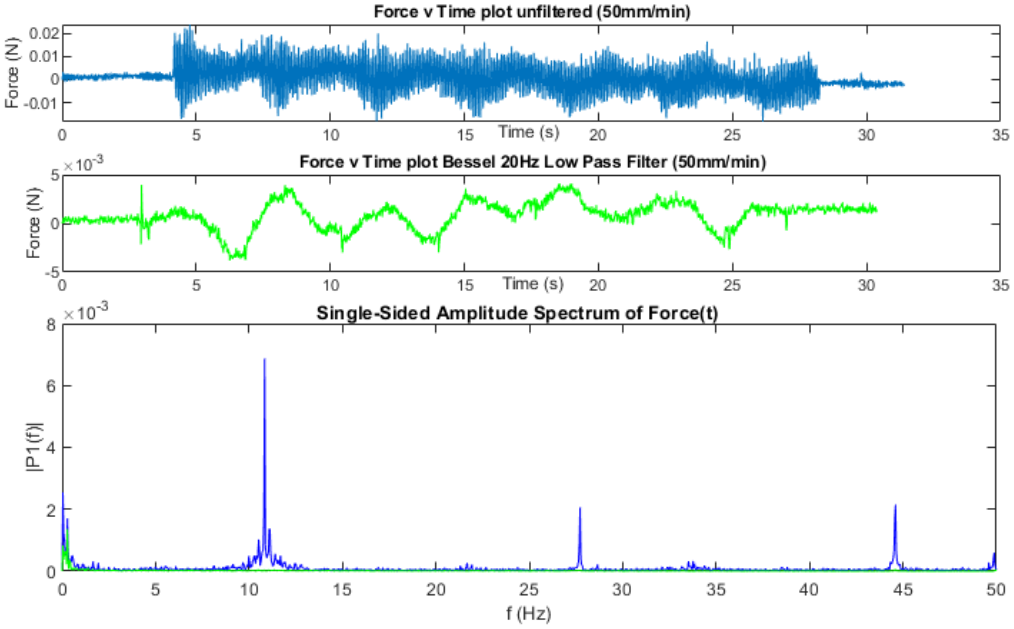

Figure 5.3 Unfiltered (top) and filtered data (middle)

Additionally, interfacing components are less likely to have any play between them when the items are loaded, this would decrease noise caused by rattling or vibrating fits.

5.1.4 Load cell check

In order to verify that the force results obtained during the comparative study were truly comparable the load cells of the custom built machine (S2M 50N HBM load cells) were placed in series with a calibrated load cell on the Instron uniaxial tensile testing machine. The load cells were placed in compression and the results recorded. The results show that the bought load cells are accurate. Some slight vibrations were picked up by the HBM load cells but these did not negatively affect the results.

5.2 Uniaxial tensile testing

5.2.1 Instron uniaxial test results and discussion

Figure 5.4 shows the Stress versus Strain graph of the 20 specimens tested on the Instron tensile testing machine, using a 100 N load cell.

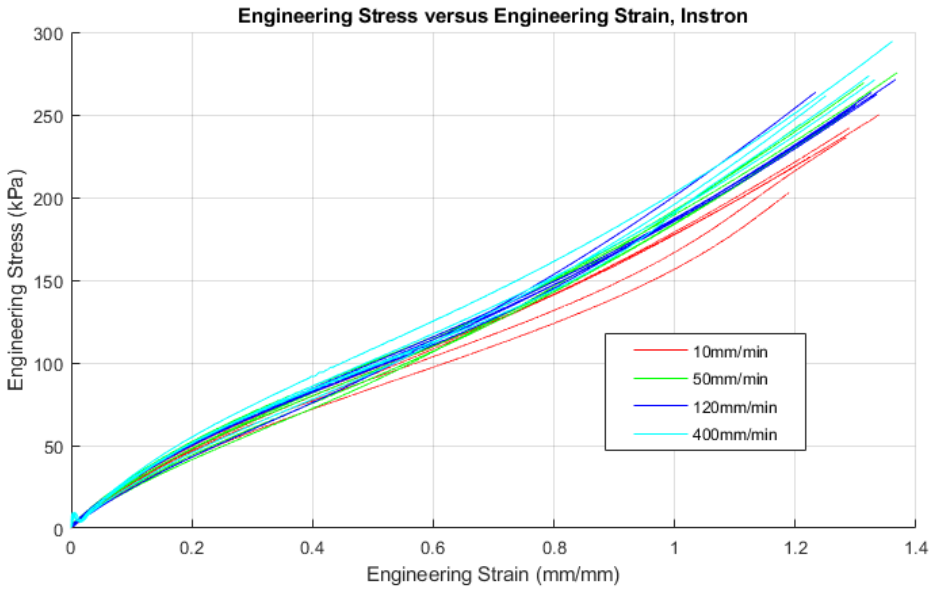

Figure 5.4 Engineering stress versus Engineering strain, testing done on Instron machine at CME, UCT

The results from the Instron testing demonstrated a few issues worth noting. The specimens exhibit strain rate dependent behaviour with the specimens tested at 10 mm/min showing consistently lower stresses between strains of 0.4 and 1.2. Likewise, the 400 mm/min tests show consistently higher stress values. This can be seen more clearly in Figure 5.5 below. The 400 mm/min tests also have a small but noticeable spike in stress at the start of the tests. This could could be a result of inertial effects due to the testing no longer being truly quasi-static or an effect of the grips or other physical mechanisms within the machinery at higher testing speeds.

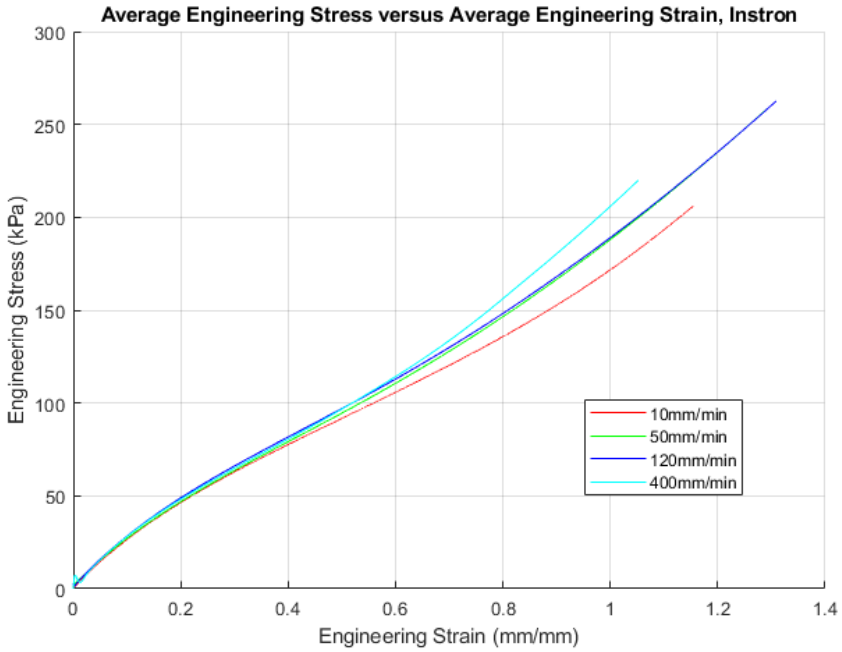

Figure 5.5 Average Stress v Average strain curve for each speed tested on Instron Uniaxial Tensile tester

The thickness of the specimens can be difficult to measure as the Dragon Skin 10 is so pliable. The specimens deform in the user's hand if held up for measurement with a vernier. To obtain more reliable measurements of thickness, the specimens were laid flat on a surface measuring table, and a height gauge used to determine thickness. It was also difficult to load the specimens into the grips on the Instron machine (Figure 5.6) without unintentionally applying a small pre-load, or inversely, leaving slack in the specimen. As the forces needed to deform the specimens are so small extra care was needed to accurately reproduce the same starting point for all specimens.

5.2.2 Custom machine results: first test and resulting changes

The custom built planar biaxial tensile testing machine was used to test the Dragon Skin 10 uniaxial tensile specimens, using the same test parameters and specimens from the same batch as those used in the Instron tests. It was the first time that the machine was used while incorporating all the sub-systems together at once with test specimens. Twenty specimens were tested at four different strain rates as specified in Section 4.3.1.

There were some clear issues in the data obtained. The results can be seen in Figure 5.7; the figure illustrates some of the technical issues encountered. Although there is some noise and other mechanical issues there were some positives from the testing. There was still significant overlap of the testing results on the custom machine and those of the Instron tensile tester, and errors could be analysed and fixed.

Figure 5.6 Specimen under tension in Instron machine

In the top left image of Figure 5.7 it can be seen that there is noise throughout the test; this is a result of the Low-Pass Filter (as discussed in subsection 5.1.3) not being activated before testing began.

In the image on the top right of Figure 5.7 there are two interruptions to the data, the first at approximately 0.3 strain: where the DIC lost tack of the specimens, briefly causing the strain to momentarily go to zero. Then at approximately 0.55 strain there is significant noise. This is a result of the user accidentally bumping the table the machine was on. This demonstrates the sensitivity of the system.

The bottom left graph of Figure 5.7 is an example of a "stepping" phenomenon which was seen in four of the 20 tests. After some investigation it was found that the cause was a slight misalignment between the two arms of each carriage and was not the result of the specimen's response to loading. This caused the arm connected to the load cell to jam in its slot. This jamming caused the force measured to go through cycles of constant force (when the arm was jammed) and then relatively quick periods of loading as the arm overcame the friction needed to move in the slot again. Results with this stepping cannot provide reliable tensile testing data. Additionally, the observed "stepping" is a safety risk to the load cells as the actual load can reach an amount greater than the safety limits put in place on the load cells if the arm jams and then frees itself while loaded above the safety limit.

The bottom right image of Figure 5.7 shows an example of a large jump in force at the start of the test - the specimen was not preloaded. The load cell was undamaged in this

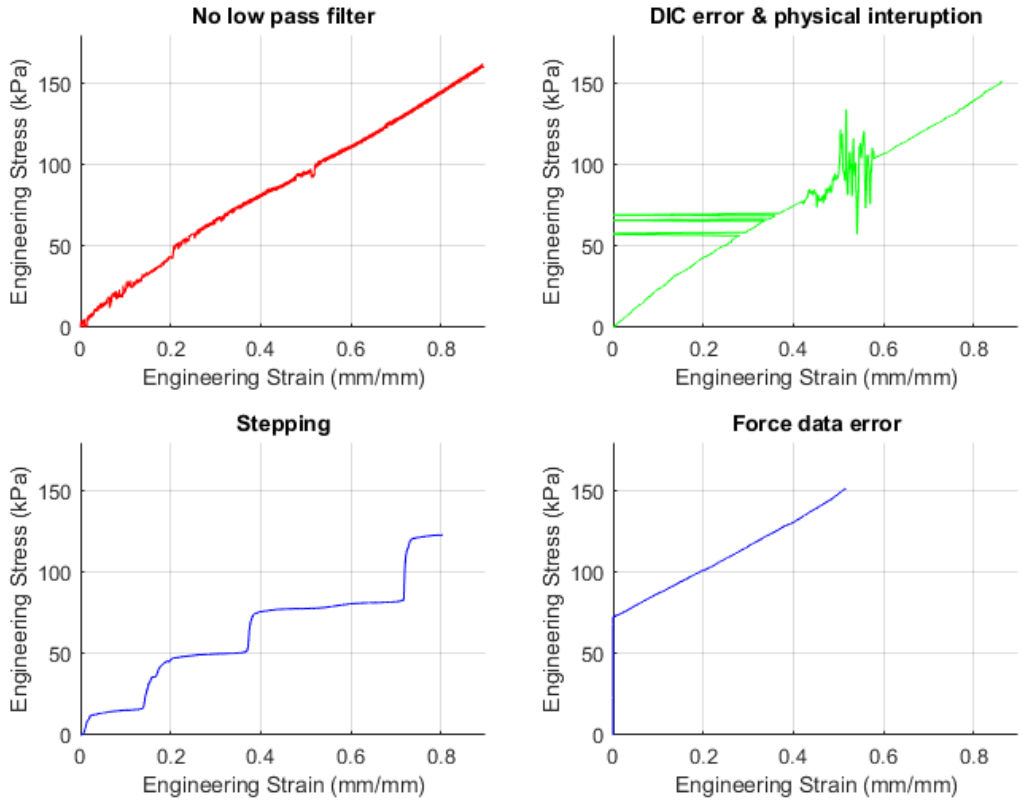

Figure 5.7 Figure showing some of the errors encountered while testing

case but such alignment errors are a risk to the safety of the load cells and the machine as a whole.

In order to address the errors discussed above modifications were made to the machine. The machine was reassembled with particular care taken to ensure the arms were aligned correctly. There were some physical changes to the carriages to make assembly easier and less likely to result in error, while also making it easier to ensure they are equidistant from the centre. This was done by making slots, as opposed to circular holes, to connect the carriage to the anti-backlash nut. This meant that the position of individual carriages could be easily adjusted without moving the carriage on the opposite end of the lead screw.

A central bushing (Figure 5.8) was designed to support the centre of lead screw as it was observed that there was a slight eccentricity in its rotation. Such an eccentricity is a concern due to unwanted fatigue effects on the central connection between the two halves of the lead screw as well a higher risk (although still relatively low at expected forces) of buckling of the lead screw.

The procedure for the test was refined to ensure specimens were loaded more reliably into the machine, which included marking the specimens to ensure the same amount of

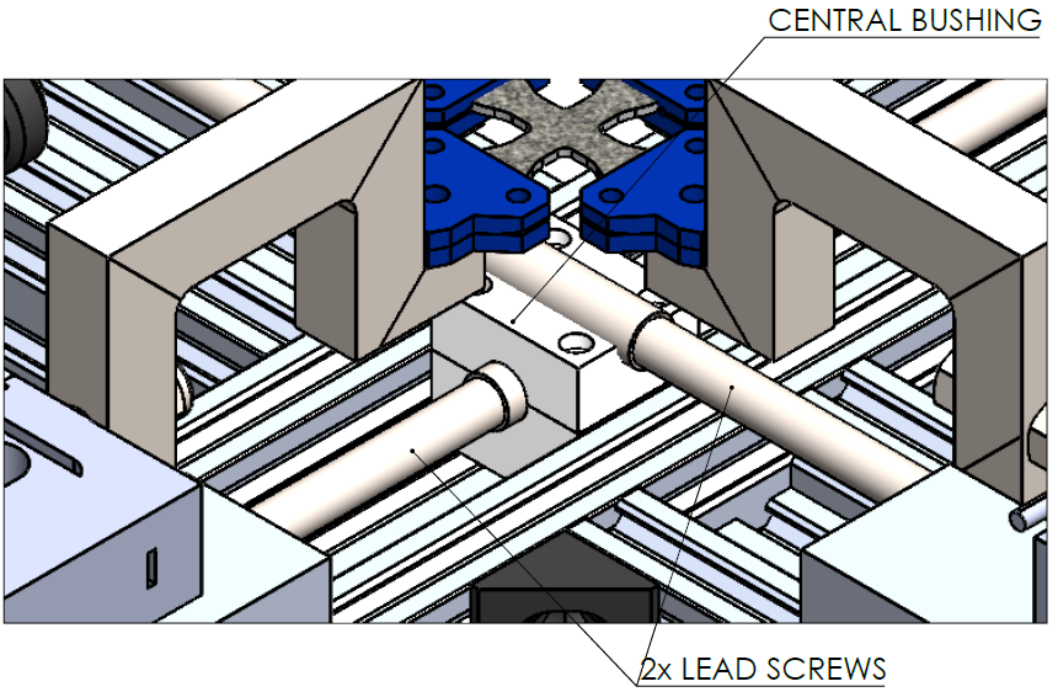

Figure 5.8 Figure showing central bushing which was added to machine to support the lead screws

each specimens was loaded into the grips. This would mitigate the risk of some specimens being accidentally pre-loaded or mounted with slack prior to testing.

5.2.3 Designed machine results; Second uniaxial test

After the changes discussed in Section 5.2.2 were implemented a second set of uniaxial tensile tests was performed. As detailed in Section 4.3.2, 20 specimens were tested in total; 10 on each axis, with half tested at 50 mm/min and half tested at 400 mm/min. The same specimens were used as those used during the Instron and first custom machine tests. Initially, each specimen was only meant to be used once, but rather than making a new set of specimens which may differ in material properties to those tested on the Instron, the same specimens were used. This meant that the second round of testing was limited to 50 and 400 mm/min due to the fact that both axes were tested as opposed to a single axis that was tested during the first round of testing. As the amount of specimens available for testing was limited, only certain speeds were retested.

Dragon Skin fits within the broad category of unfilled silicone rubber. The manufacturer claims an elongation at break of 1000% [54] and testing by Graham [26] reached strains of 700%, which was the limit of the Instron machine's extension, without rupture. Meunier et al [56] studied a comparable unfilled silicone rubber and found that any hysterisis and Mullins effect were negligible. No permanent deformation was observed during

the first set of tensile tests on these specimens, where the maximum strain was limited to 40%. As the second set of tensile tests was performed at least three weeks after the first set, the influence of repeated tension on the same specimens was considered insignificant. The likelihood of variation between the first batch of specimens and any new batch prepared thereafter, was considered to be much higher as solvent content, cure temperature humidity and duration all impact the mechanical properties of the silicone rubber. As damage from previous clamping was another potential source of error all specimens were checked for visible damage before being reused.

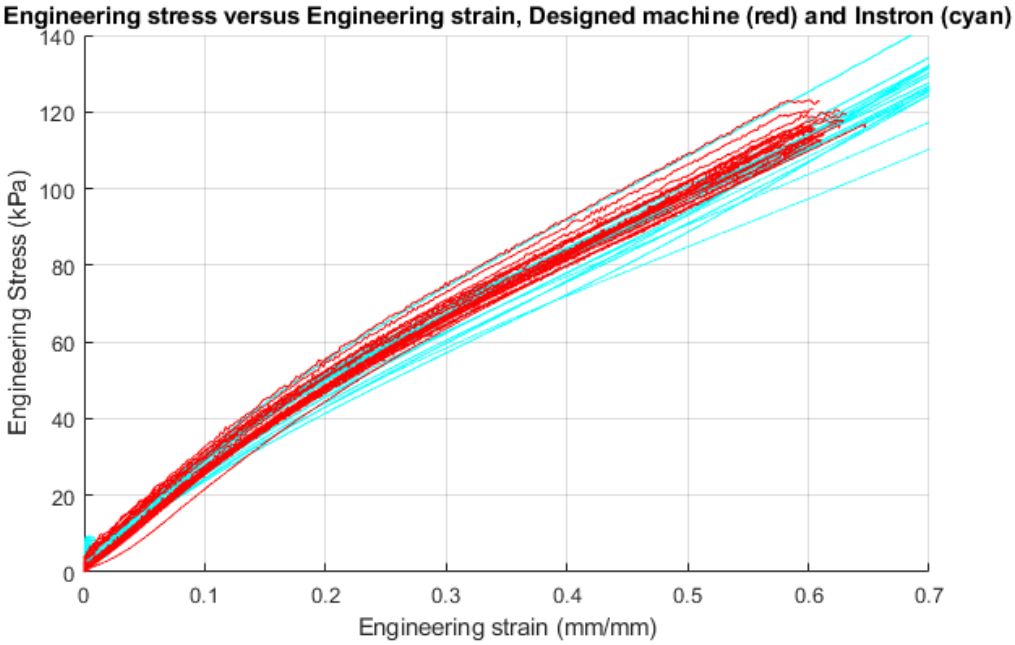

Figure 5.9 Engineering stress versus Engineering strain, testing done on custom designed machine

Figure 5.9 shows all the Instron test results in cyan and the second set of tests done on the custom designed machine in red. There was some noise recorded which was investigated and found to be from the sheet metal tray the machine was placed on. Future tests would need to be done on a more sturdy and well damped system. The vibrations were recorded only in the force measurement and not the displacement measurement of the DIC.

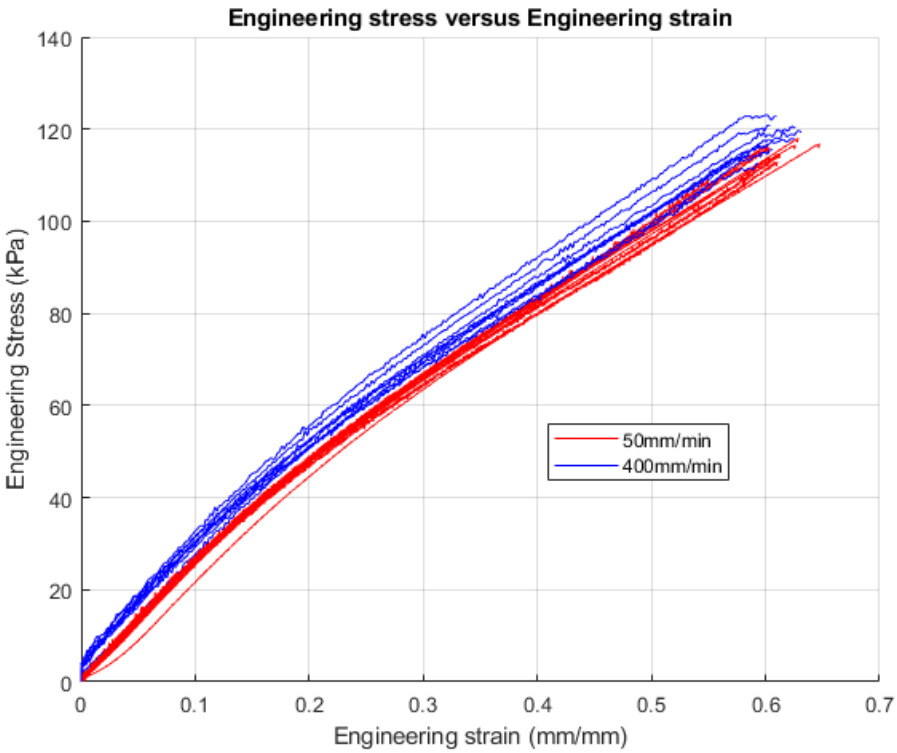

Figure 5.10 Strain rate dependence of specimens

The specimens exhibited a strain rate dependent response to loading; as seen in Figure 5.10. The 50 mm/min tensile test results were consistently lower than those tested at 400 mm/min. This is consistent with the tensile testing done on the Instron tensile testing machine as previously shown in Figure 5.5.

5.2.4 Comparison

Figure 5.11 compares the stress-strain response for all tests performed at 50 mm/min (on the Instron, designed machine white axis and red axis), while Figure 5.12 compares the data for tests at 400 mm/min. Note that the dual lines for the custom machine's data are upper and lower limits for loading curves, not an averaged load-unload test. Likewise, the green and blue bands show the full range of the data from the Instron machine at 50 mm/min and 400 mm/min respectively.

It can be seen that the stress-strain curves from both the red and white axes are within the bounds of of the data obtained during testing on the Instron machine. Therefore, for the speeds, displacements and forces tested the custom machine provides data which is equivalent to that obtained on the Instron. It must be noted that there was some difficulty placing the specimens into the grips on the Instron and it is expected that this fact is responsible for some of the variation recorded during the Instron machine tests.

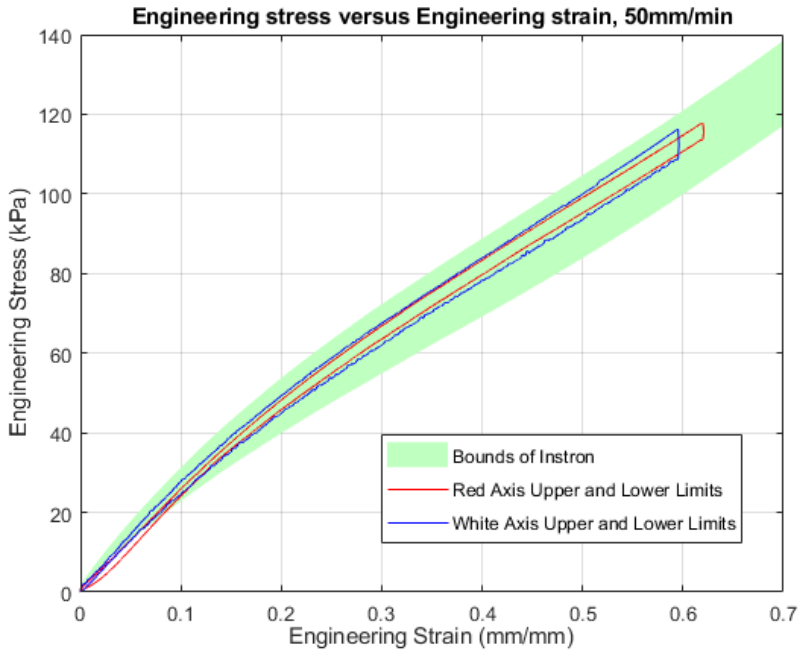

Figure 5.11 Engineering stress versus Engineering strain, comparison between Instron and custom machine at 50 mm/min

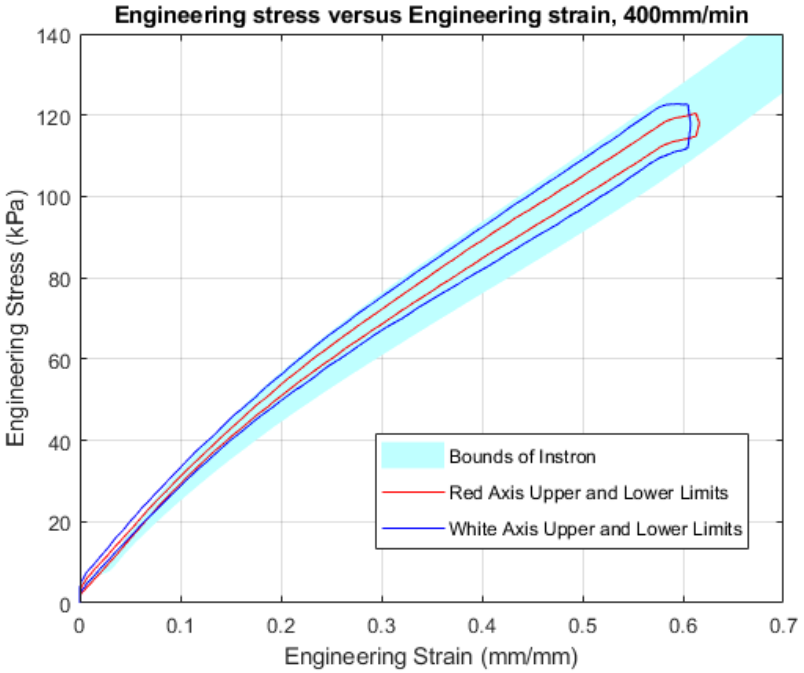

Figure 5.12 Engineering stress versus Engineering strain, comparison between Instron and custom machine at 400 mm/min

The results shown in Figures 5.11 and 5.12 have been limited to a strain below 70%, because the custom built machine was not designed for such large specimens and defor-

mations. The specimen size and expected deformations of biological biaxial specimens is significantly smaller than those used during this testing. With regards to loads encountered the custom machine did not record any forces above 5 N during testing. Although this is lower than the full desired range it does compare well with the majority of testing done on planar biaxial soft tissue specimens as seen in literature in Section 2.4.4.

From the results of the uniaxial testing it can be concluded that the design concept has been verified, as the results obtained compare favourably with those from a commercially built testing machine. The custom built machine was further used to test planar biaxial Dragon Skin 10 specimens at varying strain rates and loading ratios to verify that the machine can successfully operate as a fully operational planar biaxial tensile testing machine.

Chapter 6

Biaxial Experimental Procedure

Having successfully demonstrated the custom planar biaxial machine's capability to perform uniaxial tests on either axis, the system still needed to be tested with simultaneous biaxial tension. Unfortunately, it was not possible to locate a commercially built, calibrated planar biaxial tensile testing machine suitable for loads less than 50 N in the Western Cape province. Thus it was not possible to perform direct comparison tests for biaxial tension. The testing was done to assess whether the machine can reliably and accurately obtain results of a typical biaxial tensile test, as seen in literature, with an appropriate surrogate, such as Dragon Skin 10. The testing was not done to characterise any material but done to verify the design and build of the the planar biaxial tensile testing machine.

6.1 Biaxial Specimens

As discussed in Section 2.4.5, when performing biaxial tensile tests an area of uniform stress is desirable [30]. This can be complicated by gripping methods and the St Venant's like effects caused by said grips. It was decided to use cruciform specimens, as opposed to square specimens as is typically done when testing collagenous soft tissues. This was done as it was found that cruciform specimens could more reliably produce the uniform stress region needed for data analysis. As Dragon Skin 10 was to be used for testing rather than a soft tissue there was no material constraint which would make the amount of material needed for a cruciform specimen impractical as when dealing with human or animal tissue. The specimen dimensions are detailed in Figure 6.1.

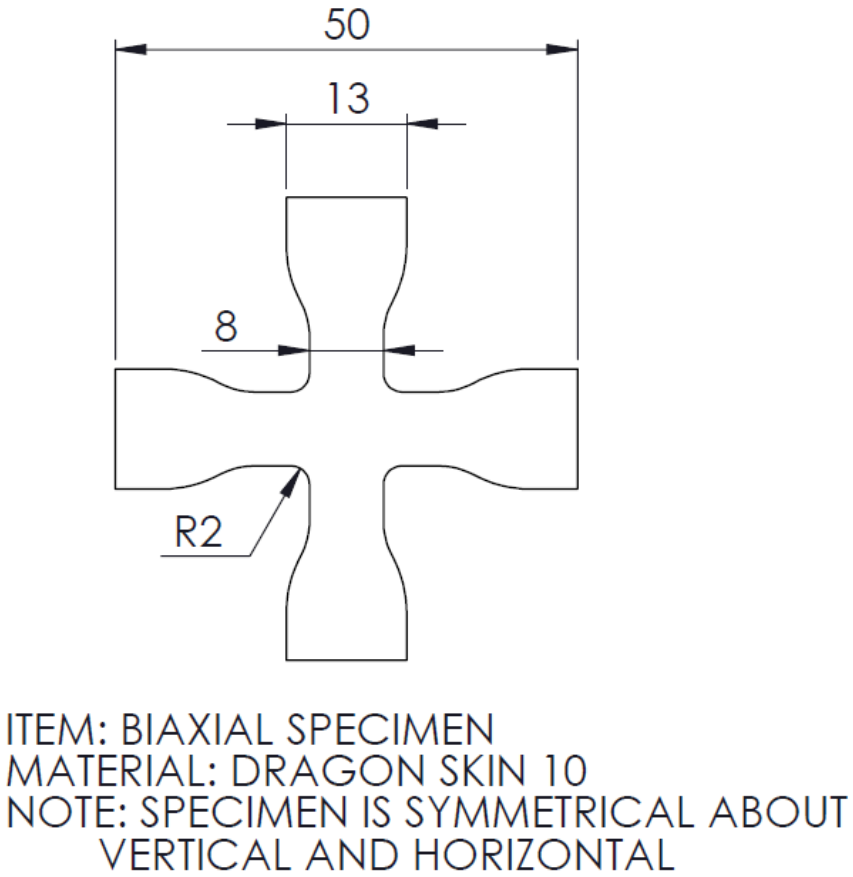

Figure 6.1 Dimensions of biaxial specimens

6.2 Biaxial testing plan and procedure

6.2.1 Biaxial commissioning testing plan

The biaxial tensile testing of the machine was designed to test a variety of loading rates. This was achieved by varying the speed and the ratio of the speeds of one axis compared to the other. Furthermore, testing was done with oscillating and varying loading in the same test.

The first round of testing involved constant speeds and ratios: where a 1:1 ratio would equate to both axes running at the same speed and 1:0 ratio would mean one axis is running at the selected speed, while the other is held stationary. The speeds for any given test are always given as the reference speed, which is the faster speed of the two axes. There were 4 speeds and 5 ratios used for testing; providing a total of 20 different possible tests. Some tests were run multiple times and one test was not run (10 mm/min at 1:0.5), this was because it was not necessary to test every ratio at every speed in order to verify the machine. Each specimen was only used once during testing. These ratios and

speeds were chosen to verify that the machine works as expected at a range of speeds and ratios expected to be used during the testing of collagenous soft tissues, as per the design requirements. Material characterisation was not a consideration when conducting these experiments. Testing was done in order of test number and test numbers were assigned randomly to help mitigate potential environmental confounding effects. The tests carried out and the number of specimens tested are shown in the Table 6.1 below.

Test num. (number of tests)	**10** *mm/min*	**50** *mm/min*	**120** *mm/min*	**400** *mm/min*
1:1	Test 1 (x2)	Test 15 (x4)	Test 12 (x2)	Test 3 (x3)
1:0.75	Test 10 (1)	Test 7 (x1)	Test 16 (x1)	Test 8 (x1)
1:0.5	No Test (x0)	Test 14 (x1)	Test 5 (x1)	Test 19 (x1)
1:0.25	Test 6 (x1)	Test 9 (x1)	Test 2 (x1)	Test 11 (x1)
1:0	Test 17 (x2)	Test 4 (x2)	Test 13 (x2)	Test 18 (x2)

Table 6.1 *Biaxial testing done using designed planar biaxial tensile testing machine. Test Number (number of tests): shown against testing speed vs speed ratio between the axes*

In order to verify the machine performance the following data needed to be obtained for analysis: DIC data for specimen surface deformation, axial force on each axis and the initial dimensions of the specimens. The controlled testing variables were the speed and total displacement of each axis independently. Table 6.2 below shows the sample frequencies used for obtaining the axial force and DIC data. As the load cells are separate to the DIC system the sample rates are different. The DIC sample rate was adjusted as the computational cost of analysing a 10 mm/min test at a high sample rate would be too great and unnecessary. Additionally, the maximum frame rate of the cameras imposed a limit on the fastest possible test speed.

Test speed (mm/min)	DIC sample frequency (Hz)	Force sample frequency (Hz)
10	1	100
50	5	100
120	10	100
400	25	100

Table 6.2 *Biaxial testing DIC and load cell sample frequency*

The second round of testing consisted of more complex loading profiles. This is necessary when performing cyclic loading on the machine when trying to establish visco-elastic properties of a material. First a single specimen was tested with repeated loading and unloading of the specimen at equal rates of 120 mm/min by 6 mm five times. There were also "asynchronous" tests with a more unconventional loading profile. Figure 6.2 displays the displacement versus time graph for both axes according to the GCode used to control the axes for the asynchronous tests.

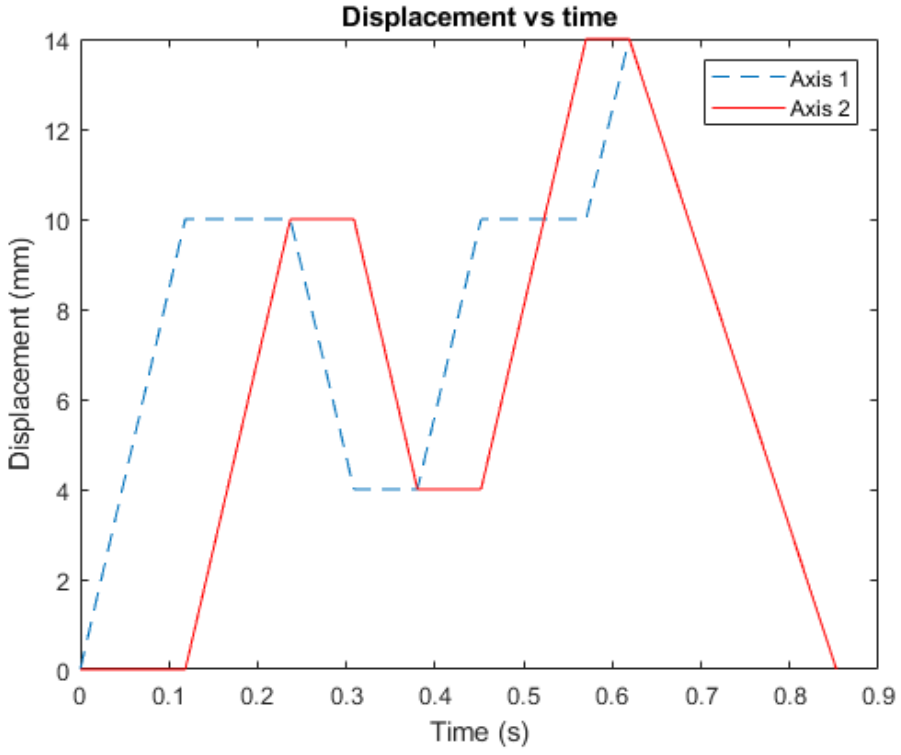

Figure 6.2 Displacement versus time graph for both axes during asynchronous biaxial testing

6.2.2 Data analysis plan

Typically in literature biaxial results are presented as stress and strain or stress and stretch results, therefore the stress and strain for each test would be recorded and analysed. Unfortunately, without the slits in the specimen arms specified in BSI ISO 16482:2014, it is not possible to consistently define the width of the gauge section of the cruciform specimen. To avoid calculating stress with an ill-defined area, which would not be an accurate representation, the force per unit of initial thickness is presented. Future biaxial testing of soft tissues should ensure that the gripping system and specimen geometry allows for a well defined gauge area. The strain used in the data analysis was the engineering strain along the two loading axes.

The testing needed to verify the following:

- the ability of the machine to run both axes simultaneously at different speeds,
- whether the gauge section remains stationary and centered during testing, and
- whether the specimen deformation remains planar.

To facilitate the above, the 3D surface deformation of the specimen was tracked with DIC.

6.2.3 Testing Procedure

The testing procedure for the biaxial testing is very similar to that detailed in Section 4.3.3. All testing was done using 3D DIC, therefore two cameras were needed for testing. From the uniaxial tensile testing results it was clear that extra care was needed to mount the specimens into the grips repeatedly. This was achieved by first setting the carriages to a known distance apart, then the specimens were marked so that they were mounted to the correct depths in the grips. If mounted to this predetermined depth and set onto the carriages the specimens were neither slack nor pre-loaded.

Chapter 7

Biaxial testing results and Discussion

This chapter details, analyses and discusses the results of the biaxial commissioning testing of the custom built planar biaxial tensile testing machine.

7.1 Biaxial tensile testing results

Figure 7.1 below shows a biaxial cruciform specimen fitted into the custom built planar biaxial testing machine during testing at CME. Lighting was carefully controlled to ensure optimum image quality for the DIC system.

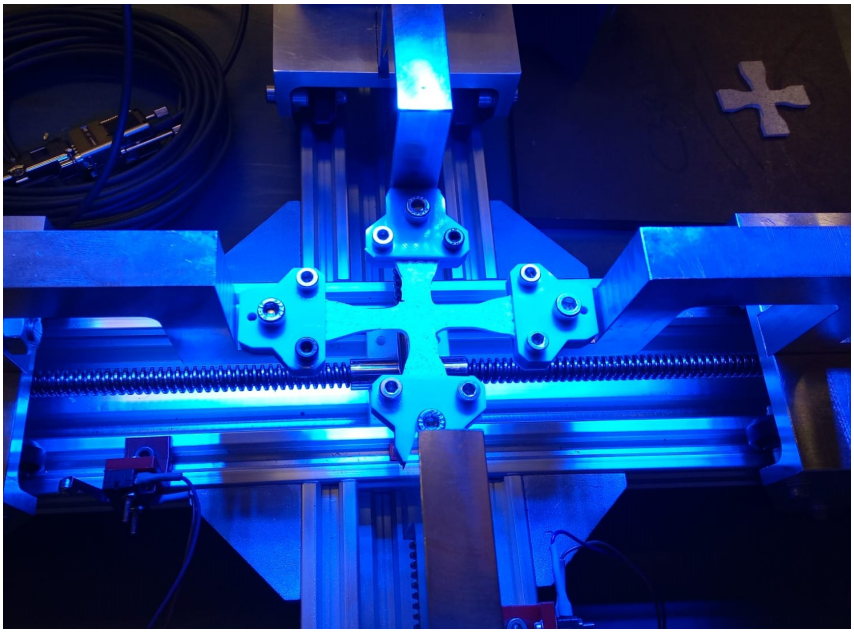

Figure 7.1 Photograph of biaxial testing specimen during testing

7.1.1 DIC strain data

The DIC data was analysed using the Istra4D software. Each test was evaluated individually using the appropriate calibration data obtained before each round of testing. The three figures below show the 1st principal strain superimposed onto an image of the specimen. The strain direction is displayed as a quiver plot and the magnitude of the strain is displayed with the colour. These specimens are in states of maximum deformation in the images below.

Figure 7.2 shows Test 15_4; which was run at 50mm/min at a displacement ratio of 1:1. The distribution of the strain across the specimen is as expected; with an area of uniform strain in the central region of interest and the strain in the arms being nominally uniform. The direction of the strains aligns with the testing axes as would be expected.

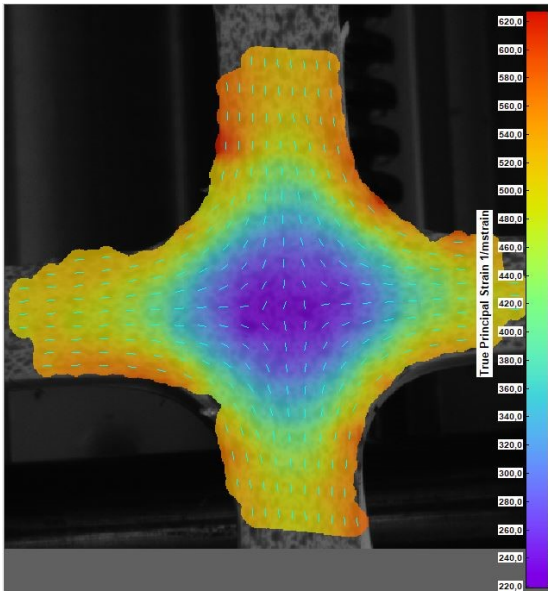

Figure 7.2 1st Principal Strain of Test 15_4 (1:1, 50mm/min) superimposed onto image of specimen during testing

Figure 7.3 shows the maximum deformation of test 17_1 where the test was run at 10mm/min at a ratio of 1:0. The direction of the 1st principle strain aligns with the reference axis and there is also some resistance provided by the specimen arms along the stationary axis as well. There is a notable variation between the strains measured in the opposite arms of the reference axis. This could be a result of a difference in thickness across the specimen, or from a misalignment in the mounting of the specimen or from mounting the one end of the specimen deeper into the grips than the other end of the specimen.

Figure 7.4 shows the principal strains of test 19_1 in which the rate of displacement was 400mm/min and the ratio was 1:0.5. It should be noted that the displacement reference

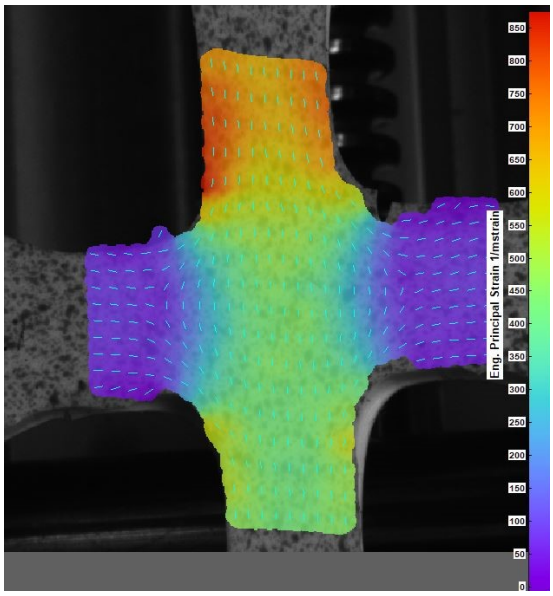

Figure 7.3 1st Principal Strain of Test 17_1 (1:0, 10mm/min) superimposed onto image of specimen during testing

axis in Figure 7.4 is horizontal, whereas it was the vertical axis in Figures 7.2 and 7.3. The resistance provided in the non-reference axis is clearly more than that in Figure 7.3 which was to be expected. There are two small regions of low strain that form above and below the the central uniform strain region.

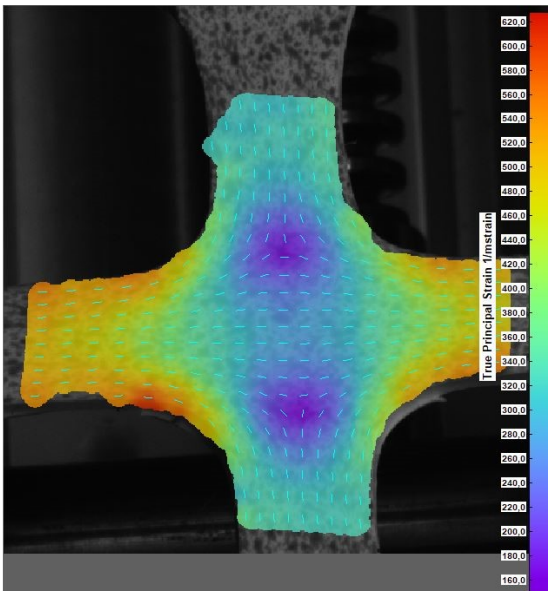

Figure 7.4 1st Principal Strain of Test 19_1 (1:0.5, 400mm/min) superimposed onto image of specimen during testing

As previously discussed the ROI at the centre of the cruciform should form a uniform strain area. In Figure 7.2 this can be seen clearly as the testing was done at a 1:1 ratio. For the Figures 7.3 and 7.4 the region is still uniform but the uniform gauge area is slightly

smaller and less obvious. Therefore when analysing the data on the Instra4D software the selection of the ROI is essential.

7.1.2 Out of plane motion

In order to verify that the deformation of the specimen was planar the Z-axis positions of 5 gauge points were plotted. One gauge point was placed at the centre of each arm of the cruciform specimen and one at the centre of the ROI. The coordinate axes and gauge points are shown in Figure 7.5.

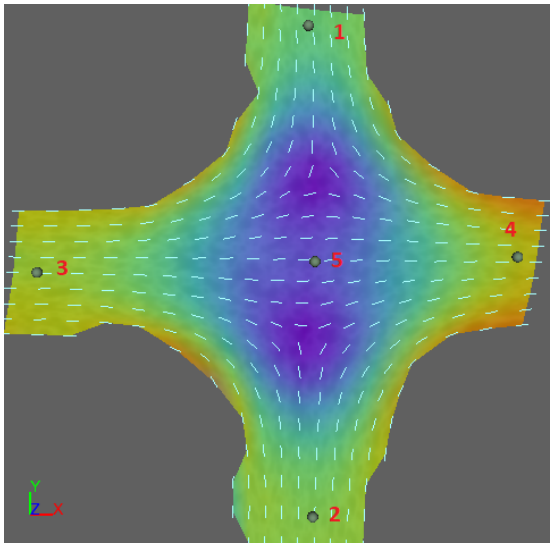

Figure 7.5 Gauge points shown on Specimen 10_1 (1:0.75, 10mm/min) during testing

Figure 7.5 displays the 1st principal stress of the specimen at its maximum deformation with the 5 gauge points in place. The position of these gauge points with respect to the Z-axis (out of plane) are shown in Figure 7.6 for four tests.

As can be seen in Figure 7.6 in tests 10_1 and 3_3 the cruciform arms depicted by gauge points 3 and 1 respectively, are not initially level with the other points. However, when a load is applied to the specimen the gauge points level out and all 5 gauge points are within 0.15mm of each other with respect to their Z-axis position in both test 10_1 and 3_3. This implies that a small initial out-of-plane offset has largely corrected and leveled out under load, and these tests may be considered as planar. It is also interesting to note that at maximum deformation the centre of the specimen (Point 5) is the lowest, which implies that the thickness of the specimen is thinner at the centre of the ROI than on the arms of the cruciform.

The self correction seen in tests 10_1 and 3_3 is not evident in test 13_2, with points 3 and 4 staying above the other gauge points throughout the test. Upon closer inspection it can be seen that the "self-correction" only happens across pairs of opposite gauge points on

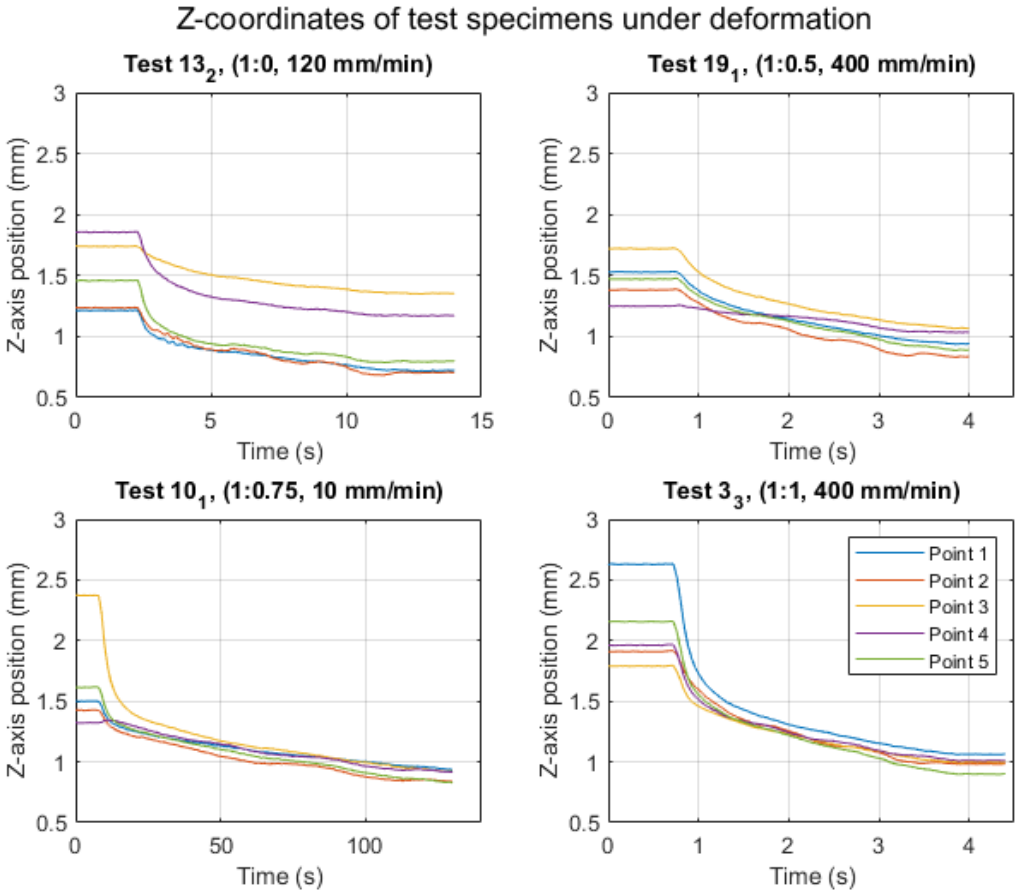

Figure 7.6 Z-axis position of the 5 gauge points on specimen 13_2, 19_1, 10_1 and 3_3 as per Figure 7.5

the same axis. Hence points 1 and 2 on the same axis will converge to the same height, but points 3 and 4 on the perpendicular axis may not converge to this height, which can be seen to a lesser extent in tests 10_1 and 19_1. It must also be noted that there was significantly less force applied across points 3 and 4 of test 13_2 as they were located on the zero displacement axis of a 1:0 test.

The out of plane motion is still too large according to BSI ISO 16482:2014; which stipulates that out of plane motion should be limited to 0.1mm. However, BSI ISO 16482:2014 is a standard for the planar biaxial testing of metals and not soft tissue. It should also be noted that the gauge points which were tracked to detect in the out of plane motion were located on the specimens which will narrow when undergoing deformation and would therefore be expected to show some out of plane motion even in a perfectly planar test.

Across the 4 tests shown in Figure 7.6 there does not seem to be a single point which is consistently out of plane. This would imply that there could be small inconsistencies when

mounting the specimens into the grips or when mounting the grips onto the machine. This would be consistent with the difficulties of mounting soft specimens reported in literature and experienced during this round of testing.

7.1.3 Translation of the Region of Interest (ROI)

It is important that the ROI remains centred during planar biaxial testing, as required by BSI ISO 16482:2014. The centre of the ROI was tracked to see if it remained centred with respect to the machine axes during loading of the specimens. Figures 7.7, 7.8 and 7.9 show the X and Y motion of the centre of the specimen during testing for 9 different specimens, grouped according to their strain ratios.

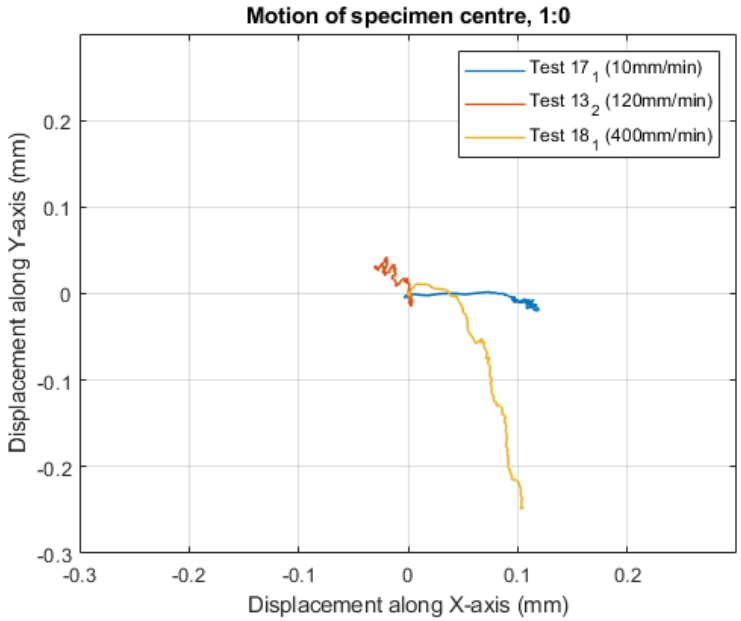

Figure 7.7 Displacement of the centre of the specimen during testing (1:0)

The motion direction appears to be random and the magnitude small. This implies that the errors are not consistent machine errors affecting testing but rather that the centre moves depending on how the specimen deforms. The maximum displacement displayed above is 0.27 mm recorded during test 18_1 in Figure 7.7. Compared to the grip displacements of 15 mm, this displacement is not significant enough to adversely affect the results nor show evidence of system machine error.

There are a number of potential causes of the drift of the centre of the ROI observed during testing. When mounting the specimens into the grips it can be very easy to load the specimen differently into the four grips due to the extremely pliable material being tested. This can be done by mounting the specimen at a slight angle relative to the loading axes or by loading the specimen further into certain grips. Additionally due to the nature of the manufacturing of the specimens there was some variation in thickness

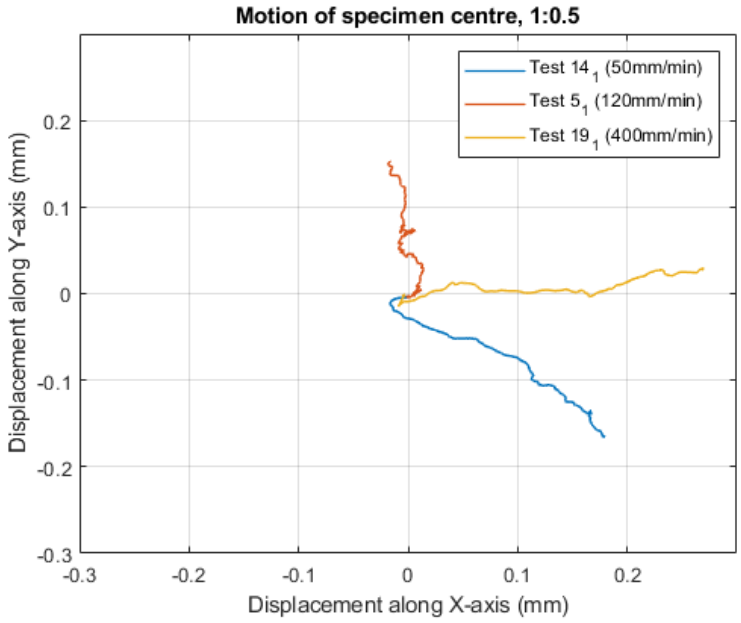

Figure 7.8 Displacement of the centre of the specimen during testing (1:0.5)

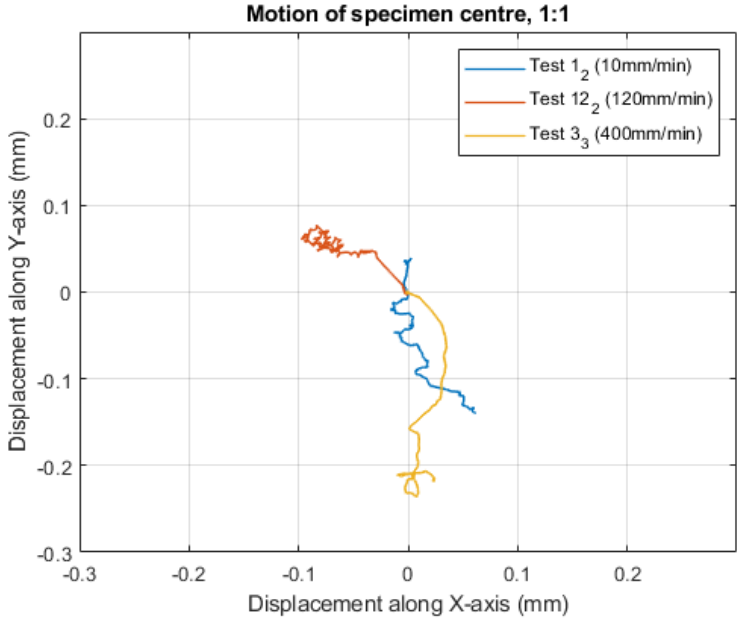

Figure 7.9 Displacement of the centre of the specimen during testing (1:1)

of the specimens, if one arm of the specimen is marginally thicker than the the opposite arm it would result in the ROI drifting towards the thicker specimen arm during loading.

7.1.4 Stress-strain response

As previously discussed, the load was normalised to Newtons per unit thickness rather than stress as the specimen geometry and pliability meant that it was not possible to define a consistent cross-sectional area. This is simplified when testing metals as specimens and means of measuring specimens are specified in standards which do not apply to the testing of silicone elastomers or biological specimens. The biaxial results are shown in Figures 7.10 to 7.14 and are grouped according to the displacement ratios of the tests performed.

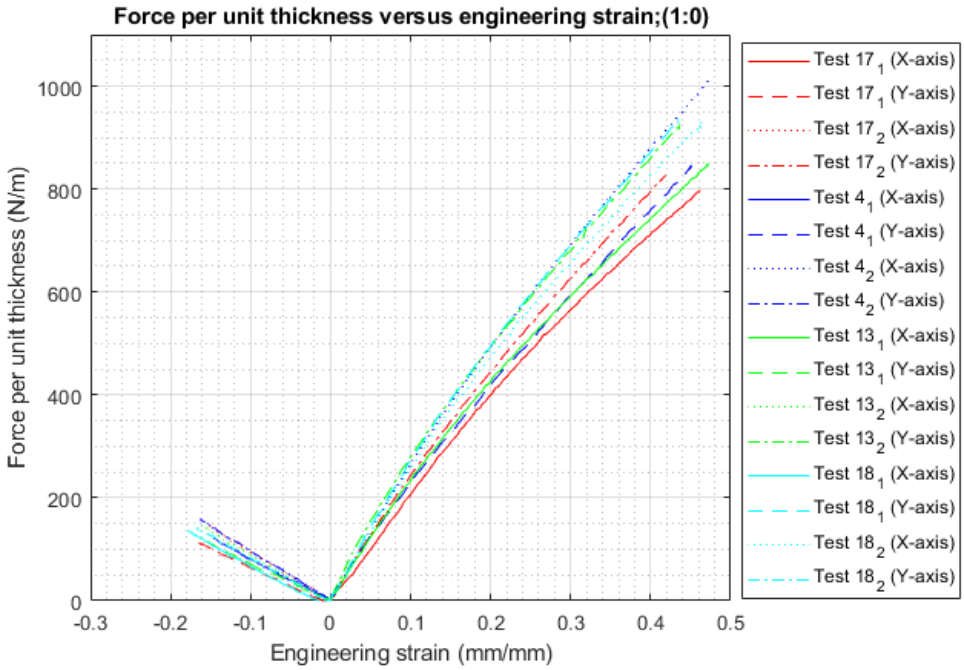

Figure 7.10 Force/Thickness versus tangential strain graph at stress ratio of 1:0

The tests performed at ratios of 1:0 and 1:0.25 both show a negative strain on the non-dominant testing axis. The results for the 1:0 testing seem well clustered (Figure 7.10). When some additional resistance is applied during the 1:0.25 testing (Figure 7.11) the results are no longer linear but there is still a negative strain along the less dominant axis. This was to be expected as lateral contraction would be observed in a uniaxial tensile test due to the Poisson effect; at the ratios of 1:0 and 1:0.25 the relatively low forces applied across the non-dominant axis are not enough to overcome this Poisson effect resulting in negative strains.

As the extension ratios increase the maximum strain decreases, conversely the strain along the non-dominant axis consistently increases. This culminates in the two axes meeting in Figure 7.14 when the strain ratio is 1:1, as would be expected. However, there were some outliers such as test 15_4 in Figure 7.14 which appears to show evidence of slack

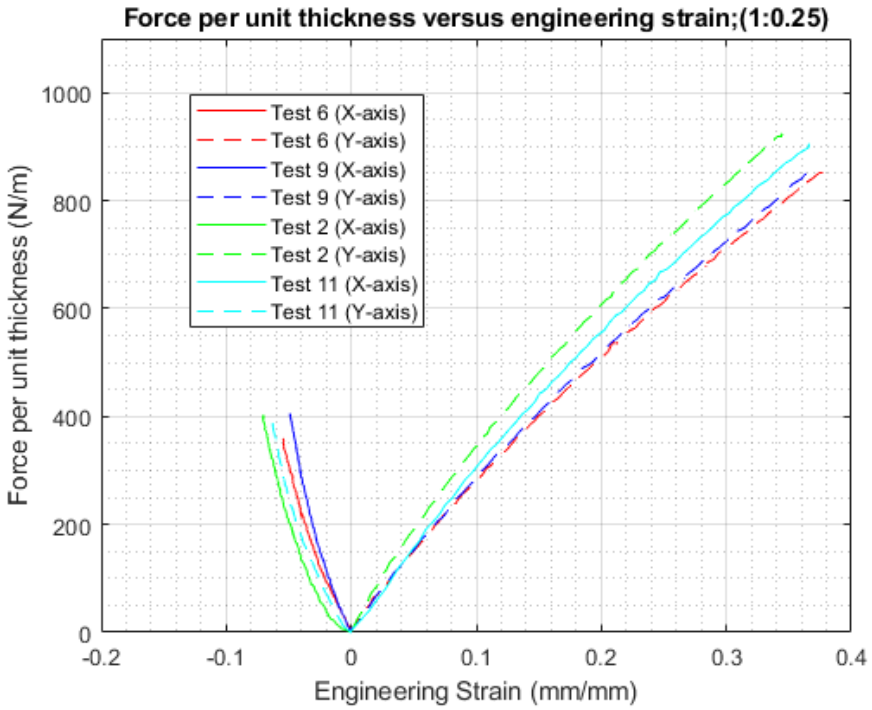

Figure 7.11 Force/Thickness versus tangential strain graph at stress ratio of 1:0.25

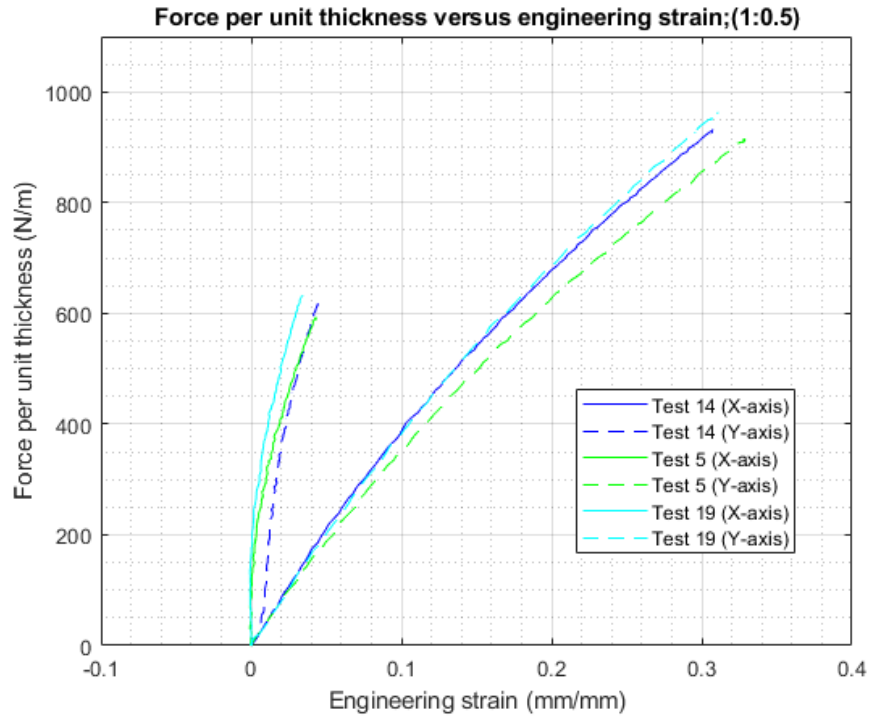

Figure 7.12 Force/Thickness versus tangential strain graph at stress ratio of 1:0.5

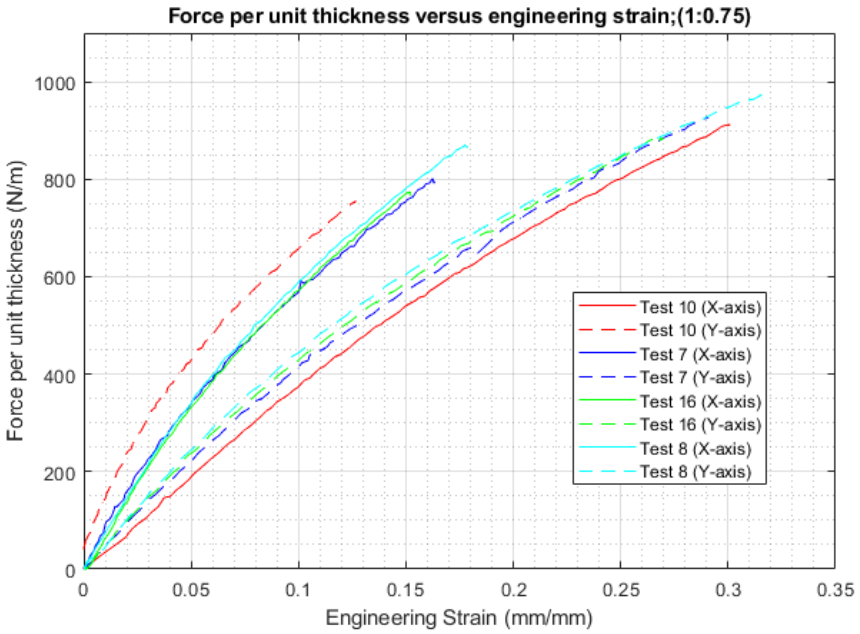

Figure 7.13 Force/Thickness versus tangential strain graph at stress ratio of 1:0.75

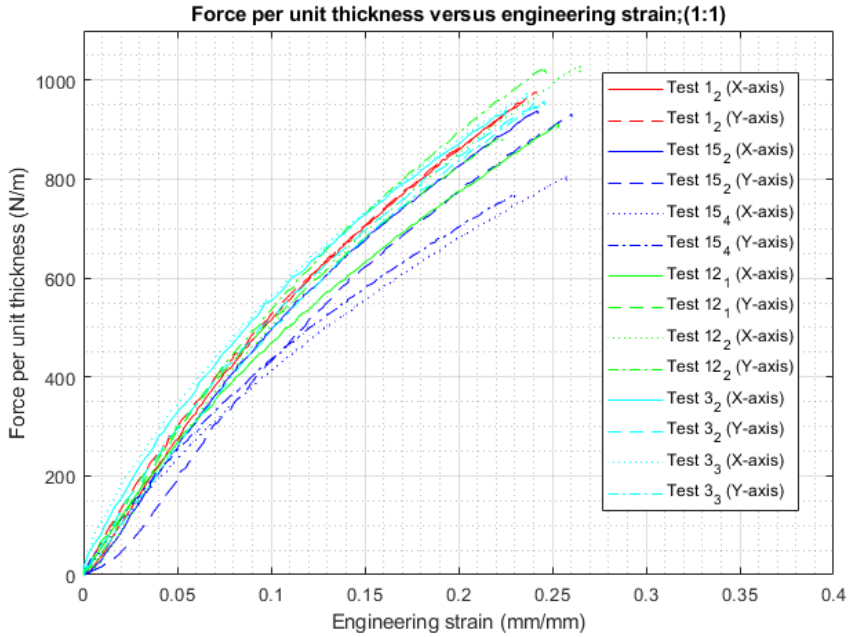

Figure 7.14 Force/Thickness versus tangential strain graph at stress ratio of 1:1

being present in the specimen when testing commenced. For the most part the data is consistent with the uniaxial results and most of the variation is believed to be a result of specimen and grip mounting inconsistencies. There was no consistent difference between

the results obtained from the two axes and the machine was able to perform all tests at the different speeds and testing ratios adequately.

7.1.5 Stress relaxation

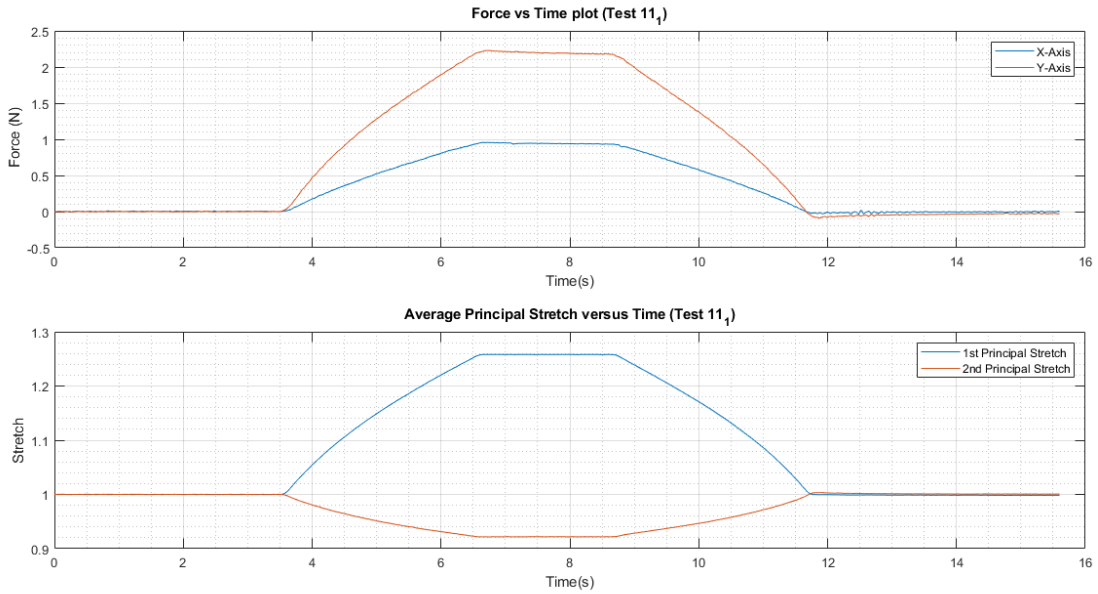

Figure 7.15 Force versus time (top) and stretch versus time (bottom) plots for Biaxial Test 11_1

Figure 7.15 shows both the force versus time (top) and stretch versus time (bottom) plots for specimen 11_1. The force and stretch for both axes of the biaxial test are shown. The graphs show both the loading and unloading of the specimen. It is interesting to note that there is slight hysteresis observed. This is made evident by the fact that when the carriages are not in motion between approximately 3.8 s to 11.8 s it can be seen that the stretch remains constant, but that there is a very slight but clear drop in force across the same time period. This was observed for all specimens and indicates stress relaxation at constant stretch, confirming that the material has a visco-elastic response.

7.1.6 Synchronous and asynchronous results

All the results shown have been done by the single loading of a specimen at a constant speed. Often biaxial soft tissue specimens undergo cyclic loading. In order to verify that the machine can apply a cyclic load and record the results correctly, a series of cyclical loading tests were performed. Figure 7.16 shows a test in which the applied displacement of both axes are the same and repeated.

The results displayed in Figure 7.16 show that the machine is capable of applying a cyclical load. There is an offset when comparing the two strains but this can be attributed

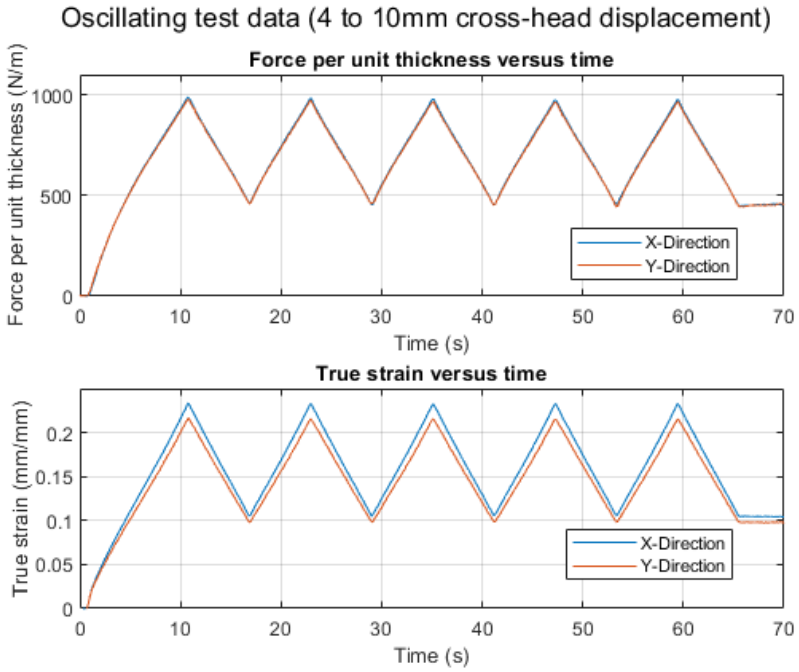

Figure 7.16 Results of synchronised oscillating test

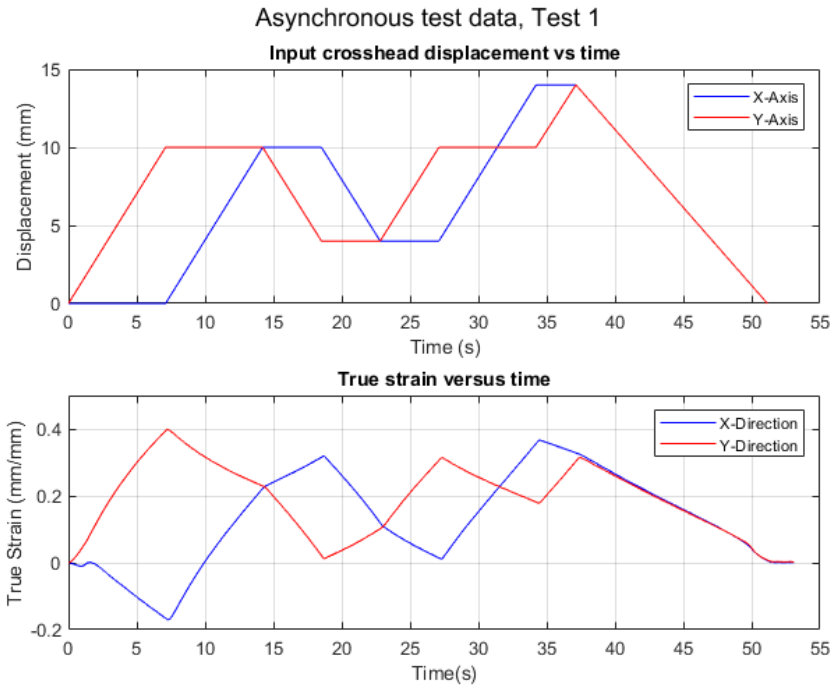

Figure 7.17 Results of asynchronous testing

to a variation in thickness of the perpendicular specimen arms. While the machine was not tested with a sinusoidal load, this can easily be achieved by adjusting the GCode: by

making the GCode follow a circular path in a 2D space, a sinusoidal loading curve would be achieved.

Figure 7.17 shows the results of an asynchronous test to show some of the more complex loading regimens that can be performed using the planar biaxial tensile testing machine. The top graph shows the intended displacement according to the GCode sent to the GRBL system, the bottom graph shows strain recorded when that GCode was applied to a specimen.

7.2 Discussion

7.2.1 Testing procedure and setup

There were some difficulties noted during testing of the biaxial specimens. Most difficulties concerned the repeatable and reliable mounting of the specimens. These could be mitigated in the future by implementing a more robust testing procedure and a better grip design. The major difficulties encountered were:

- Difficulty consistently aligning the specimens in the grips,
- difficulty consistently placing the specimens into the grips to the same depth,
- difficulty mounting the grips consistently into the machine,
- inconsistencies in calibration; the placement of the calibration plate during the initial calibration image when calibrating the DIC software determines the X, Y and Z directions which are used in post processing of the DIC data, and
- intra-specimen variability; although not as pronounced as the heterogeneous nature of biological specimens the specimens' thicknesses varied sufficiently that non-uniform deformation was detectable.

In order to mitigate the unwanted effects resulting from the aforementioned difficulties the following recommendations should be followed for future testing. Specimens should be measured and marked prior to testing to ensure that the same length of specimen is exposed (i.e. able to deform between the grips). This will allow for more consistent mounting of specimens with fewer specimens accidentally pre-loaded or slack on one or more specimen arms. This was done for later testing in this study and although it helped it did not completely resolve the issue as there were still uncertainties from the use of a ruler and pen to mark such soft and pliable specimens. Working with soft and pliable biological specimen will likely require the development of a dedicated mounting jig to assist in accurately mounting the specimens.

Additionally, the grips were mounted to the carriages using bolts which fixed the grips in place, which resulted in slight misalignments from placing the specimen into the grips or placing the grips into the machine. Therefore, these misalignments could affect the results and may cause slight inconsistencies. In order to mitigate these inconsistencies it is recommended to give the grips a rotational degree of freedom in the testing reference plane. Like the sutures attached to pulleys used in literature this would allow for small, unavoidable variations in mounting the specimens to be corrected as the specimen would be able to realign itself with the testing axes. For the grips used in the testing detailed here the bolt can be removed and testing can be performed using only the 3mm stainless steel pin which allows rotation but not translation of the grips, which would decrease the variation in results in the future.

7.2.2 Specimen and boundary conditions

As discussed in Section 7.2.1 there were some issues with the mounting and gripping of the specimens. It is hypothesised that these problems will only be exacerbated when handling soft tissue. The mounting of the specimens and grip design have a direct effect on the boundary conditions of the experiment.

Although there was no evidence of slipping during the testing, the repeatability of the mounting process was found to be a cause of variation in results. A system which allows in-plane rotation and lateral deformation would mitigate some of the inevitable errors in specimen mounting. For example; tethered sutures on pulleys would correct this but also require user dexterity to mount the specimens.

The specimen design prevented unwanted confounding effects like St Venant's effects and provided a uniform stress region in the gauge area. The forces recorded during testing were of the magnitude expected during testing planar soft tissue specimens. Therefore, the choice of Dragon Skin 10 for the commissioning testing described in this study can be considered as a reasonable material choice for a skin surrogate. However, other issues such as hygiene, and sterility were not tested during commissioning because of the use of a non-biological surrogate and will still need to be tested.

7.2.3 Machine performance

For the most part the custom built machine performed well. The individual axes produce uniaxial tensile data that is within the bounds of results obtained when using the calibrated Instron uniaxial tensile testing machine. The design, build and testing of the custom built planar biaxial tensile testing machine is considered to have been a first attempt and a proof of concept, and therefore performed well. Realistically there are design features which can be updated which will improve the performance of the machine.

As detailed in Section 7.1.2, there was some out of plane motion (Z direction) of the specimens during testing. This is undesirable and can result in unwanted bending effects or through shear of the specimens. Neither of these are measured or accounted for in post-processing of planar biaxial tensile testing. Although the measured Z displacements were small, some did exceed the amount specified by BSI ISO 16842:2014. The standard is intended to be followed for the planar biaxial testing of metals and not soft tissue, so the effects of the out of plane motion do not have as much of an effect on soft specimens as they would on a more rigid metal specimen. However, it was found that the four arms of the cruciform specimens remained planar with respect to each other during loading.

It is important to correctly align the specimens (especially when testing anisotropic collagenous tissue) with the loading axes of the machine, and in turn with those of the DIC system. This proved to be an area of difficulty during the commissioning testing of the machine. To ensure better alignment of the respective axes it is suggested that a calibration plate holder be made to align the calibration target with the machine axes for the first calibration image. This was done using the square faces of the stainless steel U-arms during the later biaxial testing and worked acceptably. However, a dedicated, more robust way of aligning the DIC and machine axes would be better and can be used for other grip/arm configurations. Furthermore, to ensure better specimen alignment to the grips, and therefore the machine, it is proposed that grips that allow for in plane rotation and contra-lateral boundary motion be used. This can be done in the form of tethers or rakes for example, or alternatively similar grips to those used during the commissioning testing can be used if they are not fixed, ie only attached via a pin that allows rotation.

The sanitary requirements of the machine were not tested and will still need to be investigated. The use of aluminium and stainless steel for the majority of the machine components should mean that it will not be negatively affected by the use of biological specimens and can be easily cleaned with bleach or alcohol, although hard to reach areas of the device are a concern for cleaning.

Chapter 8

Conclusion and Recommendations

The aim of this investigation was to design, build and test a planar biaxial tensile testing machine with the intention of using the machine to test skin and soft membrane tissues in the future. The machine was designed and built as two orthogonal and independent axes. Each axis consists of a lead screw of half left-handed and half right-handed thread driven by a stepper motor with gears connecting the screw to the motor. Force was measured using a 50 N load cell on each axis and deformation was measured using a non-contact DIC system. Uniaxial tensile testing was done on a silicone elastomer on each axis independently and results were compared to those obtained using an Instron uniaxial tensile testing machine with the same specimens. Machine and procedure adjustments were made as needed and then planar biaxial tensile testing was performed on silicone elastomer cruciform specimens.

8.1 Uniaxial tensile testing on custom machine

The custom machine detailed in Chapter 3 was designed and constructed as part of this investigation. The machine concept was verified by performing tests on the two axes independently and then comparing them to the results obtained when using an Instron uniaxial tensile testing machine while testing the same Dragon Skin 10 silicone elastomer as a skin surrogate. The commissioning tests performed on the individual axes were: displacement tests, speed tests, safety system checks and finally full uniaxial tensile tests.

After initial testing on the first axis there were some errors detected in the results obtained using the custom machine, which were resolved by minor modifications to the machine. These changes included making the machine easier to assemble, adding a bushing to support the lead screw, adjusting the testing procedure and using a 20 Hz low pass filter on load cell data. These changes resulted in a significant improvement in the results. Both axes were tested at 50 and 400 mm/min and the results fell within the bounds of

the data obtained when using the calibrated Instron tensile testing machine on the same tensile testing specimens at the same rates. Therefore the machine design was verified when testing the specimens uniaxially.

The specimens were a source of difficulty from manufacture through to testing. Initially during fabrication, the speckling of the silicone specimens was more difficult than anticipated. After several methods were tried, an airbrush was found to be the best way to speckle the specimens with a special silicone based product used in special effects (Psycho Paint, Smooth-On). During testing the specimens proved difficult to repeatably mount due to their soft and pliable nature.

8.2 Planar biaxial tensile testing

Planar biaxial tensile testing was then performed using the custom machine. This testing was intended to prove the machine's ability to test specimens over a wide range of speeds and displacement ratios for both axes. A further requirement was to quantify any undesirable translation of the specimen during testing both in and out of the reference plane. Biaxial testing was done on cruciform Dragon Skin 10 specimens at four different speeds and 5 different strain ratios between the axes. The speeds were: 10, 50, 120 and 400 mm/min, and the ratios were: 1:1, 1:0.75, 1:0.5, 1:0.25 and 1:0.

Minor out of plane motion of the specimen was observed, which is attributed to minor inconsistencies in mounting height of the specimen arms. The out of plane displacement was not considered large enough to negatively affect the results for soft tissue specimens. The U-shaped arms used for testing are also a potential source of some out of plane motion as the arms will tend to open and bend when loaded. Calculations were done to ensure this would not be the case however at the forces observed during this investigation.

There was also some in-plane drift of the ROI observed during testing; this was to be expected due to minor intra-specimen variation in thickness and due to inconsistencies in mounting the specimen perfectly in the centre of the machine. The in-plane drift was random and small in magnitude. It was concluded that it was not a result of machine error. These difficulties are most likely a result of the soft and pliable nature of the specimens, which can be accidentally mounted into the grips and the machine with unwanted preloads or slack across the specimen. These difficulties were also widely reported in literature when dealing with soft biological membranes. A jig to ensure the correct mounting of specimens would mitigate these errors and is recommended for future testing.

Clamp grips were used for both the uniaxial and biaxial testing performed. Some of the difficulties and errors encountered during testing can be mitigated by redesigning the grips. By using a design that allows in-plane rotation within the reference plane and allows contra-lateral deformation of the specimen boundaries these expected human

mounting errors can be corrected as the specimen would realign itself when loaded. The clamped grips were successful in that there was no evidence of slipping during testing and their modular design made them relatively easy to use.

As a whole the machine performed the planar biaxial tensile tests well. The results obtained were repeatable and as anticipated. The machine performed well for all speeds and ratios tested; however, more testing at higher loads is still needed. Although there is room for improvement, as a first design and proof of concept the investigation is considered a success. Testing on skin and other collagenous membrane tissue can be undertaken with confidence at the rates and loads used in this study.

8.3 Recommendations

From this investigation the following recommendations for future use of the custom tensile testing machine are made.

- Create jig to align the DIC calibration plate with the machine axes. This will ensure that the testing axes align correctly with the axes used by the DIC software during post processing of the data.
- Create jig to hold specimens while mounting into grips and/or the machine; this will reduce the errors caused by poor repeatability of mounting of specimens observed in this investigation.
- Design of new grips for testing biological specimens; from the testing done in this study and from literature it is believed that a system which will allow some in-plane rotation and contra-lateral motion would be preferable.
- Investigation into the cleanliness of the device when used with biological specimens. This includes the potential use of an environmental chamber as well as the effects of the specimens and saline bath on the machine.
- Although testing was performed at a wide range of testing speeds the testing was limited to a relative small range of loads. This was due to the nature of the specimens tested. In order to fully validate the machine further, testing at higher loads (above 5 N but less than 50N) is needed. An investigation into whether closed loop control would be worth while, in order to perform load control testing. It was not needed for the load range tested in this study.

Bibliography

[1] G. A. Holzapfel, "Biomechanics of soft tissue," in *The HANDBOOK OF MATERIALS BEHAVIOR MODELS, Volume III, Multiphysics Behaviors*, Boston: Composite Media ed. Academic Press, 2001, ch. 10, pp. 1049–1063.

[2] F. H. Silver, J. W. Freeman, and D. Devore, "Viscoelastic properties of human skin and processed dermis," Tech. Rep., 2001, pp. 18–23.

[3] A. Ní Annaidh, K. Bruyère, M. Destrade, M. D. Gilchrist, and M. Otténio, "Characterization of the anisotropic mechanical properties of excised human skin," *Journal of the Mechanical Behavior of Biomedical Materials*, 2012, ISSN: 17516161. DOI: 10.1016/j.jmbbm.2011.08.016. eprint: 1302.3022.

[4] M. S. Sacks, "Biaxial mechanical evaluation of planar biological materials," *Journal of Elasticity*, vol. 61, pp. 199–246, 2000, ISSN: 03743535. DOI: 10.1023/A:1010917028671.

[5] *Biotester — cellscale*, Nov. 2021. [Online]. Available: https://www.cellscale.com/products/.

[6] A. Curry, "Design, manufacture and commissioning of a low pressure quasistatic bulge tester for skin and membrane tissue," MSc dissertation, University of Cape Town, 2020.

[7] D. Fischer, "The design and construction of a bulge testing device platform for human skin tissue applications," MSc dissertation, University of Cape Town, 2020.

[8] G. Limbert, "Mathematical and computational modelling of skin biophysics: A review," in *Proceedings of the Royal Society A: Mathematical, Physical and Engineering Sciences*, vol. 473, Royal Society Publishing, Jul. 2017. DOI: 10.1098/rspa.2017.0257.

[9] P. A. J. Kolarsick, M. A. Kolarsick, and C. Goodwin, "Anatomy and Physiology of the Skin," *Journal of the Dermatology Nurses' Association*, vol. 3, no. 4, pp. 203–213, Jul. 2011, ISSN: 1945-760X. DOI: 10.1097/JDN.0b013e3182274a98.

[10] A. Pissarenko, W. Yang, H. Quan, K. A. Brown, A. Williams, W. G. Proud, and M. A. Meyers, "Tensile behavior and structural characterization of pig dermis," *Acta Biomaterialia*, vol. 86, pp. 77–95, Mar. 2019, ISSN: 18787568. DOI: 10.1016/j.actbio.2019.01.023.

[11] J. W. Jor, M. P. Nash, P. M. Nielsen, and P. J. Hunter, "Estimating material parameters of a structurally based constitutive relation for skin mechanics," *Biomechanics and Modeling in Mechanobiology*, vol. 10, no. 5, pp. 767–778, Oct. 2011, ISSN: 16177959. DOI: 10.1007/s10237-010-0272-0.

[12] S. L. Evans and C. A. Holt, "Measuring the mechanical properties of human skin in vivo using digital image correlation and finite element modelling," *Journal of Strain Analysis for Engineering Design*, 2009, ISSN: 03093247. DOI: 10.1243/03093247JSA488.

[13] G. A. Holzapfel and R. W. Ogden, "On planar biaxial tests for anisotropic nonlinearly elastic solids. A continuum mechanical framework," *Mathematics and Mechanics of Solids*, 2009, ISSN: 10812865. DOI: 10.1177/1081286507084411.

[14] A. Kalra, A. Lowe, and A. Al-Jumaily, "Mechanical Behaviour of Skin: A Review," *Journal of Material Science & Engineering*, 2016, ISSN: 21690022. DOI: 10.4172/2169-0022.1000254.

[15] K. Langer, "ON THE ANATOMY AND PHYSIOLOGY OF THE SKIN I. The cleavability of the cutis," *British Journal of Plastic Surgery*, pp. 3–8, 1978.

[16] M. Ottenio, D. Tran, A. Ní Annaidh, M. D. Gilchrist, and K. Bruyère, "Strain rate and anisotropy effects on the tensile failure characteristics of human skin," *Journal of the Mechanical Behavior of Biomedical Materials*, vol. 41, pp. 241–250, 2015, ISSN: 18780180. DOI: 10.1016/j.jmbbm.2014.10.006.

[17] J. McGrath, R. Eady, and F. Pope, "Anatomy and Organization of Human Skin," in, ch. Chapter 3:

[18] P. G. Agache, C. Monneur, J. L. Leveque, and J. De Rigal, "Mechanical properties and Young's modulus of human skin in vivo," *Archives of Dermatological Research*, 1980, ISSN: 0340-3696. DOI: 10.1007/BF00406415.

[19] L. Falland-Cheung, M. Scholze, P. F. Lozano, B. Ondruschka, D. C. Tong, P. A. Brunton, J. N. Waddell, and N. Hammer, "Mechanical properties of the human scalp in tension," *Journal of the Mechanical Behavior of Biomedical Materials*, 2018, ISSN: 18780180. DOI: 10.1016/j.jmbbm.2018.05.024.

[20] O. A. Shergold, N. A. Fleck, and D. Radford, "The uniaxial stress versus strain response of pig skin and silicone rubber at low and high strain rates," *International Journal of Impact Engineering*, 2006. DOI: 10.1016/j.ijimpeng.2004.11.010.

[21] C. Pailler-Mattei, S. Bec, and H. Zahouani, "In vivo measurements of the elastic mechanical properties of human skin by indentation tests," *Medical Engineering and Physics*, 2008, ISSN: 13504533. DOI: 10.1016/j.medengphy.2007.06.011.

[22] F. M. Hendriks, D. Brokken, J. T. W. M. van Eemeren, C. W. J. Oomens, F. P. T. Baaijens, and J. B. A. M. Horsten, "A numerical-experimental method to characterize the non-linear mechanical behavior of human skin," *Skin Research and Technology*, 2003, ISSN: 0909752X. DOI: 10.1034/j.1600-0846.2003.00019.x.

[23] S. D. Waldman and J. Michael Lee, "Boundary conditions during biaxial testing of planar connective tissues. Part 1: Dynamic behavior," Tech. Rep. 10, 2002, pp. 933–938. DOI: 10.1023/A:1019896210320.

[24] N. Kumaraswamy, H. Khatam, G. P. Reece, M. C. Fingeret, M. K. Markey, and K. Ravi-Chandar, "Mechanical response of human female breast skin under uniaxial stretching," *Journal of the Mechanical Behavior of Biomedical Materials*, 2017, ISSN: 18780180. DOI: 10.1016/j.jmbbm.2017.05.027.

[25] T. K. Tonge, L. S. Atlan, L. M. Voo, and T. D. Nguyen, "Full-field bulge test for planar anisotropic tissues: Part I-Experimental methods applied to human skin tissue," *Acta Biomaterialia*, 2013, ISSN: 17427061. DOI: 10.1016/j.actbio.2012.11.035.

[26] A. Graham, "Design and implementation of a high strain rate biaxial tension test for elastomeric materials and biological soft tissue," MSc dissertation, University of Cape Town, 2020.

[27] L. Treloar, "The Physics of Rubber Elasticity," *Oxford Univ. Press*, 1975.

[28] R. Rivlin and D. Saunders, "Large elastic deformations of isotropic materials, vii. Experiments on the deformation of rubber," *Philos. Trans. R. Soc*, pp. 251–288, 1951.

[29] Y. Lanir and Y. C. Fung, "Two-dimensional mechanical properties of rabbit skin-I. Experimental system," *Journal of Biomechanics*, vol. 7, no. 1, pp. 29–34, 1974, ISSN: 00219290. DOI: 10.1016/0021-9290(74)90067-0.

[30] M. S. Sacks and W. Sun, "Multiaxial Mechanical Behavior of Biological Materials," *Annual Review of Biomedical Engineering*, 2003, ISSN: 1523-9829. DOI: 10.1146/annurev.bioeng.5.011303.120714.

[31] *574 series planar biaxial test machine - testresources, inc.* Nov. 2021. [Online]. Available: https://www.testresources.net/test-machines/planar-biaxial-test-machines/574-series-planar-biaxial-test-machine/.

[32] A. Hannon and P. Tiernan, *A review of planar biaxial tensile test systems for sheet metal*, 2008. DOI: 10.1016/j.jmatprotec.2007.10.015.

[33] G. Ferron and A. Makinde, "Design and development of a biaxial strength testing device," *Journal of Testing and Evaluation*, no. 16, pp. 253–256, 1988.

[34] G. Sommer, A. J. Schriefl, M. Andrä, M. Sacherer, C. Viertler, H. Wolinski, and G. A. Holzapfel, "Biomechanical properties and microstructure of human ventricular myocardium," *Acta Biomaterialia*, vol. 24, pp. 172–192, 2015. DOI: 10.1016/j.actbio.2015.06.031. [Online]. Available: http://dx.doi.org/10.1016/j.actbio.2015.06.031.

[35] A. J. Skulborstad, S. M. Swartz, and N. C. Goulbourne, "Biaxial mechanical characterization of bat wing skin," *Bioinspiration and Biomimetics*, vol. 10, no. 3, Jun. 2015, ISSN: 17483190. DOI: 10.1088/1748-3190/10/3/036004.

[36] R. Aydin, S. Brandstaeter, F. Braeu, M. Steigenberger, R. Marcus, K. Nikolaou, M. Notohamiprodjo, and C. Cyron, "Experimental characterization of the biaxial mechanical properties of porcine gastric tissue," *Journal of the Mechanical Behavior of Biomedical Materials*, pp. 499–506, 2017. DOI: 10.1016/j.jmbbm.2017.01.028.

[37] Y. Lanir and Y. C. Fung, "Two-dimensional mechanical properties of rabbit skin-II. Experimental results," *Journal of Biomechanics*, vol. 7, no. 2, 1974, ISSN: 00219290. DOI: 10.1016/0021-9290(74)90058-X.

[38] M. S. Sacks and C. J. Chuong, "Orthotropic mechanical properties of chemically treated bovine pericardium," Tech. Rep. 5, 1998, pp. 892–902. DOI: 10.1114/1.135.

[39] C. Bellini, P. Glass, M. Sitti, and E. S. Di Martino, "Biaxial mechanical modeling of the small intestine," *Journal of the Mechanical Behavior of Biomedical Materials*, vol. 4, no. 8, pp. 1727–1740, Nov. 2011, ISSN: 17516161. DOI: 10.1016/j.jmbbm.2011.05.030.

[40] G. D. O'Connell, S. Sen, and D. M. Elliott, "Human annulus fibrosus material properties from biaxial testing and constitutive modeling are altered with degeneration," *Biomechanics and Modeling in Mechanobiology*, vol. 11, no. 3-4, pp. 493–503, Mar. 2012, ISSN: 16177959. DOI: 10.1007/s10237-011-0328-9.

[41] S. E. Szczesny, J. M. Peloquin, D. H. Cortes, J. A. Kadlowec, L. J. Soslowsky, and D. M. Elliott, "Biaxial tensile testing and constitutive modeling of human supraspinatus tendon," *Journal of Biomechanical Engineering*, vol. 134, no. 2, 2012, ISSN: 01480731. DOI: 10.1115/1.4005852.

[42] B. Cruz Perez, J. Tang, H. J. Morris, J. R. Palko, X. Pan, R. T. Hart, and J. Liu, "Biaxial mechanical testing of posterior sclera using high-resolution ultrasound speckle tracking for strain measurements," *Journal of Biomechanics*, 2014, ISSN: 18732380. DOI: 10.1016/j.jbiomech.2013.12.009. arXiv: NIHMS150003.

[43] V. Deplano, M. Boufi, O. Boiron, C. Guivier-Curien, Y. Alimi, and E. Bertrand, "Biaxial tensile tests of the porcine ascending aorta," *Journal of Biomechanics*, 2016, ISSN: 18732380. DOI: 10.1016/j.jbiomech.2016.05.005.

[44] J. Lu and H. Y. S. Huang, "Biaxial mechanical behavior of bovine saphenous venous valve leaflets," *Journal of the Mechanical Behavior of Biomedical Materials*, 2018, ISSN: 18780180. DOI: 10.1016/j.jmbbm.2017.10.028.

[45] S. Jett, D. Laurence, R. Kunkel, A. R. Babu, K. Kramer, R. Baumwart, R. Towner, Y. Wu, and C. H. Lee, "An investigation of the anisotropic mechanical properties and anatomical structure of porcine atrioventricular heart valves," *Journal of the Mechanical Behavior of Biomedical Materials*, 2018, ISSN: 18780180. DOI: 10.1016/j.jmbbm.2018.07.024.

[46] H. Fehervary, J. Vastmans, J. V. Sloten, and N. Famaey, "How important is sample alignment in planar biaxial testing of anisotropic soft biological tissues? A finite element study," *Journal of the Mechanical Behavior of Biomedical Materials*, 2018. DOI: 10.1016/j.jmbbm.2018.06.024. [Online]. Available: www.elsevier.com/locate/jmbbm.

[47] H. Fehervary, M. Smoljkić, J. Vander Sloten, and N. Famaey, "Planar biaxial testing of soft biological tissue using rakes: A critical analysis of protocol and fitting process," *Journal of the Mechanical Behavior of Biomedical Materials*, 2016, ISSN: 18780180. DOI: 10.1016/j.jmbbm.2016.01.011.

[48] W. Sun, M. S. Sacks, and M. J. Scott, "Effects of Boundary Conditions on the Estimation of the Planar Biaxial Mechanical Properties of Soft Tissues," *Journal of Biomechanical Engineering*, 2005, ISSN: 01480731. DOI: 10.1115/1.1933931.

[49] M. S. Sacks, "A Method for Planar Biaxial Mechanical Testing That Includes In-Plane Shear," *Journal of Biomechanical Engineering*, 1999, ISSN: 01480731. DOI: 10.1115/1.2835086.

[50] "BSI ISO 16842:2014: Metallic materials — Sheet and strip — Biaxial tensile testing method using a cruciform test piece," British Standards Policy and Strategy Committee, Standard, 2014.

[51] E. Rizzuto, S. Carosio, and Z. Del Prete, "Characterization of a Digital Image Correlation System for Dynamic Strain Measurements of Small Biological Tissues," *Experimental Techniques*, vol. 40, no. 2, pp. 743–753, Apr. 2016, ISSN: 17471567. DOI: 10.1007/s40799-016-0075-z.

[52] M. Palanca, G. Tozzi, and L. Cristofolini, *The use of digital image correlation in the biomechanical area: A review*, 2016. DOI: 10.1080/23335432.2015.1117395.

[53] Y. Barranger, P. Doumalin, J. C. Dupré, and A. Germaneau, "Digital image correlation accuracy: Influence of kind of speckle and recording setup," *EPJ Web of Conferences*, vol. 6, 2010, ISSN: 2100014X. DOI: 10.1051/epjconf/20100631002.

[54] *Dragon skin series addition cure silicone rubber compounds*, Smooth-On, Nov. 2021.

[55] *Psycho paint platinum silicone paint base*, Smooth-On, Nov. 2021.

[56] L. Meunier, G. Chagnon, D. Favier, L. Orgéas, and P. Vacher, "Mechanical experimental characterisation and numerical modelling of an unfilled silicone rubber," *Polymer Testing*, vol. 27, no. 6, pp. 765–777, 2008, ISSN: 0142-9418. DOI: https://doi.org/10.1016/j.polymertesting.2008.05.011. [Online]. Available: https://www.sciencedirect.com/science/article/pii/S0142941808000986.

Appendices

Appendix A

Drawings

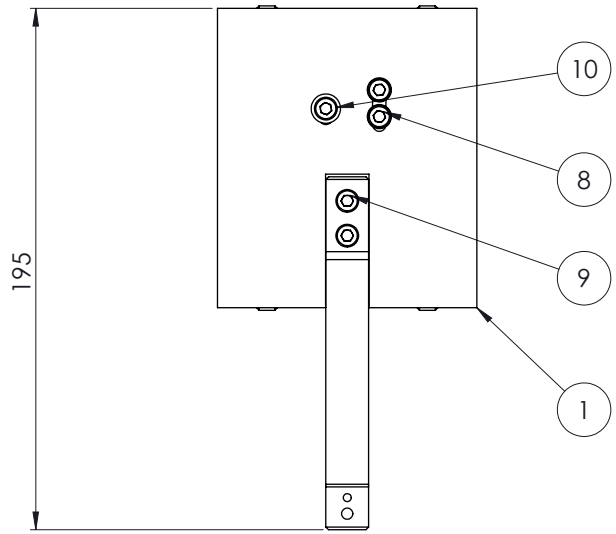

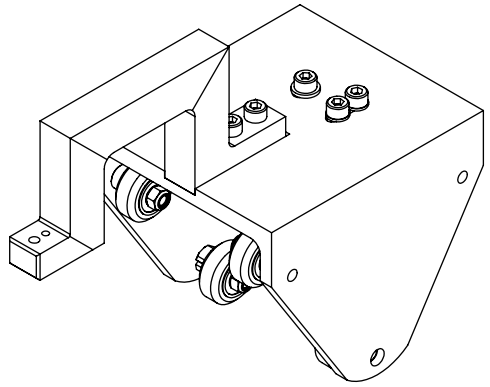

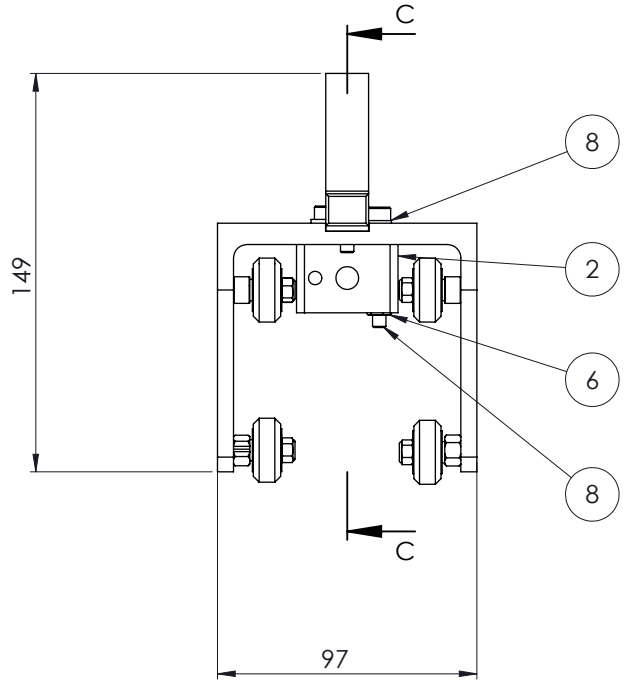

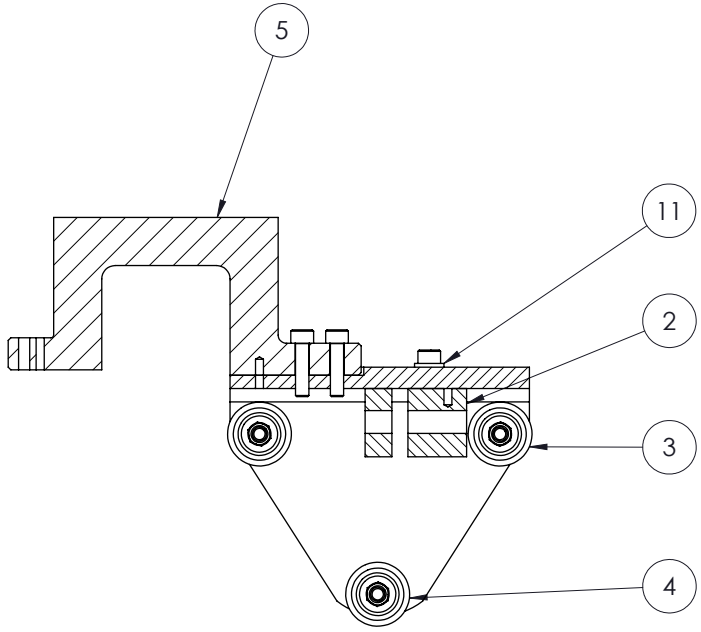

SECTION C-C

ITEM NO.	PART NUMBER	QTY.
1	Bi Cbeam Carriage 1	1
2	Anti-Backlash Nut (Bi)	1
3	Wheel (fixed)	4
4	Wheel (floating)	2
5	Bi Arm 1	1
6	ISO - 4034 - M5 - N	2
7	Washer ISO 7092 - 5	2
8	B18.3.1M - 5 x 0.8 x 40 Hex SHCS -- 22NHX	2
9	B18.3.1M - 5 x 0.8 x 20 Hex SHCS -- 20NHX	2
10	B18.3.1M - 5 x 0.8 x 16 Hex SHCS -- 16NHX	1
11	B18.22M - Plain washer, 5 mm, narrow	1

A3 Landscape	University of Cape Town Department of Mechanical Engineering		
	Title: BIAXIAL CARRIAGE 1 SUB-ASSEMBLY		
Assembly Drawing	Scale: 1:2	Date: 2021/11/29	of Carriage 1 Sub-Assembly
	Drawn By: JONATHAN CAINE		Drawing Number

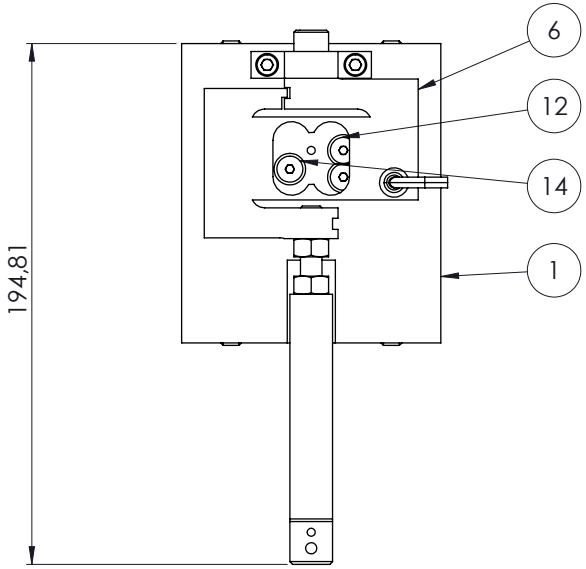

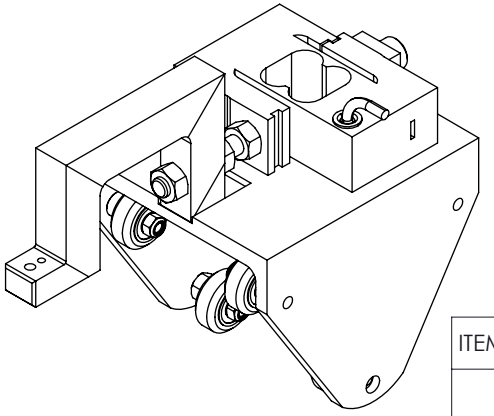

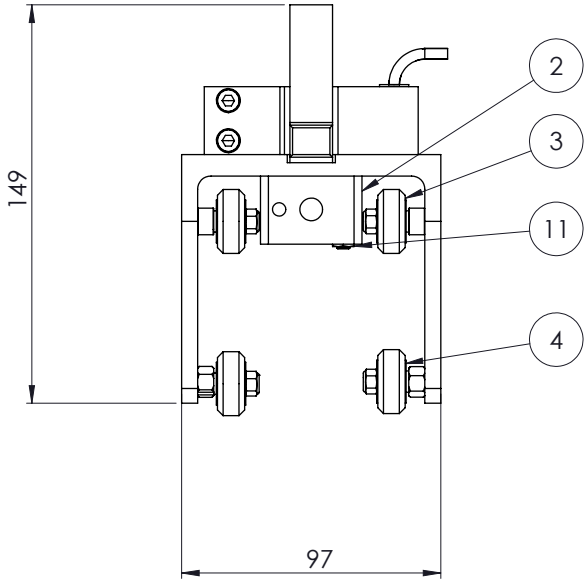

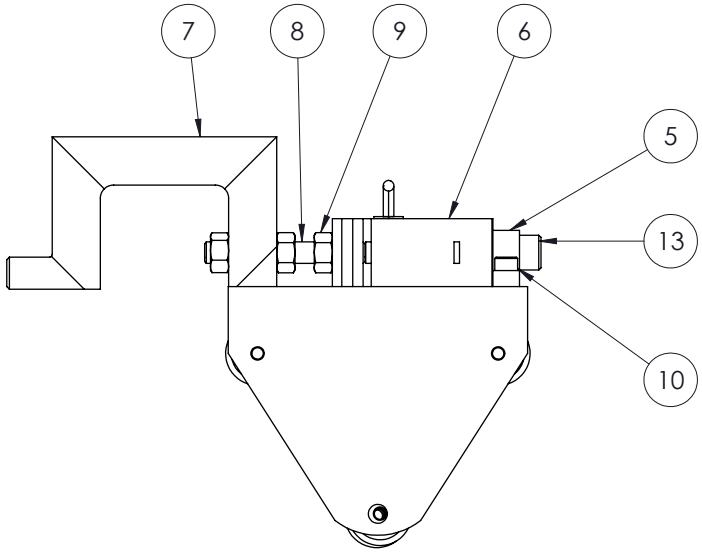

ITEM NO.	PART NUMBER	QTY.
1	Bi Cbeam Carriage 2	1
2	Anti-Backlash Nut (Bi)	1
3	Wheel (fixed)	4
4	Wheel (floating)	2
5	LC Bolt Clamp	1
6	K-S2M (load cell)	1
7	Bi Arm 2	1
8	AM -- M8 x 60 N	1
9	B18.2.4.1M - Hex nut, Style 1, M8 x 1.25 --D-N	3
10	B18.3.1M - 5 x 0.8 x 16 Hex SHCS -- 16NHX	2
11	ISO - 4034 - M5 - N	2
12	B18.3.5M - 5 x 0.8 x 35 Socket FCHS -- 35N	2
13	B18.3.1M - 8 x 1.25 x 20 Hex SHCS -- 20NHX	1
14	B18.3.5M - 5 x 0.8 x 16 Socket FCHS -- 16N	1
15	Spec and grips	1

A3 Landscape	University of Cape Town Department of Mechanical Engineering			
	Title: BIAXIAL CARRIAGE 2 SUB-ASSEMBLY			
Assembly Drawing	Scale: 1:2	Date: 2021/11/29	Carriage 2 Sub-Assembly	of
	Drawn By: JONATHAN CAINE		Drawing Number	

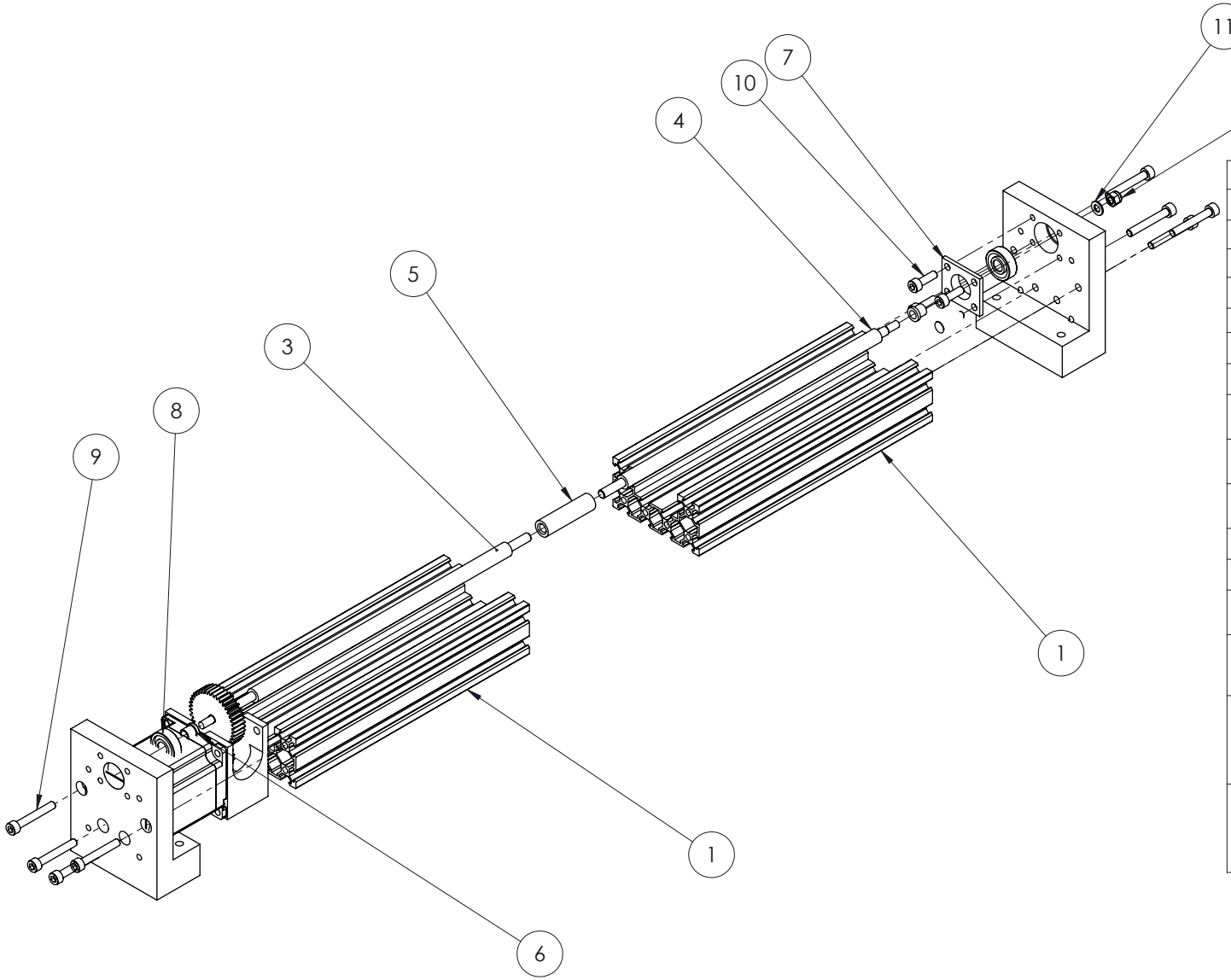

ITEM NO.	PART NUMBER	QTY.
1	C-Beam 40x80 (split)	2
2	C-Beam End Mount 2	2
3	Lead Screw (left)	1
4	Lead Screw (Right)	1
5	Sleeve	1
6	Bearing sleeve	2
7	Bearing Clamp	1
8	SKF - 608 - 8,SI,NC,8_68	2
9	ISO 4762 M5 x 35 - 22N	8
10	ISO 4762 M5 x 16 - 16N	4
11	Washer ISO 7089 - 5	1
12	ISO 7040-M5-N	1
13	Motor Mount (Biaxial)	1
14	Stepper motor NEMA 23HS7430	1
15	ISO - Spur gear 1M 20T 20PA 12FW --- S20A75H50L5.0N	1
16	ISO - Spur gear 1M 40T 20PA 10FW --- S40A75H50L6.0N	1

A3 Landscape	University of Cape Town Department of Mechanical Engineering		
	Title: BIAXIAL CBEAM SUB-ASSEMBLY		
Assembly Drawing	Scale: 1:2	Date: 2021/11/29	of CBeam Sub-Assembly
	Drawn By: JONATHAN CAINE		Drawing Number

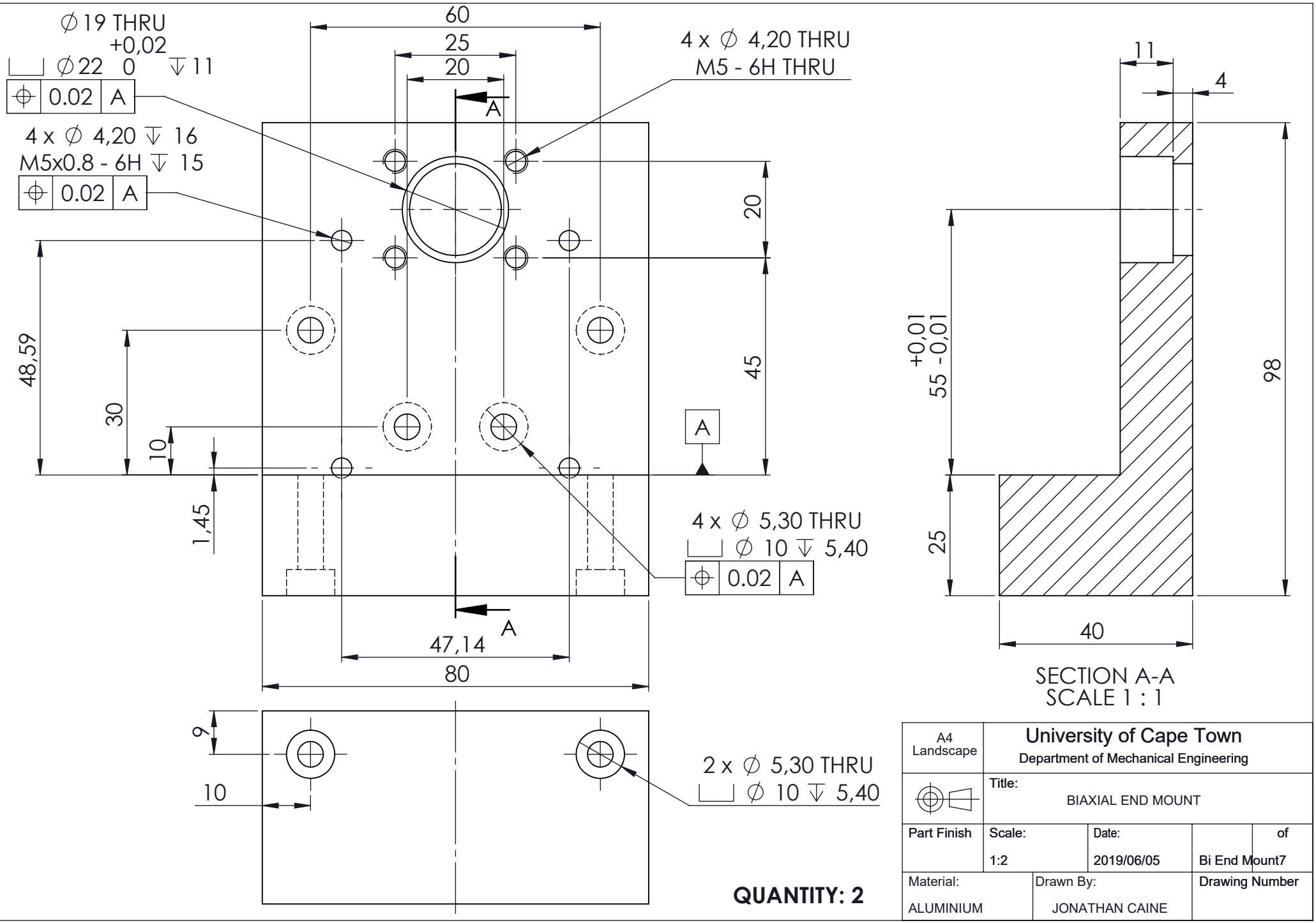

A4 Landscape	University of Cape Town Department of Mechanical Engineering		
	Title: BIAXIAL END MOUNT		
Part Finish	Scale: 1:2	Date: 2019/06/05	of Bi End Mount7
Material: ALUMINIUM	Drawn By: JONATHAN CAINE		Drawing Number

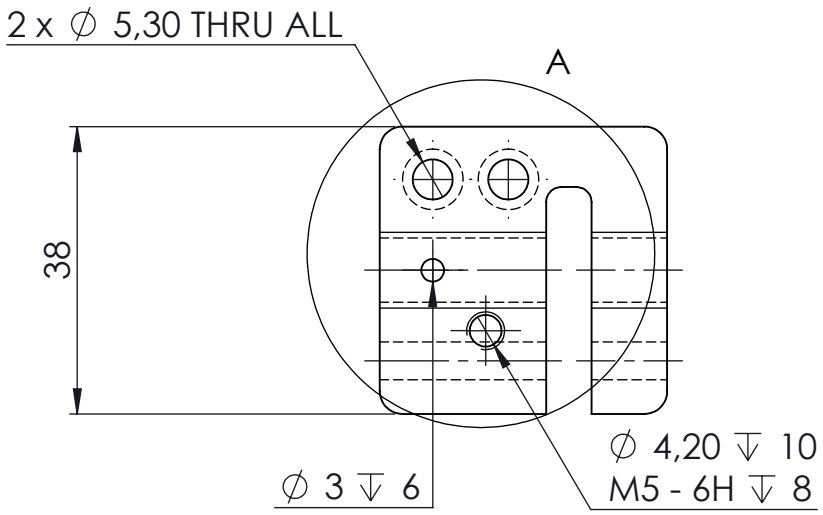

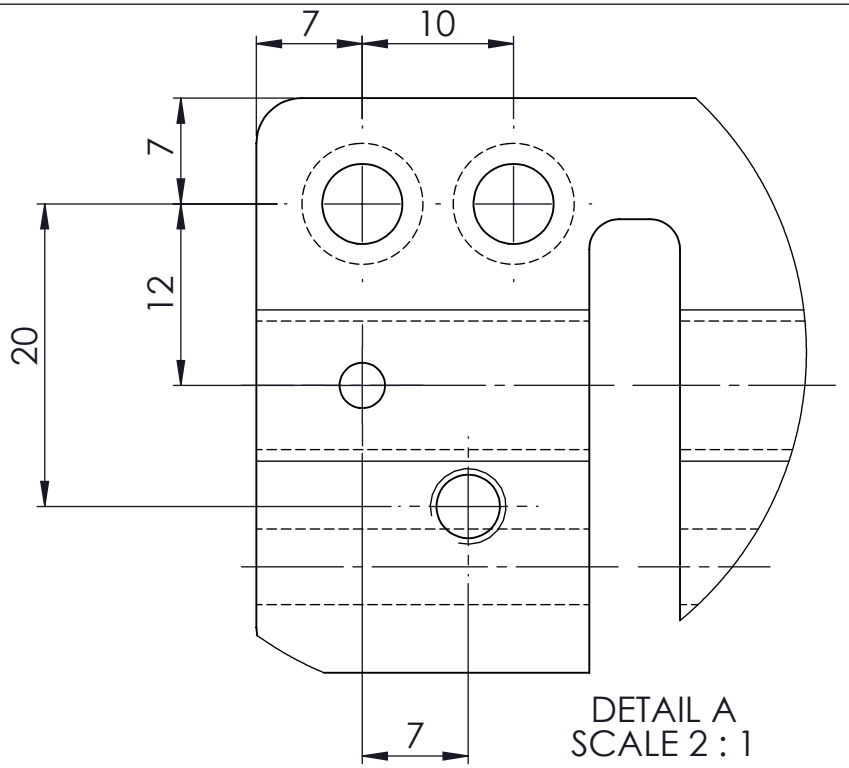

DETAIL A
SCALE 2 : 1

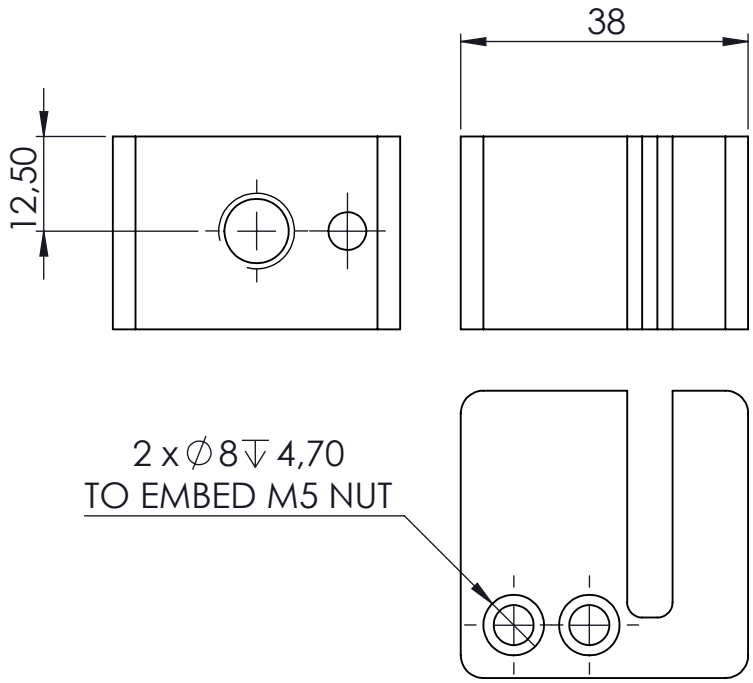

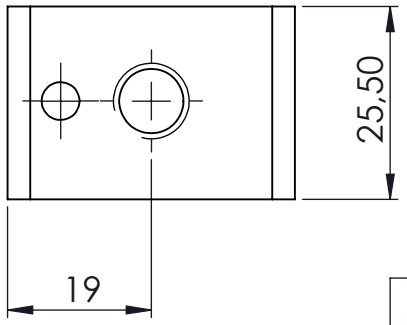

QUANTITY: 2
(1 LEFT HAND & 1 RIGHT HAND)

A4 Landscape	University of Cape Town Department of Mechanical Engineering			
	Title: BIAXIAL ANTI-BACKLASH NUT			
Part Finish	Scale: 1:1	Date: 2019/06/05	Bi AB Nut	of 7
Material: SUSTARIN C	Drawn By: JONATHAN CAINE		Drawing Number	

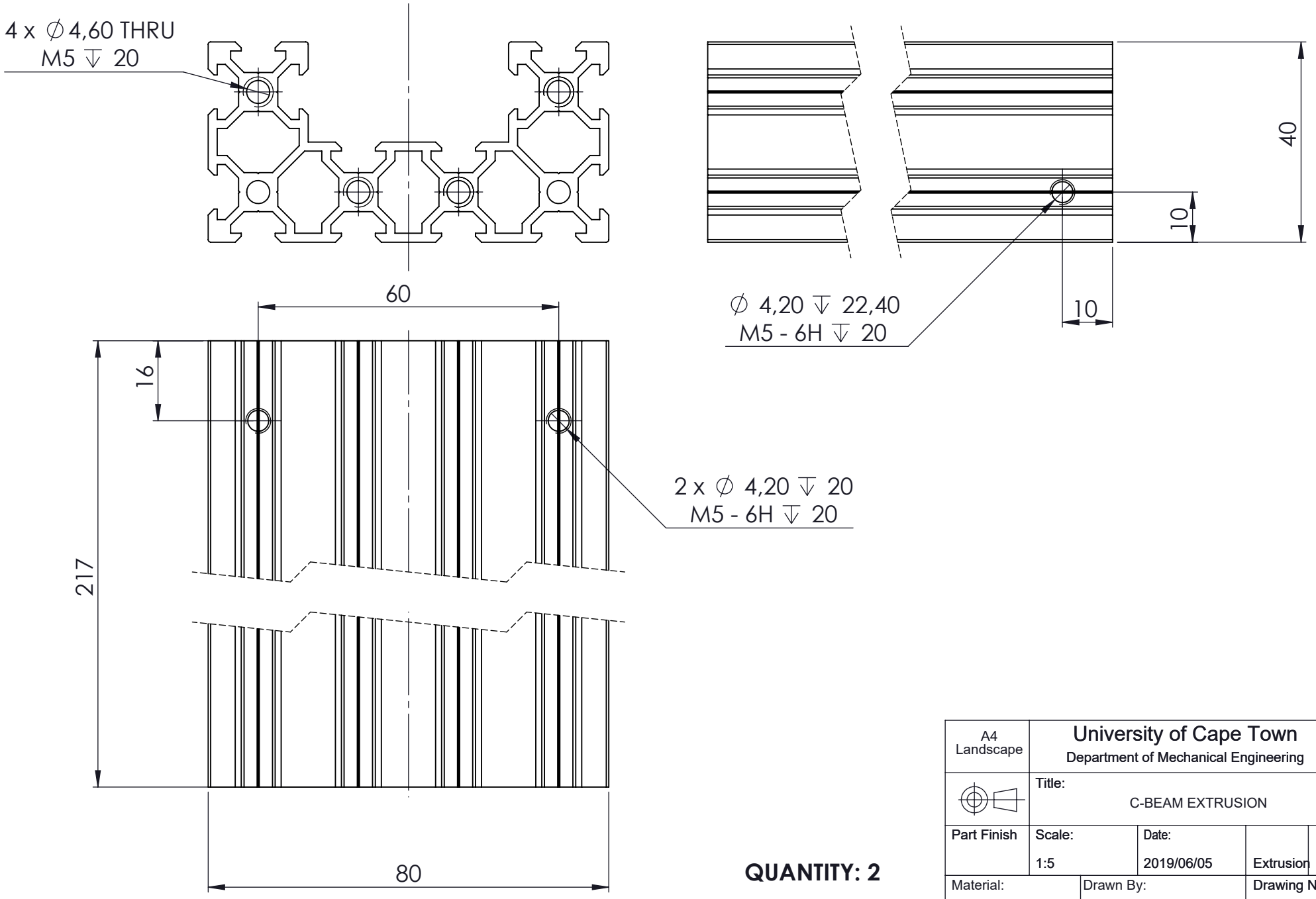

QUANTITY: 2

A4 Landscape	University of Cape Town Department of Mechanical Engineering			
	Title: C-BEAM EXTRUSION			
Part Finish	Scale: 1:5	Date: 2019/06/05	Extrusion	of 7
Material: ALUMINIUM	Drawn By: JONATHAN CAINE		Drawing Number	

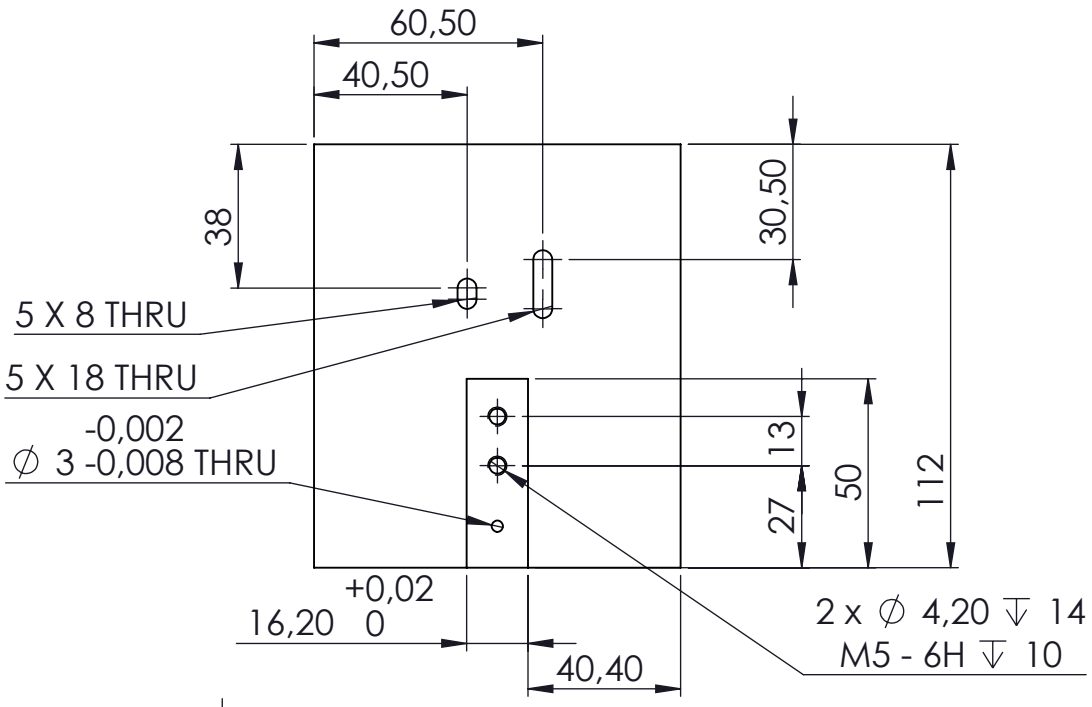

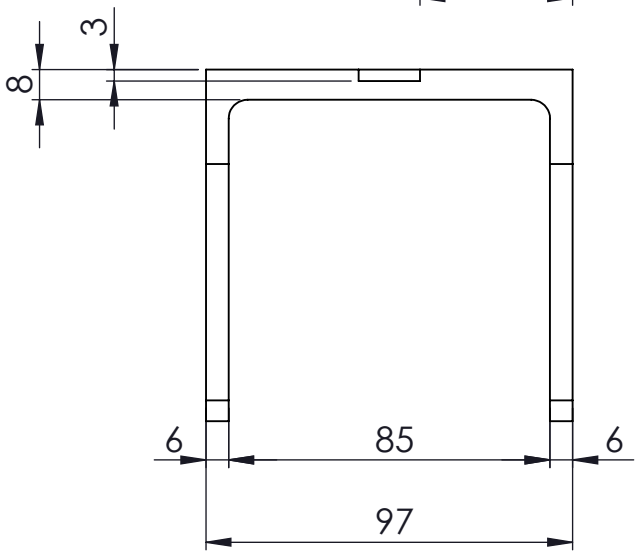

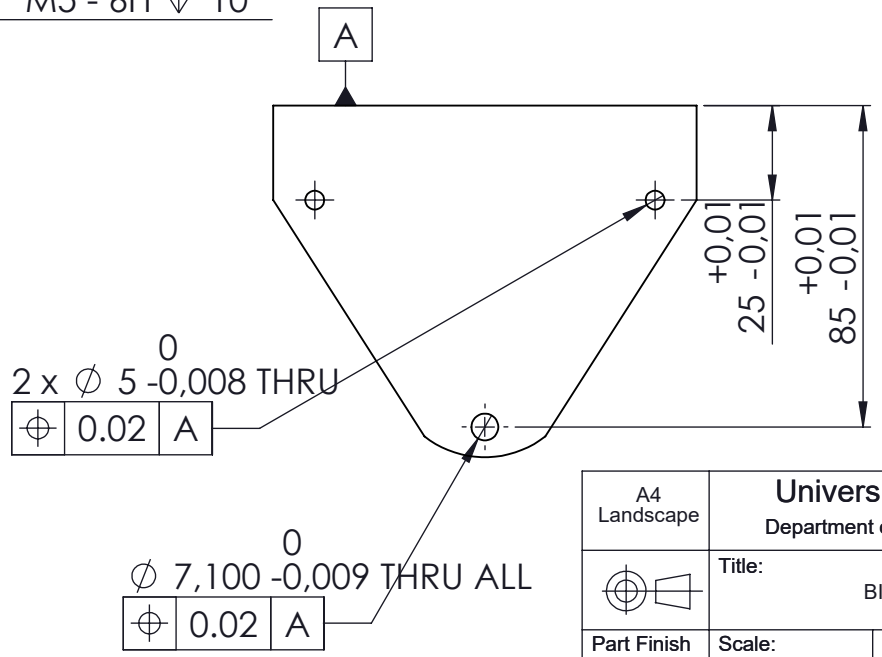

QUANTITY: 1

A4 Landscape	University of Cape Town Department of Mechanical Engineering		
	Title: BIAXIAL CARRIAGE 1		
Part Finish	Scale: 1:2	Date: 2019/06/05	Bi Carriage 1 of 7
Material: ALUMINIUM	Drawn By: JONATHAN CAINE		Drawing Number

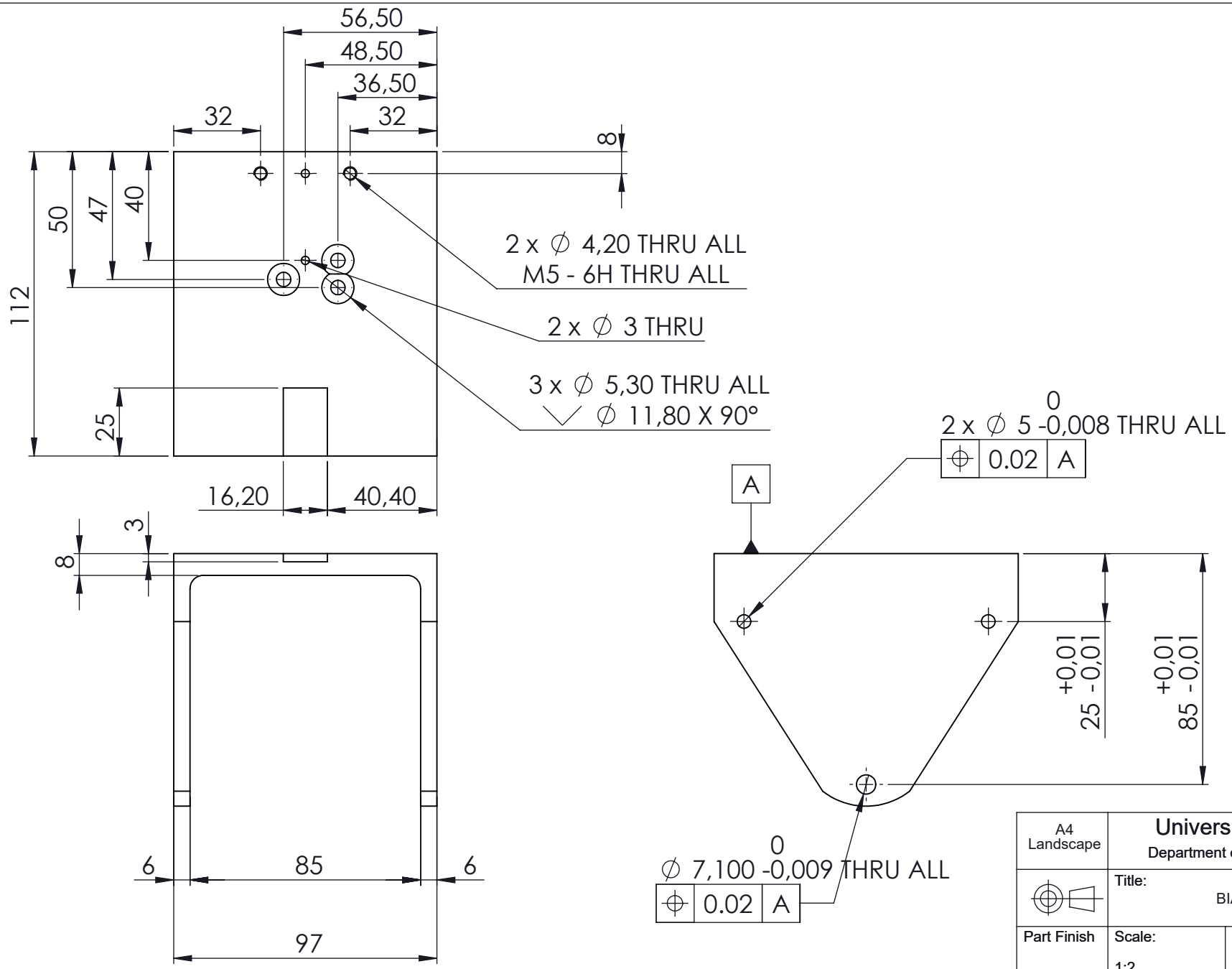

QUANTITY: 1

A4 Landscape	University of Cape Town Department of Mechanical Engineering		
	Title: BIAXIAL CARRIAGE 2		
Part Finish	Scale: 1:2	Date: 2019/06/05	Bi Carriage 2 7 of
Material: ALUMINIUM	Drawn By: JONATHAN CAINE		Drawing Number

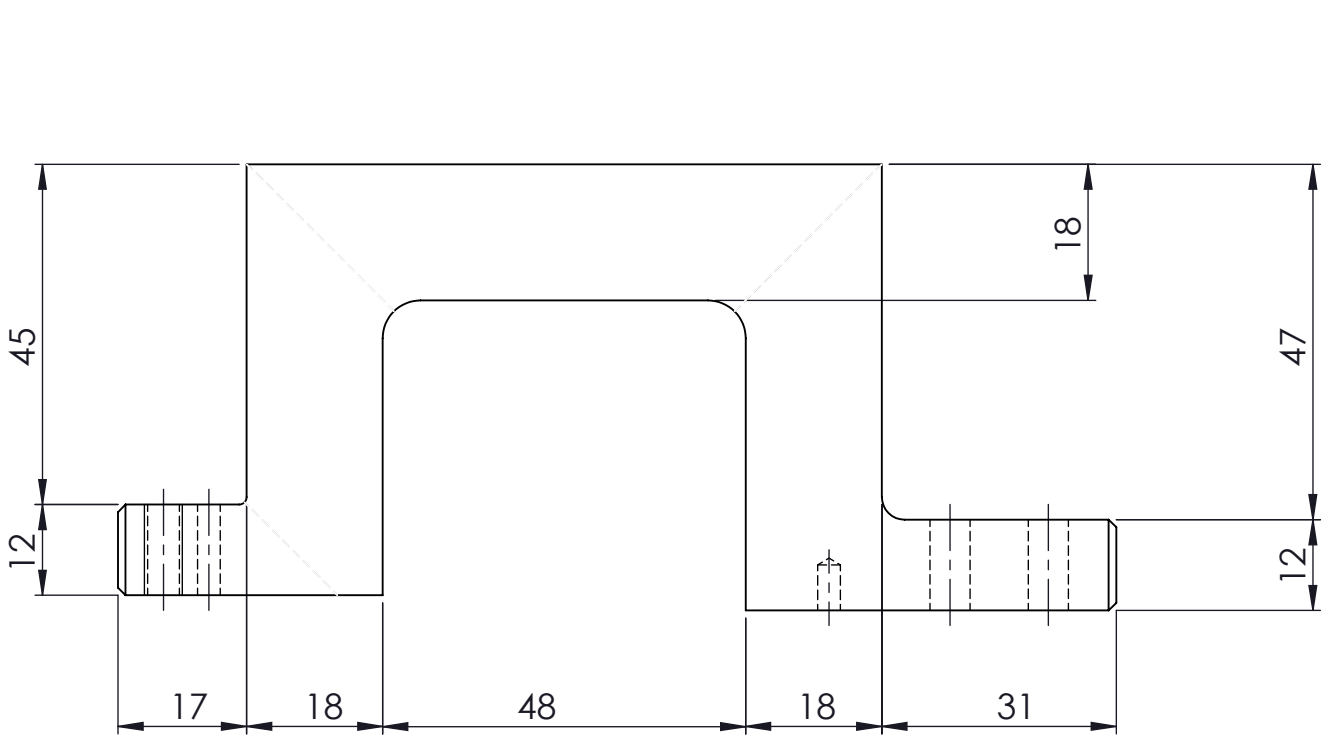

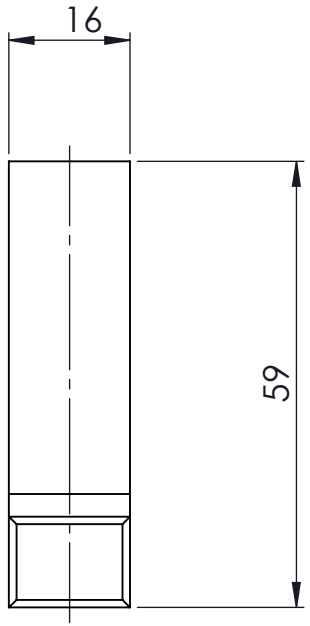

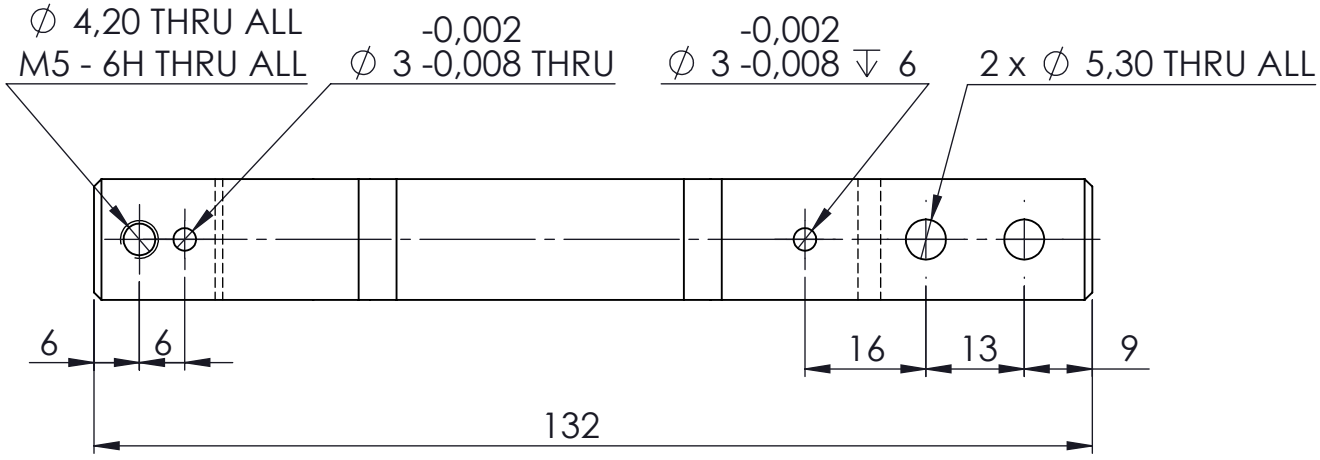

QUANTITY: 1

A4 Landscape	University of Cape Town Department of Mechanical Engineering			
	Title: BIAXIAL ARM 1			
Part Finish	Scale: 1:1	Date: 2019/06/05	Bi Arm 1	of 7
Material: STAINLESS STEEL	Drawn By: JONATHAN CAINE		Drawing Number	

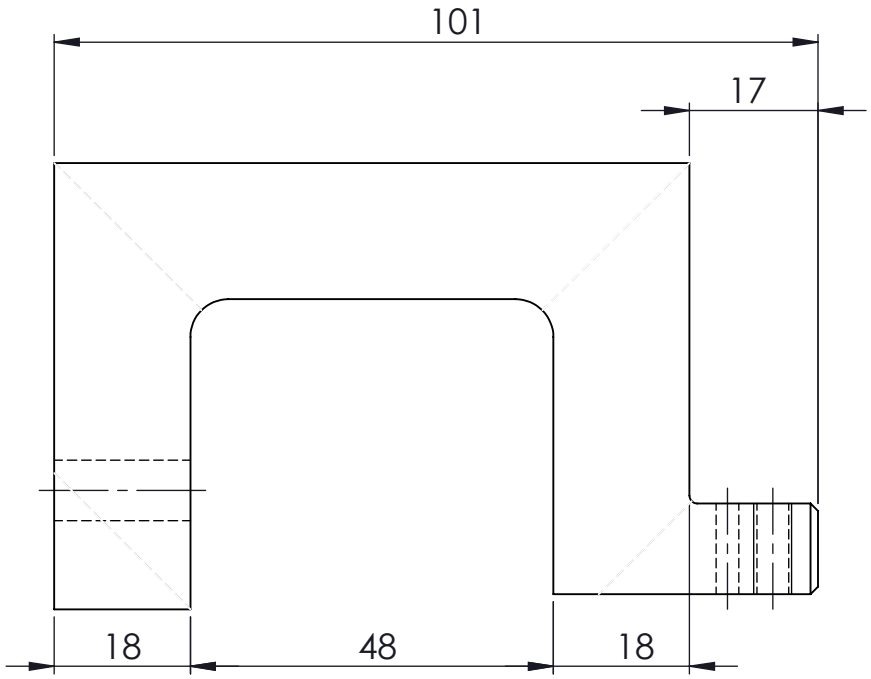

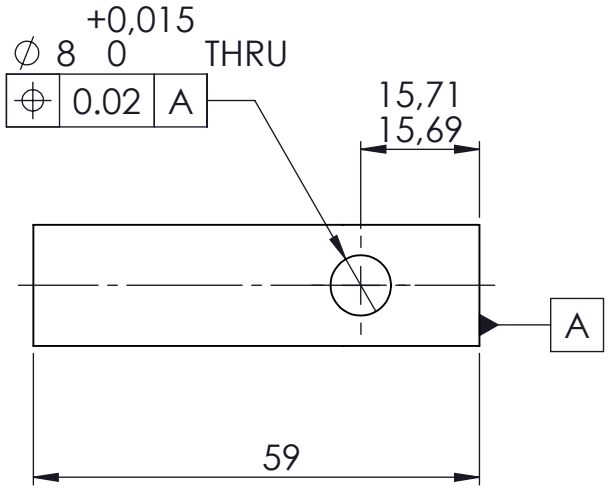

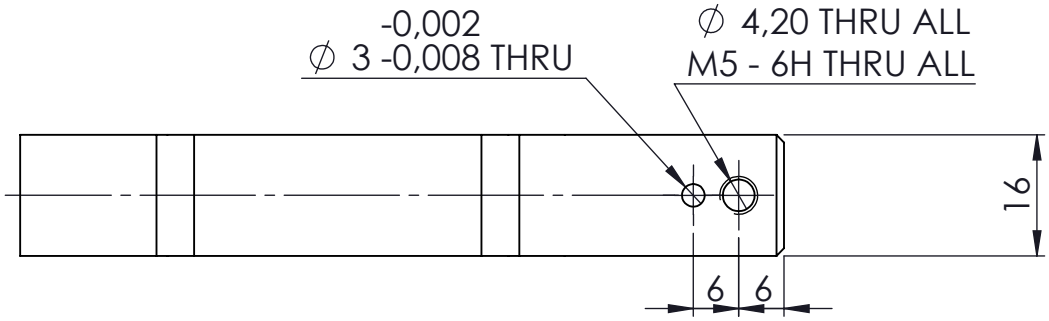

QUANTITY: 1

A4 Landscape	University of Cape Town Department of Mechanical Engineering			
	Title: BIAXIAL ARM 2			
Part Finish	Scale: 1:1	Date: 2019/06/05	Bi Arm 2	of 7
Material: STAINLESS STEEL	Drawn By: JONATHAN CAINE		Drawing Number	

Appendix B

Concept Selection

Concept Selection		A		B		C		D		E/F		G		H	
Requirement	Importance	Score	Weighted Score	Score	Weighted Score	Score	Weighted Score	Score	Weighted Score	Score	Weighted Score	Score	Weighted Score	Score	Weighted Score
Allow unobstructed motion in x direction	10	4	40	5	50	5	50	5	50	5	50	5	50	5	50
Ability to accurately locate bearings to guide	8	4	32	4	32	3	24	5	40	5	40	4	32	4	32
Constrain rotation in the xy plane	6	4	24	5	30	5	30	5	30	5	30	4	24	4	24
Constrain rotation in the xz plane	6	4	24	4	24	5	30	3	18	5	30	5	30	5	30
Constrain rotation in the yz plane	4	3	12	3	12	4	16	3	12	5	20	4	16	5	20
Constrain motion in the y direction	6	5	30	5	30	5	30	5	30	5	30	5	30	5	30
Constrain motion in the z direction	6	3	18	3	18	5	30	3	18	5	30	5	30	5	30
Cost	5	5	25	5	25	5	25	5	25	2	10	5	25	5	25
Ease of manufacture	5	5	25	5	25	4	20	5	25	3	15	4	20	4	20
Weight	5	5	25	5	25	5	25	5	25	4	20	5	25	5	25
Ease of assmbly	4	5	20	4	16	4	16	5	20	4	16	4	16	4	16
	65	47	**275**	48	**287**	50	**296**	49	**293**	48	**291**	50	**298**	51	**302**

Description of Concepts

A	4 wheels located in the xy-plane, equally spaced
B	3 wheels located in the xy-plane, plus one in the xz plane to counter moment during loading
C	3 wheels located in the xy-plane, plus 3 in the xz plane
D	3 wheels located in the xy-plane (Displayed below)
E	3 linear bearings on guide rod
F	Igus T rail, with 3 bearings (use extrusion as light weight base)
G	3 wheels located in the xz plane
H	2x 3 wheels located in the xz plane

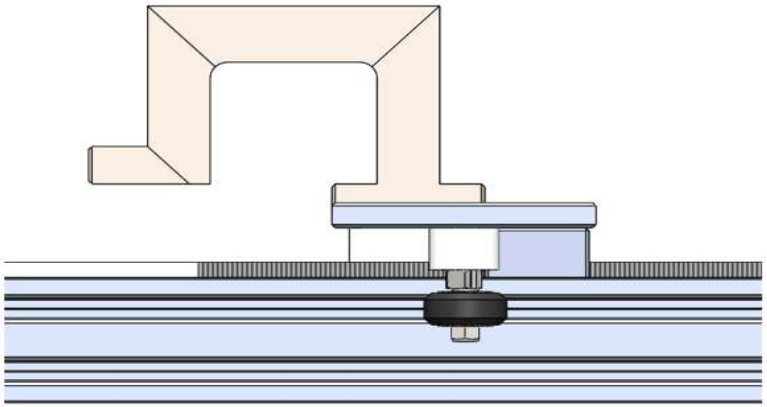

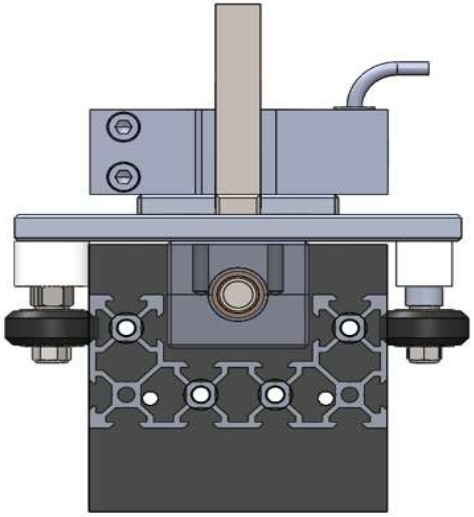

Appendix C

Lead-Screw Calculations

```
%
%
%   Lead Screw calculations
%   Jonathan Caine
%
%
%% Input Parameters

clear

alpha = 2*pi*((15)/360);        % angle of thread
p = 0.003;                      % pitch (m)
nt = 1;                         % number of threads
L = nt*p;                       % Lead(m)
d_o = 0.010;                    % outer diameter (m)
d_i = 0.0062;                   % inner diameter
dm = (d_i + d_o) / 2;           % mean diameter
F = 200;                        % Load (N)
coef_st = 0.25;                 % Coefficient of friction (static)
coef_dy = 0.18;                 % Coefficient of friction (dynamic)
C = 1;                          % End condition constant
Ey = 200E9;                     % Youngs Modulus of screw
Lc = 0.5;                       % column length


coef_sl = 0.5;                  % Coefficient of friction of steel
L_sl = 0.02;                    % Length of shrink fit on sleeve (m)
d_sl_i = 0.006;                 % Inner diameter of sleeve
d_sl_o = 0.012;                 % outer diameter of sleeve
E_sl = 200E9;                   % Youngs modulus of sleeve
v = 0.3;                        % Poisson's ratio of screw
v_sl = 0.3;                     % Poisson's ratio of sleeve


%% Lead Screw Calculations

Torque = (F * dm/2) * ( (pi*coef_st*dm + L*cos(alpha)) / (pi*dm*cos(alpha) -↙
coef_st*L) );

eff = (F*L) / (2*pi*Torque);          % efficiency

F_crit = (C * pi^3 * Ey * d_i^4) / (Lc^2*64);            % critical buckling force

def = (4*F*Lc) / (pi*d_i^2*Ey) ;                         % deformation

Torsion = 16*Torque/(pi*d_i^3);

Stress_norm = -4*F/(pi*d_i^2);

Stress_bearing = -2*0.38*F/(pi*dm*1*p);              % bearing stress on thread

Stress_bending = 6*0.38*F/(pi*d_i*1*p);              % bending stress on thread

%% Sleeve Calculations
```

```
sf = 3; % safety factor

r_i = d_sl_i/2; r_o = d_sl_o/2;
F_sleeve = sqrt(F^2 + (Torque/r_i)^2);
Norm = F_sleeve/coef_sl;
P = sf*Norm /(2*pi*L_sl*r_i);

A = ( P * r_i^2 )/ (r_o^2 - r_i^2);
B = ( P * (r_i^2) * (r_o^2) )/ (r_o^2 - r_i^2);
sig_Ho = A+(B/r_i^2);
sig_Hi = -P;

%shrink_all = (r_i / Ey)*(sig_Ho + v * (-P)) - (r_i / E_sl)*(sig_Hi + v_sl * (-P))
shrink_all = (r_i / Ey) * (sig_Ho - sig_Hi);             % if both are stainless steel
```

Appendix D

Set-up instructions

1. Ensure motor is connected to Arduino Uno
2. Ensure all limit switches are correctly connected (Y+, Y-)
3. Ensure machine (and machine path) are clear of any foreign objects (tools, stationary etc)
4. Connect Arduino Uno to PC
5. Before connecting Arduino Uno/GRBL Shield to power supply unit (PSU) ensure the unit is turned on and set to 12 v.
6. Connect Arduino Uno/GRBL Shield to PSU
7. Connect to the Arduino Uno on the Universal Gcode Sender software
8. Ensure all motor settings are correct (They will appear on the Universal GCode Sender once connected)
9. Home the machine. Watch to make sure machine is operating properly. Hit emergency stop in case of error.

Appendix E

Ethics Clearance

APPLICATION FORM

Please Note:
Any person planning to undertake research in the Faculty of Engineering and the Built Environment (EBE) at the University of Cape Town is required to complete this form **before** collecting or analysing data. The objective of submitting this application *prior* to embarking on research is to ensure that the highest ethical standards in research, conducted under the auspices of the EBE Faculty, are met. Please ensure that you have read, and understood the **EBE Ethics in Research Handbook** (available from the UCT EBE, Research Ethics website) prior to completing this application form: http://www.ebe.uct.ac.za/ebe/research/ethics1

APPLICANT'S DETAILS		
Name of principal researcher, student or external applicant		Jonathan Caine
Department		Mechanical Engineering
Preferred email address of applicant:		Cnxjon003@myuct.ac.za
If Student	Your Degree: e.g., MSc, PhD, etc.	MSc
	Credit Value of Research: e.g., 60/120/180/360 etc.	120
	Name of Supervisor (if supervised):	Dr Reuben Govender
If this is a researchcontract, indicate the source of funding/sponsorship		-
Project Title		Design, build and test a planar biaxial tensile testing machine for skin and other collagenous soft tissues.

I hereby undertake to carry out my research in such a way that:

- there is no apparent legal objection to the nature or the method of research; and
- the research will not compromise staff or students or the other responsibilities of the University;
- the stated objective will be achieved, and the findings will have a high degree of validity;
- limitations and alternative interpretations will be considered;
- the findings could be subject to peer review and publicly available; and
- I will comply with the conventions of copyright and avoid any practice that would constitute plagiarism.

SIGNED BY	Full name	Signature	Date
Principal Researcher/ Student/External applicant	Jonathan Caine	Signed by candidate	**05 Apr 2019**

APPLICATION APPROVED BY	Full name	Signature	Date
Supervisor (where applicable)	Dr Reuben Govender	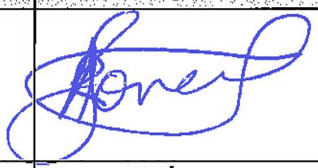	**05 Apr 2019**
HOD (or delegated nominee) Final authority for all applicants who have answered NO to all questions in Section1; and for all Undergraduateresearch (Including Honours).	George Vicatos	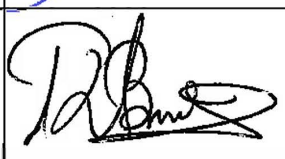	11/4/19

UNIVERSITY OF CAPE TOWN
Faculty of Health Sciences
Animal Ethics Committee

Room E53-46 Old Main Building
Groote Schuur Hospital
Observatory 7925
Telephone [021] 406 6492
Email: sumayah.arlefdien@uct.ac.za
Website: www.health.uct.ac.za/fhs/research/animalethics/forms

01 April 2019

Dr R Govender
Mechanical Engineering
Upper Campus
UCT

Dear Dr Govender

PROTOCOL TITLE: Mechanical Properties of Membrane Tissues

FHS AEC REF NO: 019/014

Thank you for submitting your request for approval of use of animal material for scientific purposes to the Faculty of Health Sciences (FHS) Animal Ethics Committee (AEC).

I am pleased to inform you that the FHS AEC EXCO has **approved** your request, which will terminate on **30 April 2022.**

Number of animal material & species: 2Kg -Sheep, Cow, Pig Intestines

Please quote the FHS AEC REF NO (above) in all future correspondence.

Please note that the approval of this protocol imposes the following obligations on the principal investigator (PI):

1. To submit an annual mandatory progress report. The first annual report for this protocol is due on **28 February 2020**. The forms can be accessed from http://www.health.uct.ac.za/fhs/research/animalethics/forms
2. To submit a final mandatory report on the **30 April 2022**, please access the final report form from: http://www.health.uct.ac.za/fhs/research/animalethics/forms
3. Ensuring that all study participants perform within the confines of the procedures and experimental design of the protocol as approved, or as amended.

4. Ensuring that all study participants comply with all applicable national legislation, UCT policies, FHS AEC policies and standard operating procedures (SOPs) and national standards (SANS 10386: 2008).

My best wishes for a successful research and /or teaching endeavour.

Yours sincerely

PROF PJ COMMERFORD
CHAIR, FHS AEC

Faculty of Health Sciences
Animal Ethics Committee (AEC)

USE OF ANIMAL MATERIAL FOR SCIENTIFIC PURPOSES

- Current forms to be downloaded from the Administrative Forms web page at http://www.health.uct.ac.za/fhs/research/animalethics/forms
- This application form is to seek ethics approval for the Use of Animal Material for Scientific Purposes.
- Please print double-sided where possible.
- **Important:** Animals not specifically killed for this study.

This application must be typed and one signed completed form submitted to:
Mrs Sumayah Ariefdien
Animal Research Ethics Committee
E 53 Room 46, Old Main Building, Groote Schuur Hospital, Observatory, 7700
Telephone: +27 21 404 6492
An electronic copy of the original application (Word format which is saved as a PDF file) is to be forwarded to fhsanimalresearch@uct.ac.za and sumayah.ariefdien@uct.ac.za

For office use only	
Application No:	019_014
Animal Material:	Intestines
Species:	Sheep, Pig, Cow
Source:	
Date received:	26.08.2019
Date approved	

1. TITLE OF APPLICATION	Mechanical Properties of Membrane Tissues

2. DETAILS OF APPLICANT	
Title (e.g. Prof, Dr, Mr, Ms)	**Dr**
Forenames & Surname	**Reuben A. Govender**
Qualifications (e.g. PhD)	**PhD**
Position or appointment	**Senior Lecturer**
If applicant is a **student**, please provide **name of supervisor**	

3. CONTACT DETAILS	APPLICANT	SUPERVISOR (if applicant a student)
Address for correspondence	**Mechanical Engineering Library Rd South Upper Campus University of Cape Town Rondebosch 7701**	
Telephone number, extension	**021 650 4526**	
Cell phone number	**082 730 2048**	
Fax number		
E-mail address	**Reuben.govender@uct.ac.za**	

4.1 ANIMAL MATERIAL REQUESTED	
Species and Strain	**Sheep, cow, pig – intestines processed into "sausage casings"**
Amount of animal material required	**Approx. 0.5kg of intestine per student project (2.0kg total)**
Describe Animal Material (e.g. tissues) (max 250 words)	
Sausage skins (cleaned intestinal membranes) from sheep / pigs / cows will be used for commissioning a newly designed and built bulge / inflation tester. The device measures the mechanical stiffness and strength of thin membranes, and is intended to ultimately assist with characterisation of human membrane tissues and their artificial replacements.	

5.1 SOURCE OF ANIMAL MATERIAL
Please indicate the source/supplier of the animal material and where and when it was sourced. Please note that an abattoir registration number is required if the animal material is sourced from an abattoir. Was material ethically sourced? Please explain.
Intestines will be purchased as "natural sausage casings" from Freddy Hirsch Group (www.freddyhirsch.co.za), who are suppliers of sausage casings, spices and butcher's equipment in wholesale quantities to retail butchers and the meat processing industry. The Freddy Hirsch Group is supplied by several abattoirs, as they sell both halaal-certified products and non-halaal products.

5.2 ANIMALS KILLED
Briefly explain, if known, how and why animals were killed.
This study will not use tissue from any animal that was not destined for slaughter at a commercial abattoir.

6. STUDY PARTICIPANTS:		
Name	**Department**	**Role**
Dr Reuben Govender	**Mechanical Engineering**	**Principal Investigator**
Jonathan Caine	**Mechanical Engineering**	**PG Student (Lab Work involves handling specimens)**
Daniel Pons	**Mechanical Engineering**	**PG Student (Lab Work involves handling specimens)**
Andrew Curry	**Mechanical Engineering**	**Research Assistant**
Deharen Pillay	**Mechanical Engineering**	**UG Student (Lab Work involves handling specimens)**

DU	ION OF STUDY				
PE	hich the application is required ed three years)	Years	2	Months	2
St	May 2019	End date		July 2021	

PU	OSE (select category)				
Resea	X	Teaching/training		Other (specify)	

9. Briefly describe what you will be doing

If a hypothesis is being tested (explanatory research) please state what it is.

This project is investigating different ways of quantifying the mechanical properties (stiffness, failure strains and stresses etc) of biological membrane tissues. The PI's PG students in Mechanical Engineering have been designing and building the experimental apparatus (bulge tester and planar biaxial tensile tester) to perform these experiments. To date, the early commissioning work on the apparatus has been completed with engineering surrogate materials (latex and silicon elastomers). Further improvements to the apparatus specifically the imaging system used for strain measurements and the gripping system for delicate specimens, require that specimens are prepared from biological tissues. For this level of commissioning work, animal intestines that have been processed into "natural sausage casing" are an ideal material – they are of similar composition / properties to the ultimate material of interest, can be sourced inexpensively in suitable quantities and specimens can easily be prepared.

The desired outcome of this phase of the project is a calibrated testing apparatus and mature testing protocol, such the investigations of human membrane tissues or material destined for human clinical applications (e.g. artificial skin cultured for burn treatment) may proceed. This will clearly require a further application to the appropriate ethics committee.

10. SIGNATURES

Applicant Signature: _____ Date 26 MARCH 2019

NOTE: Please note that an Annual or Final Report is required in order to maintain AEC approval.